東海大学大学院　令和 4 年度博士論文

Fundamental Study on Improvement of Salt Damage Resistance of Mortar with Various Blast Furnace Slag based on Chloride Ion Immobilization Capacity

（各種高炉スラグ微粉末配合モルタルの塩化物イオン固定化性能に基づく耐塩害性向上に関する基礎的研究）

指導　伊達　重之　教授

東海大学大学院総合理工学研究科
総合理工学専攻
サッパアーサー　プラン
SUBPA-ASA PRANG

Abstract

Deterioration and maintenance of concrete structures have become a focus of social attention. Regarding this point, blast furnace slag, one of the industry by-products, has been actively studied in recent years, not only from the viewpoint of SDGs but also as an admixture that is expected to improve durability. The effect of improving durability by utilizing blast furnace slag is based on the ability to suppress chloride ions' diffusion and immobilize the hydrated structure. However, the use of blast furnace slag cement, which is inferior in initial strength to ordinary Portland cement, and the replacement of blast furnace slag with cement reduces the productivity of precast products, so there are few cases of use compared to cast-in-place concrete. In addition, the fineness of blast furnace slag on the suppression of chloride ion diffusion is not significant, and in particular, there are few research cases on chloride ion immobilization performance.

In this study, to improve the durability of steam curing products by blending blast furnace slag, various materials and blending conditions (blast furnace) that affect mechanical properties and durability against salt damage (suppression of chloride ion penetration and immobilization performance). Furthermore, focusing on the effects of slag Blaine value, basicity, substitution rate, etc. and manufacturing conditions (preparation time, presence/absence of steam, secondary curing, etc.), the purpose is to acquire and organize technical information that contributes to the manufacture of high-quality precast products was decided.

This study aims to improve the durability of precast products that steam curing by blending blast furnace slag, various materials, and blending conditions (a blast furnace) when the effect of mechanical properties and durability of salt damage (percolation control of chloride ion and immobilization performance).

In addition, it focused on the effects of manufacturing conditions (e.g., preplacing time, presence or absence of steam, secondary curing, etc). to obtain and organize technical information that will contribute to the manufacture of high-quality precast products.

The experimental methods in this study were The effective diffusion coefficient evaluated the effect of suppressing the permeation of chloride ions by the electrophoresis method (Rapid Chloride ion Penetration Test; JSCE-G571-2003). There is no established method for "quantification of chloride ion immobilization amount," which is the main theme of this paper. Therefore, it devised an originally devised quantification method. After the cement paste was hardened and crushed, the sample size was adjusted to eliminate the influence of the difference in the amount of physical adsorption. The prepared material was soaked in 5 wt% saline solution, which is 10 times its mass, for 28 days, then washed and dried. Immediately, it was confirmed that the quantification of Friedel's salt could be performed accurately by XRD analysis by the corundum internal standard method. The findings obtained in this study. The main findings are as the mechanical characteristics by measuring the pore size distribution by injecting mercury confirmed that the structure became denser as the fineness (Blaine value) and substitution rate increased. In particular, it was confirmed that the one using 6000 Blaine had almost no decrease in strength due to slag replacement concerning the plain product (non-replacement product). Further, the effective diffusion coefficient of chloride ion was found as the higher the Blaine value, the smaller the effective diffusion coefficient. Second, it was confirmed.

The production efficiency of precast concrete products have been conducted so far. For example, it has been reported that the utilization of blast furnace slag has a positive effect and a negative effect, such as cracking and strength reduction. Given these past data, incorporating the influence of various manufacturing parameters on the improvement of durability obtained in this research into the product manufacturing plan can reduce environmental load and manufacture high-quality precast products. Therefore, technology development can be expected. In addition, the Japan Society of Civil Engineers has proposed an estimation formula for the chloride ion concentration that contributes to the estimation of the remaining service life. On the other hand, the effect of immobilization performance is not considered or reflected. In the future, based on this knowledge, it will be possible to improve the accuracy of the prediction formula.

Keywords: effective diffusion coefficient; blast furnace slag; chloride ion penetration; chloride prediction

Acknowledgments

The authors appreciate the Department of Architecture and Civil Engineering support, Graduate School of Science and Technology, Tokai University, Japan. Furthermore, sincere gratitude to the number of persons and teammates without whom I might not have written the thesis and to whom I am forever grateful.

Prof. Shigeyuki Date, first and foremost, is my research advisor, for whom I have the most appreciate profound respect. I am very grateful for his encouragement, scientific guidance, valuable critics, patience, and constant support at Tokai University. I sincerely appreciate his dedication and work initiating making this research possible.

Teammates who were making the friendliest environment to work and learn. Indeed, the last 3 years of my journey would not have been joyful and memorable without them. Furthermore, I would like to express my gratitude to my college Ph.D. candidate at Tokai university, Mizuki Takigawa, for continuous advice to rail me on this road and for being a friend and a great source of inspiration. Furthermore, I am very grateful to the master's students at Tokai University, Kazuki Mochida, for their assistance in commitment to this work.

Watanuki international scholarship foundation, the author appreciates the scholarship from Watanuki International Scholarship Fund. The financial support from the scholarship has helped me a lot in my life in Japan.

Friends, the authors appreciate Panumas Saingam and Nattaya Morawan for their support and suggestions. Ornalin Techatadakul, my sister who always has my back.

Psychiatrist Dr. Somrak Santibenjakul, I appreciated the doctors who took care and gave suggestions to me during my Ph.D. life. I could imagine if the author did not has you on my back. Without you, this work would never be possible.

Family, last but not least, words cannot express enough appreciation and love for my family for their constant faith in me, encouragement, patience, and neverending love throughout my up and downs. Without them, this work would never be possible.

Table of Contents

List of Tables

List of Figures

Technical terms used

Cement: a binder or a substance used in construction that sets, hardens, and can bind other materials together. Various types of cement are used as a component in the production of mortar, and concrete, composed of cement and aggregate to form a strong building material.

Ordinary Portland cement: a high-quality and general purpose native suitable for most applications. This product has been specifically designed to reduce the carbon intensity of cement production and complies with the specification for Portland-limestone cement.

High-early strength Portland cement: special purpose cement containing a high C_3S to gain faster strength development. This product was mainly used for cold weather construction and emergency relief projects due to its rapid hardening properties.

Fly Ash: a byproduct from burning pulverized coal in electric power generating plants. During combustion, mineral impurities in the coal (clay, feldspar, quartz, and shale) fuse in suspension and float out of the combustion chamber with the exhaust gases. As the fused material rises, it cools and solidifies into spherical glassy particles called fly ash. Fly ash chemically reacts with the byproduct calcium hydroxide released by the chemical reaction between cement and water to form additional cementitious products that improve many desirable properties of concrete.

Carbon-Free Fly Ash: a byproduct from burning pulverized coal in electric power generating plants. The difference between fly ash and carbon free fly ash is that the presence of unburned carbon in fly ash is much higher than CfFA.

Blast-furnace slag: the molten slag is cooled and solidified by rapid water quenching to a glassy state; little or no crystallization occurs. This process results in the formation of sand size (or frit-like) fragments, usually with some friable clinker-like material. The physical structure and gradation of granulated slag depend on the chemical composition of the slag, its temperature at the time of water quenching, and the method of production. Ground granulated blast furnace slag (GGBFS) has cementitious properties when crushed or milled to excellent cement sized particles, making it a suitable partial replacement for or additive to Portland cement.

Aggregate: generally natural sand which has been washed and sieved to remove particles larger than 5 mm, and coarse aggregate is gravel which has been crushed, washed, and sieved so that the particles vary from 5 up to 50 mm in size.

Mortar: a workable paste used to bind building blocks such as stones, bricks, and concrete masonry units together, fill and seal the irregular gaps between them, and sometimes add decorative colors or patterns in masonry walls. Mortar includes pitch, asphalt, and soft mud or clay, used between mud bricks in its broadest sense. Mortar comes from Latin mortarium, meaning crushed.

Concrete: a composite material composed of coarse aggregate bonded with a fluid cement that hardens over time. Most concretes used lime-based concretes such as Portland cement concrete or concretes made with other hydraulic cement, such as cement fond. However, asphalt concrete, frequently used for road surfaces, is also a type of concrete. The cement material is bitumen, and polymer concretes are sometimes used where the cementing material is a polymer.

Precast Concrete: a construction product produced by casting concrete in a reusable mold or "form" then cured in a controlled environment, transported to the construction site, and lifted into place. In contrast, standard concrete is poured into site-specific forms and cured on site.

In-site Concrete: pour the concrete into forms at the building site; this is so-called in situ concrete. The other method is called precast concrete, in which building components are manufactured in a central plant and later brought to the building site for assembly.

Admixtures: ingredients in concrete other than Portland cement, water, and aggregates added to the mixture immediately before or during mixing. There are two kinds of admixtures: chemical admixtures and mineral admixtures.

High-range water-reducing admixture: chemical admixtures used to make high-strength concrete. They can reduce the water demand and cement content and make a low cement ratio. Generally, these additives allow a 12-40% reduction in water content with standard or enhanced workability, generating slumps over 150mm without bleeding and segregation.

Slump test: measures the consistency of concrete in that specific batch. It is performed to check the surface (also known as workability or fluidity) of freshly made concrete and, therefore, the ease with which concrete flows.

Pre-Curing Time: a period before the freshly made concrete elements were exposed to steam curing in the steam curing process.

Steam curing or accelerate curing: a method of actually agegh early age strength in concrete. The most commonly adopted curing techniques are steam curing at atmospheric pressure, warm water curing, boiling water curing, and autoclaving.

Maturity: a concept that concrete strength and other properties are directly related to age and temperature.

Equivalent age: a concept used to stimulate strength development of heat-treated concrete, reference temperature usually at 20℃.

Nurse-Saul function: is a method to predict the strength of concrete that assumes the rate of strength development of the exponential function of temperature.

Arrhenius law: strength estimation method assumes the rate of strength development of the linear function of temperature.

RH: a measure of the current amount of water vapor in the air relative to the total amount of water vapor in the air at its current temperature and is expressed as a percentage.

Compressive strength: measures the ability of concrete to withstand loads that will decrease the size of the concrete. Compressive strength is tested by breaking cylindrical concrete samples in a particular machine designed to measure this type of strength.

Hydration reaction: chemical reaction that occurs when water reacts with alkene or an alkyne substance. The heat of this exothermic reaction is most influenced by C_3S and C_3A, mix proportion, fineness of binder, and curing temperature.

Cement hydration products: the reaction products between cement and water are termed "hydration products." In concrete (or mortar or other cementitious materials), there are typically four main types: Calcium silicate hydrate: this is the main reaction product and is the main source of concrete strength.

Mold: a hollow container used to shape molten or hot liquid material when it cools and hardens.

Demolding: the process of separating the component from the mold and it becomes one of the critical aspects in the processing of polymers. During the molding process, the polymer typically sticks to the mold.

Blain fineness: of slag or carbon-free fly ash measured by the method by JIS A 6206 and expressed in terms of specific surface (cm^2/g).

Pozzolan: defined in the ACI Committee 216 report as a siliceous material.

Binder: The volume of cementitious materials includes cement and mineral admixtures (fly ash, silica fume (SF), and slags).

Chapter 1

Introduction

1.1 Research background

Concrete is more widely used than any other manufactured material and has been a construction staple for centuries. However, several theories on the deterioration of reinforced concrete (RC) show that direct current (DC) tends to corrode steel reinforcement, and chlorides are chemically bound by the cement paste (tricalcium aluminate, C_3A) [1].

In marine environments, a significant reason for the collapse of RC structures is the corrosion of steel reinforcements, which creates a course for the penetration of chloride through the concrete surface [2], which comes into contact with internal reinforcement, leading to rebar oxidation and corrosion. Therefore, chloride-induced reinforcement corrosion is considered to be the main cause of concrete deterioration. In addition, rust occupies volume and creates tensile stresses in the concrete, resulting in spalling and cracking [3].

Chloride-induced corrosion is the most significant problem affecting aging concrete structures, especially in maritime environments or areas where salts are utilized. Chlorides can be incorporated into concrete or diffused from the outside environment [4], such as from saltwater or deicing salt. When Cl^- reaches the reinforcing steel, it combines with hydroxide to produce the passive oxide layer, which penetrates and causes a crack. Cl^- can cause a breakdown in the passive steel oxide layer, which drives the corrosion reaction. Steel corrosion in concrete can be reinforced by oxygen starvation, especially when oxygen is only at the cathodic areas of steel in solution at the anode. According to [5], carbonation and chloride diffusion processes require several years to reach the reinforcing steel in concrete during the period of corrosion initiation. Equations for Fick's law of diffusion may be used to numerically predict the time it takes for chloride diffusion or carbonation to pass through the concrete covering and initiate corrosion in the RC structure. Covering thickness, quality of concrete, and the environment are possible factors that affect the structure's initial properties and age. Chloride levels at various depths in concrete and carbonate depth are another possible reason. The passive layer is damaged from the point of corrosion

initiation to the first signs of corrosion damage. Therefore, the corrosion period can be estimated using modeled equations that calculate the corrosion time and rate, which determine the deterioration of RC in a given environment. For example, corrosion of a concrete infrastructure due to seawater reduces the ultimate service life of an RC structure.

The durability of concrete constructions is intimately connected to the durability of the component concrete material. Therefore, the environmental effect is increased with Portland cement, which causes the expansion and deterioration of concrete. The leading chemical causes of concrete deterioration are alkali-silica reactions, alkali-carbonate reactions, carbonation, sulfate attacks, chloride attacks, and steel corrosion. A combination of various factors also frequently causes the deterioration of concrete structures. In addition to those given above, acting alone or in combination, other factors such as high structural stresses, thermal stresses, shrinkage, poor quality of materials, and inadequate maintenance may exacerbate the situation [6]. One of the major factors contributing to the corrosion of marine RC structures is the chloride induced corrosion of steel reinforcements, which substantially impacts structural service life [7]. This has been intensively researched for decades, prompted by the rising maintenance costs resulting from the impacts of seawater exposure on coastal structures [8]. Although concrete is the ideal material to protect steel reinforcement due to increased alkalinity, RC marine structures are highly vulnerable to corrosion due to chloride attacks. The severity of the attack is dependent on climatic conditions, among other factors [8].

When partially penetrating the concrete, chloride is captured to react with C_3A to obtain calcium chloroaluminate ($3CaO{\cdot}Al_2O_3{\cdot}CaCl_2{\cdot}10H_2O$), called Friedel's salt, and also reacts with C_4AF to form calcium chloroferrite ($3CaO{\cdot}Fe_2O_3.\ CaCl_2.10H_2O$). The unbound fraction of chloride is referred to as free chloride. It is an aqueous solution in the void of concrete (pore solution). This free chloride is part of the chlorine. Polysaccharides that can diffuse into concentrated concrete of free chloride are lower in number. Moreover, the pore solution reduces alkalinity in concrete to catch large amounts of chloride. The advantage of using high C_3A cement is good chloride corrosion resistance. On the other hand, sulfate corrosion resistance requires cement with low C_3A, which is a contradiction [9].

The aforementioned study revealed that chloride ion permeability into RC structures induces corrosion, disrupting and reducing the structure's performance, and concrete shrinks and cracks as a result. The diffusion coefficient of the chloride ion in the offshore construction was used to evaluate the durability of concrete and mortar. By first decreasing chloride ion penetration, reinforcement corrosion could be delayed [6].

The moisture content of concrete significantly impacts its long-term durability [10]. Water absorption is generally caused by structural porosity (interlayer C-S-H), porous paste, and the aggregate interface zone, particularly in the early stages. Additionally, the physical adsorption of chloride caused by the C-S-H gel can assist in chloride immobilization.

The mechanism of concrete deterioration caused by chloride ion infiltration and carbonation is as follows: (1) Friedel's salt is formed when mono-sulfate (AFm) reacts with chloride ions; (2) Friedel's salt is carbonated; (3) chloride ions immobilized in Friedel's salt dissolve into the pore solution; (4) there is an increase in chloride ion concentration in the pore solution, resulting in increased chloride ion penetration into the concrete through concentrating and diffusion cycles. Due to the acidity of HCl, the alkalinity of the concrete slightly decreases from 12.5-13.5 to grades 11, 10, and 9, respectively. The area where the film was destroyed has a negative electric potential in an electrolysis reaction. "Anodic reaction" is the term referring to this type of reaction [6].

Blast furnace slag (BFS) as a byproduct of pig iron manufacturing, and features high latent hydraulic property. BFS is used as an admixture in Portland BFS cement at 40% to 45%. The advantage of Portland BFS cement is that its long-term strength is more enhanced, and it has higher resistance to seawater and chemicals. In addition, the diffusion coefficient of chloride ions makes the cement suitable for offshore structures. Furthermore, alkali aggregate reactivity is suppressed, the cement can be used with recycled aggregates, and lower heat release rate effectively suppresses thermal cracking [11].

Chloride damage resistance is required when BFS is used. The hardened concrete is denser than ordinary Portland cement [11], as it has a solid capability for incorporating chloride ions.

A previous study [11] focused on the mechanisms of chloride penetrated in concrete and reinforcing steel corrosion, which developed corrosion protection, repair strategies, and detection techniques to develop reliable and practical design approaches

for durability and corrosion protection for concrete reinforcing steel. To develop mechanistic and practical models (deterministic or probabilistic), the study can be used to design durable concrete structures. Furthermore, it can be used to predict the deterioration and maintenance optimization of existing concrete structures to achieve a specified design life.

BFS can improve the resistance of cementitious materials to sulfuric acid attack as the influence of concrete quality on diffusion coefficients is related to the concrete pore structure. Time dependence is due to the hydration of cement particles and chemical reactions of seawater ions with hydration products, which reduce the pore structure.

When BFS is used, sulfuric acid has a small effect in terms of erosion; instead, the high strength concrete or mortar becomes more durable, owing to the enhanced capacity to withstand sulfuric acid. Furthermore, BFS can suppress the penetration of chloride ions, inhibit steel corrosion, and reduce time dependent strains [6].

BFS was used as the aggregate to investigate corrosion initiation on RC structures in one study [16]. That study focused on the physical and chemical attacks on RC structures during their service life and investigated whether any protections might be placed to mitigate the degeneration caused by these attacks. It was found that the concrete performance may be improved by including mineral additives in cement, such as silica fume, BFS, and fly ash.

A literature review reveals many studies of BFS containing concrete in various countries. However, few studies have examined its use in reducing chloride ion permeability as the main factor of corrosion reactions.

1.2 Purposes of this dissertation

This study utilizes BFS as cement to investigate the performance of concrete in terms of delaying chloride ion penetration, which affects corrosion reactions. Furthermore, an experiment was conducted to examine improvements in the performance of an alternative concrete using BFS as cement replacement, focusing on chloride diffusion on concrete with BFS. This study aims to develop products for use in the precast concrete industry toward extending the life of concrete structures, especially reinforced concrete structures, in marine environments.

1.3 Dissertation outline

Chapter 1 summarizes the current state of deterioration of concrete structures, which is the background of the research. The deterioration mechanism has repair and reinforcement and the current state of various material utilization techniques for improving durability.

Chapter 2 summarizes examples of deterioration and repair of marine structures, which is also a problem in the author's home country of Thailand.

Chapter 3 summarizes a literature survey on blast furnace slag blended concrete, which is being actively utilized to reduce environmental effect. In the previous studies, the main positive effects are the crack suppression effect by reducing the heat of hydration and improving salt damage resistance, while the negative effects are the decrease in initial strength and the risk of cracks due to self shrinkage increases have been reported. Increases have been reported. Most of these studies are for concrete in which blast furnace slag 4000 Blaine is replaced with cement by 45 to 50%. There are some cases where the substitution rate is as low as 30%, and the substitution rate is as high as 70%, but the findings are insufficient. On the other hand, considering the application of the results of this study to the manufacture of precast products, it is not realistic to use a large amount of substitution compounding exceeding 50%. Therefore, the replacement rate in this study was set to 45% and half the value (22.5%).

Chapter 4 summarizes the experimental methods in this study. The effective diffusion coefficient evaluated the effect of suppressing the permeation of chloride ions by the electrophoresis method (Rapid Chloride ion Penetration Test; JSCE-G571-2003). There is not established method for "quantification of chloride ion immobilization amount," which is the main theme of this paper. Therefore, it devised an originally devised quantification method. After the cement paste was hardened and crushed, the sample size was adjusted to eliminate the influence of the difference in the amount of physical adsorption. The prepared material was soaked in 5 wt% sodium chloride solution, which is 10 times its mass, for 28 days, then washed and dried. Immediately, it was confirmed that the quantification of Friedel's salt could be performed accurately by XRD analysis by the corundum internal standard method.

Chapter 5 summarizes the findings on improving the salt damage resistance of mortar obtained in this study. The higher the powderiness of the blast furnace slag fine powder used, the better the salt damage resistance, the minimum substitution factor

exists for performance improvement, and the performance deterioration when steam curing is compared to normal curing. In addition, it was found that the preface time was about a percentage, and the effective diffusion coefficient was not affected, but the immobilization performance increased as the preface was longer. The findings regarding salt damage resistance are as follows.

< Mechanical characteristics >

By measuring the pore size distribution by injecting mercury, it was confirmed that the structure became denser as the fineness (Blaine value) and substitution rate increased. In particular, it was confirmed that the one using 6000 Blaine had almost no decrease in strength due to slag replacement concerning the plain product (non-replacement product).

< Durability 1: Effective diffusion coefficient of chloride ion >

- The higher the Blaine value, the smaller the effective diffusion coefficient. It was confirmed that the 6000 Blaine 45% replacement product was halved compared to the non-replacement product.
- The above effect is in the case of 45% replacement, but it is confirmed that the difference from the non-replacement product is slight at half the replacement rate, and it is necessary to set a replacement rate of more than 22.5% in order to improve durability.
- There was almost no significant difference between 0.5 hrs. and 3.0 hrs. in terms of the effect of the pre-preparation time of steam curing.
- It was confirmed that steam curing increased the effective diffusion coefficient by about 9.4% compared to the standard curing product, which hindered the improvement of salt damage resistance.
- It was confirmed that the service period of the structure can be extended by about 30% by replacing the blast furnace slag 6000 Blaine product by 45%.

< Durability 2: Chloride ion immobilization performance >

- It was found that the greater the degree of Blaine and the replacement rate, the increased the immobilization performance. It was confirmed that 6000 Blaine 45% replacement increased by about 65.4% in comparing with the non-replacement product.

- Although the effect of slag basicity on durability has not been seen so far, in this study, it was found that the immobilization ability was increased by 1.5 times by slightly increasing the basicity (1.8 → 2.0).
- Regarding the effect of the pre-preparation time of steam curing, the amount of immobilization increases for 3.0 hrs. compared to 0.5 hrs., unlike the result of the effective diffusion coefficient. Furthermore, it was found that the effect became more pronounced as the Blaine value increased.
- In addition to the effect of reducing the effective diffusion coefficient, further extension of the life of the structure is expected, given the immobilization capacity.

Chapter 6 is a summary of this research. Considering the existing data on the utilization of blast furnace slag for precast concrete products, we contributed to the reduction of environmental load by incorporating the knowledge on the influence of various manufacturing parameters on the improvement of salt damage resistance obtained in this study into the product manufacturing plan. At the same time, technological development for the production of high-quality precast products can be expected. In addition, the Japan Society of Civil Engineers has proposed an estimation formula for the chloride ion concentration that contributes to the estimation of the remaining service life, but the effect of immobilization performance is not considered or reflected. In the future, based on this knowledge, it will be possible to improve the accuracy of the prediction formula.

1.4 Summary

The research uses industrial by-products in construction materials as part of the technological development of the sustainable construction industry. This study focuses on various cementum admixtures to understand the effects of admixture addition on concrete productivity and durability and to spread the technology to reduce the environmental burden.

It would be possible to conduct demonstration experiments on the applicability of these items at precast product manufacturing sites and concrete construction sites to analyze the scope of application of this technology and the cost effectiveness of its

introduction. In addition, this research aims to use the results of this research as primary data for promoting the use of admixtures.

The utilization of industrial by-products for construction materials as part of technological development for sustainable construction projects was developing construction performance. This research focused on cement based admixtures used in Thailand, grasped the effects of admixtures on concrete productivity and durability, and aimed to popularize environmental load reduction technology following:

- Effect of admixture addition on freshness and effect characteristics that are directly related to productivity
- Effects of various additives on various durability
- Improvement/improvement effect of admixture to improve concrete performance

Chapter 2

Environmental effect

2.1 Introduction

Premature or early collapse of reinforced concrete (RC) infrastructure in marine environments can have significant economic, environmental, and sustainability consequences; hence it should be avoided wherever feasible. However, despite decades of research, the specific mechanisms involved in the onset and development of reinforced corrosion in maritime settings and the potential structural damage that results remain a mystery. That is not reasonably sufficient to avoid long-term durability by preventing sound design.

Concrete offers protection against reinforcement corrosion in excellent conditions by providing physical shielding, such as a suitable quantity of concrete cover, or by slowing the corrosion of the bars by the usually high pH of the concrete around them. There is currently a substantial body of data from actual RC structures demonstrating exceptional resistance to reinforcement corrosion in various marine and other conditions, including immersion, tidal, splash, and marine, salt laden atmospheres [12-15]. It was feasible to conduct extensive examinations in several of these situations [14, 16-18]. Despite chloride concentrations beyond any widely recognized chloride threshold criteria, showed extremely low or insignificant degrees of reinforcement corrosion or corrosion damage [19, 20].

In addition, the residual pH of the concrete was determined in certain situations, and it was generally found to be high, indicating substantial reserves of concrete alkalinity and, therefore, a protective effect. If the chloride barrier had been recognized many years ago, some structures would have been condemned erroneously, with possibly enormous consequences and wasteful expenditures.

The immediate question raised by the above is why there appears to be a mismatch between current reinforcement corrosion criteria and actual field observations for high-quality concrete structures, i.e., those with high strength, low permeability, and high remaining alkalinity but also very high chloride concentrations. Many of the traditionally desirable practical factors remain valid, as will be seen, but

the reasons for them may now be understood in a new light, one that is compatible with the long-term durability of well built reinforced concrete structures.

One of the more alarming and perplexing recent findings is that very localized and severe corrosion loss has been recorded in specific RC structures when (hairline) cracking has permeated through to the reinforcement and after lengthy exposure periods [16, 17]. While fracture width is commonly an essential characteristic, our findings imply that crack depth is far more critical, as detailed below. They can also be regarded as evidence of a more significant problem, namely structural degradation that allows for early corrosion start in certain circumstances and perhaps also gradual alkalinity loss, which allows for further corrosion facilitated by the presence of chlorides.

Importantly, this finding supports the idea that concretes and concrete covers that are compromised or damaged in some manners are more likely to cause reinforcement corrosion problems. In the same way, poor quality, porous concretes are prone to cause reinforcement corrosion. Many of these difficulties are recognized in isolation as possible problems for RC structures but have not been studied in the context of generating circumstances for eventual chloride related corrosion of reinforcement, as discussed in the second half of the study. When combined with new information on pitting corrosion induced start and final loss of concrete alkalis, these interpretations give a more comprehensive picture of what is commonly referred to as "chloride induced" corrosion.

2.2 Marine environment effect

2.2.1 Effect of chloride on Marine Corrosion Conditions

The conditions inside concrete usually are (mostly) wet [21], with any pore waters largely stagnant, maybe with chlorides, possibly with air (oxygen, carbon dioxide), and initially significantly pH buffered due to concrete's high alkalinity. Gaseous oxygen (O_2) diffuses slower than water into high-quality concrete, while gaseous carbon dioxide (CO_2)diffuses even slower. On the other hand, the availability of oxygen in dissolved oxygen in water is more crucial.

Steel corrosion can occur under oxygenated conditions, consuming both (O_2) and (H_2O) (oxidation cathodic reaction), as well as anoxic conditions, such as with

imperfections and inclusions (e.g., MnS inclusions) [22], consuming only H_2O and releasing gaseous H_2 after water disassociation (hydrogen evolution cathodic reaction) [23]. The first occurs early in the corrosion process while there is still some O_2 (as well as H_2O) accessible, whereas the second occurs in anoxic conditions at the metal corrosion product contact. However, oxygen must be available outside the rusts, as oxygen is still the ultimate electron acceptor [24, 25]. Corrosion will come to a halt if there is no oxygen as the ultimate electron acceptor in the abovementioned circumstances. The conditions inside the concrete remain the same regardless of whether these processes are in action.

The corrosion of steels in stationary environments, such as chloride solutions, is largely independent of the kind and concentration of salts present [26]. To prove the importance of stagnant conditions [27] by discovering that chloride content had minimal effect on corrosion. They also observed that increasing the rotation of the specimen, or the velocity of the water at the corrosion contact, increased corrosion. However, field research has shown that this influence is reduced as rust layers build up [28].

Many electrochemical studies for reinforcement corrosion have been carried out in test cells using stirred solutions (including artificial concrete pore fluids, natural or artificial seawater, or saltwater) or rotating samples (electrodes) to speed up responses and avoid corrosion product accumulation [29]. However, the findings of such testing have little bearing on actual concrete deterioration.

The use of stirred solutions [30] may help explain the seemingly unusual result commonly stated in the concrete corrosion literature [31], that corrosion in concretes occurs when the pH of the pore water solution goes below around 11. Although this may be true for pitting corrosion in chloride rich solutions, it is not valid for general corrosion regardless of chloride concentration [32]. As will be discussed more below, this divergence is crucial.

2.2.2 Corrosion initiation on Marine Corrosion Conditions

The reinforcement corrosion has been linked to critical chloride level [20] , which is still the case in many publications, such as [33, 34]. However, recent experimental findings have shed fresh light on these long held beliefs.

Even seawater as mixing water and thus with very high available chloride concentrations at the steel bar and elsewhere, even after allowing for bound chlorides [35], which Model concrete specimens exposed for up to 12 years and examined by breaking at approximately yearly intervals, have shown that there is an initial degree of corrosion, but that this then stops or dramatically reduces [36]. Similar findings have been reported elsewhere [37, 38] for a variety of RC beams closer to full size than the laboratory samples utilized in the 12 years investigation. Corrosion did not advance with time for specimens with high strength (as determined by rebound hammer) and hence low permeability. However, corrosion was more severe in the more permeable concretes, even if it was insufficient to shatter the specimens even after 12 years in the studies. The data generally revealed corrosion behavior similar to that indicated in **Figure 2.1** at t_i It should be emphasized that the period 0-t_i was near to zero since the specimens were dipped with chlorides from the start, as previously stated (i.e., with seawater). The bold trend applies for high quality, low permeability concrete. The Tutti model [19] is the conventional model that assumes t_i defines the commencement of serious corrosion damage initiated by an excessive chloride concentration.

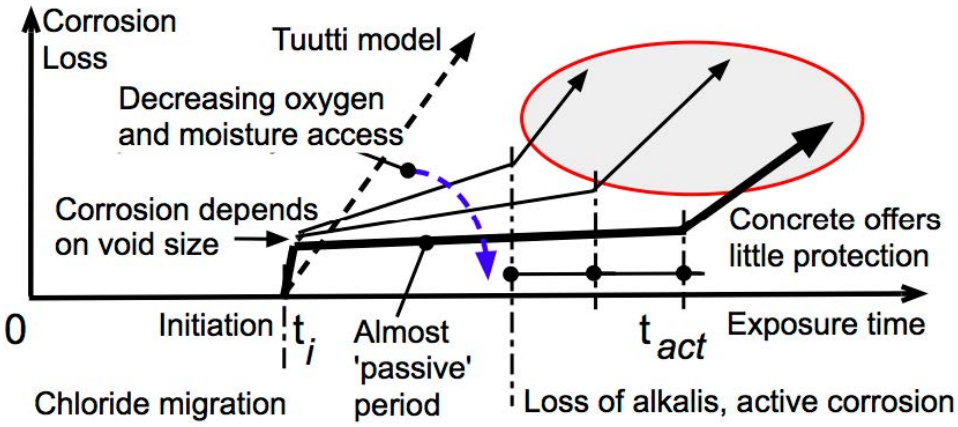

Figure 2.1 Model for the progression of reinforcement corrosion [35]

Corrosion was most frequent on the lower side of the (6 mm diameter) steel bar, according to physical examination of the internal specimens by breaking them up. Therefore, the specimens were cast horizontally and were away from the (vertical) casting direction. There was hardly any rusting everywhere else.

Microscope with fine detail after sectioning, numerous cross sections of the specimens at right angles to the steel bar direction revealed localized corrosion of the steel bar with voids in the concrete that were exactly adjacent but not necessarily aligned (**Figure 2.2b**). When the concrete was cast, the cavities in concrete and resulting localized corrosion of the steel were always the steel bar closest to the shaking table, that is, under the bar. Localized corrosion and cavities under horizontal reinforcing bars have been seen in practice for concrete beams [39], demonstrating a clear correlation between experimental results and reality. This is in contrast to the common assumption in most academic publications, such as [40, 41], that corrosion occurs everywhere around the bars.

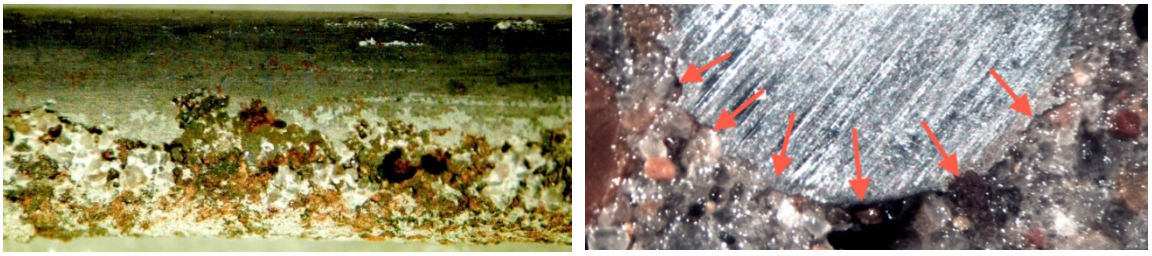

(a) One side of a steel bar (b) cross-section of concrete

Figure 2.2 Corrosion evident [39]

Pitting corrosion is the corrosion mechanism involved [36]. Only under the influence of increased chloride concentrations and elevated pH conditions is this thermodynamically achievable [32]. This will result in rusting (corrosion products) both within and outside the corrosion pits. Within the voids, oxygen will be absorbed as corrosion progresses. If the surrounding concrete is impenetrable to corrosion, corrosion will eventually halt due to a lack of oxygen. In other circumstances, the rate of inward passage of oxygen (and sometimes water) from outside, generally the external environment, will determine the long-term corrosion. This will be very slow for high-quality, low-permeable concretes, resulting in a significant decrease in corrosion rate after time t_i, as illustrated by the bold trend in **Figure 2.2**. The subsequent corrosion rate will be higher for low-quality (increased permeability) concretes, as seen in **Figure 2.2**.

Large voids are expected at the concrete steel interface in concretes that have been improperly compacted around reinforcing bars. Due to the greater oxygen

availability in the more extensive voids, this will create more rust. Rust may cause fractures in the concrete cap, allowing more oxygen to enter (and water). As a result, severe corrosion damage might occur. As previously mentioned, many studies [40, 41] thought that corrosion occurred all around the bars; however, **Figure 2.2** demonstrates that corrosion is considerably more limited, occurring at the bottom of horizontally oriented bars, which is consistent with findings in practice [28]. Only exceptionally porous concretes and vertically oriented bars would allow general bar corrosion the Consequences of Choosing a Preferential Location. The ramifications of the corrosion's privileged location, the resulting build up of corrosion products, and the influence on concrete cracking spalling or delamination of the cover appear to have escaped investigation.

2.2.3 Corrosion initiation in Concretes of Low Permeability on Marine Corrosion Conditions

The onset of corrosion following touch (**Figure 2.1**) is caused by a fundamentally different process from the one described previously. This was recently discovered [36] using laboratory specimens identical to those stated above. The theory was that the primary concrete alkaline substance $Ca(OH)_2$ had gradually disintegrated over time, facilitated by the presence of chlorides, and then leached out of the concrete matrix. The loss of this material essentially exposed the concrete matrix, allowing oxygen to enter the concrete and, once enough leaching had occurred, the reinforcing as well. As a result of the lack of local alkalinity, reinforcing corrosion became possible. These findings should be interpreted as indicating that the more permeability concretes have more interior surface areas exposed to alkali dissolution, rather than implying that they directly allowed for increased species diffusion through the more permeable concrete. Alkali dissolving, not alkali diffusion, is the rate-limiting process (and thus permeability). It should be evident that for high-quality, low-permeability concretes, the loss of concrete alkalinity is unlikely to occur during the usual lifespan of many functional structures, as specific actual reinforced concrete structures have demonstrated [16-18].

2.2.4 Marine environment effect on RC structure

Chloride is abundant in seawater and approximately 90% of the chloride in seawater is in the form of chloride compounds. The chloride salts in seawater include sodium chloride (NaCl) at approximately 27,000 ppm, magnesium chloride ($MgCl_2$) at approximately 3,200 ppm and calcium chloride ($CaCl_2$) at approximately 500 ppm. The total chloride content of concrete is the sum of the contents of 2 types of chlorides.

(1) Bound chloride is the product of a hydration reaction involving calcium chloro-aluminate hydrate as Friedel's salt. Therefore, the pore distribution on the gel surface does not affect the rusting process.

(2) Free chloride is chloride dissolved in pore water that could diffuse into concrete, where the chloride concentration is lower, and increases the alkalinity as the concrete condenses, which would lead to the release of a large amount of chlorite and delay corrosion of a reinforcement.

Chloride damage resistance from BFS is needed when the hardened concrete is denser than ordinary Portland cement, so reducing chloride ion concentrations is also important [42, 43]. Iron and steel slag are steelmaking slag that contains iron oxide (FeO) and magnesium oxide (MgO). The primary components are limestones (CaO) and silica (SiO_2), in addition to other components of BFS, including alumina (AL_2O_3) and magnesium oxide (MgO), as well as a small amount of sulfur (S). Thus, in steel slag production, the slag contains metal elements (such as iron) in oxide form. However, the refinement time for steel slag is short, and the amount of limestone in the raw material is high. Therefore, a portion of the auxiliary limestone material may remain undissolved as free lime [44]. Ordinary Portland cement has four primary constituents, tricalcium silicate ($3CaO{\cdot}SiO_2$), dicalcium silicate ($2CaO{\cdot}SiO_2$), tricalcium aluminate ($3CaO{\cdot}Al_2O_3$), and tetra-calcium alumino-ferrite ($4CaO{\cdot}Al_2O_3Fe_2O_3$), and some of the compounds in BFS can be supportive in ordinary Portland cement.

2.2.5 Corrosion reaction in RC structure

In previous studies [45-47], the primary causes of cracks in concrete structures came from drying-induced shrinkage. The addition of BFS to cement increases the amount of C-S-H gel produced; therefore, along with the cement type and curing age,

the proportion of BFS impacts the degree of cement hydration. A study has shown that the penetration of chloride ion into reinforced concrete structures causes corrosion, reducing concrete structure performance. This results in concrete shrinkage and cracking. The durability of concrete and mortar was evaluated by measuring the diffusion coefficient of chloride ions in an offshore structure. An initial reduction in chloride ion penetration delays reinforcement corrosion [48].

When exposed to HCl, which is acidic, the alkalinity of concrete gradually decreases from an average level of 12.5-13.5 to grades 11, 10, and 9. In an electrolysis reaction, the area where the film is destroyed has a negative electric potential, and the associated reaction is called an "anodic reaction." An example is shows in the following equation:

$$Fe \rightarrow Fe^{2+} + 2e^{-} \tag{2.1}$$

The resulting electron passes through the entire film area with a catholic electric potential. If it reacts with water and oxygen, it forms a hydroxyl ion $[(OH)^{-}]$, which can be written as follows:

$$4e^{-} + O_2 + 2H_2O \rightarrow 4[OH^{-}] \tag{2.2}$$

Simultaneously, the excess Fe^{2+} reacts with water and oxygen to form ferric hydroxide (rust), as shown in the following equations:

$$Fe^{2+} + 2(OH)^{-} \rightarrow Fe(OH)_2 \tag{2.3}$$

$$4Fe(OH)_2 + O_2 + H_2O \rightarrow 4Fe(OH)_3 \tag{2.4}$$

Additionally, Fe^{2+}, which is negative, reacts with water to complete its octet, as shown in the following equation:

$$Fe^{2+} + 2Cl^{-} \rightarrow FeCl_2 \tag{2.5}$$

$$FeCl_2 + 2H_2O \rightarrow Fe(OH)_2 + 2HCl \tag{2.6}$$

A previous study investigated physical and chemical attacks on reinforced concrete structures throughout their service life and investigated precautions that could

be taken to prevent the deterioration caused by these attacks. Earlier studies had indicated that the addition of minerals, such as silica fume, BFS, and fly ash, to cement could increase concrete performance [11].

2.3 Environment effect from cement production

Sustainable construction primarily tries to mitigate the construction industry's negative environmental impacts. Over the last few decades, there has been a significant effort in the building industry to use industrial waste, by-products, or recycled materials to reduce carbon dioxide emissions and protect natural resources. If material is entirely sustainable, it must have low embodied and operational energy. The quantity of energy required to make material is referred to as embodied energy.

Concrete is by far the most extensively used building material, with more than 10 billion tons manufactured each year throughout the global [49]. The building industry consumes many natural resources and contributes to air pollution due to this consumption. As a result, cement may pose a threat to the long-term viability of concrete. Carbon dioxide emissions are the most significant greenhouse gas emissions that have an impact on long-term development. One of the primary causes of global warming is the critical carbon dioxide emitted during ordinary Portland cement (OPC) manufacturing. Nearly one ton of carbon dioxide is discharged into the atmosphere for every ton of cement produced.

The cement industry alone is thought to be responsible for 6-7 percent of all carbon dioxide emissions was previously estimated that replacing each ton of OPC by 50% would save roughly 500,000 tons of CO_2. According to the SCA, using slag cement as a cement alternative in concrete can save 3 million metric tons of carbon dioxide per year. BFS has a low embodied energy or carbon dioxide emission, ranging from 120 to 160 kg/ton on average, owing to its status as a coproduct material. On the other hand, OPC consumes substantial resources and emits around 820 kg/ton of CO_2. Consequently, the difference in emissions between OPC and BFS is roughly 670 kg carbon dioxide per ton.

The utilization of BFS can save a bunch of costs on resources. Environmental restrictions in many nations, on the other hand, demand that industrial waste be disposed of as little as possible and those waste products be reused. One of the goals of sustainable steelmaking is to limit the amount of trash and the number of materials that

end up in landfills. Concrete mineral admixtures may be an essential tool in this effort. They are industrial wastes or by-products of other production processes that require relatively little energy to manufacture. Cement can be lowered by including a larger quantity of extra cementing ingredients, cutting emissions, and mixing energy consumption [50].

BFS was previously discarded in landfills, but due to its superior cementitious characteristics, it is currently being utilized as a supplementary cementitious materials (SCM) to replace OPC in concrete. It can also improve mortar or concrete's strength, durability, and other qualities. Furthermore, BFS has been used as slag particles in concrete for decades. According to one estimate, the concrete industry consumes 8 billion tons of natural resources each year. Any initiatives to lessen this reliance on virgin resources will thus aid in building a more sustainable future [51]. As a result, the use of BFS in concrete has expanded significantly in recent years, with 75 million tons predicted by 2020 [50].

BFS is a construction material that is beneficial to the environment. According to recent studies, slag polluted with dangerous metals can be used safely and beneficially in concrete applications. In addition, metals that are harmful to the environment can be immobilized in hydration products [49]. Its durability strongly influences concrete's service life. The longer the service life of concrete, the more durable it is. AAR, sulfate attack, steel corrosion, and freeze-thaw are the most common concrete durability issues. The addition of BFS to the cement improves its long-term durability. In addition, the consumption of cement decreases as the service life of constructions grows. As a result, incorporating BFS into concrete could aid in the creation of stable structures.

Chapter 3

Blast furnace slag

3.1 Introduction

BFS is defined “as the non-metallic product consisting essentially of silicates and alumina silicates of calcium, and other bases that are developed in a molten condition simultaneously with iron in a blast furnace” by ASTM C 125-16 [52] has been widely used in the construction industry for more than 80 years. When the mixture of iron-ore, coke, and limestone is placed in a blast furnace, molten iron and molten slag are produced at about 1500 ℃ temperature. Typically, 200-400 kg of liquid slag is generated for every ton of hot metal produced.

Molten iron and liquid slag accumulate at the bottom of the blast furnace, where the less dense molten slag forms a layer above the molten iron. Molten slag is channeled out of the furnace as liquid resembling molten lava by floating on the top of the molten iron and can be separated in the skimmer. The chemistry of BFS is relatively uniform. It mainly contains silica, alumina, and lime, combined with magnesia, sulfur, and oxides such as iron oxide and manganese oxide. Three significant types of BFS that are granulated, air-cooled and expanded slags can be produced depending on the cooling and solidifying methods of molten slag.

BFS is obtained by rapidly quenching the molten slag using high pressure water jets. It is glassy granular particles having generally smaller than 5 mm particle size like sand. The GBFS is often used after further processed by drying and then grinding to an excellent powder. GBFS can be used to directly replace ordinary cement with varying replacement ratios between 30% and 85%. If the molten slag is directed into pits or ground bays where solidification occurs under the prevailing atmospheric conditions, it will form air-cooled blast furnace slag (ABFS) with crystalline structured rock like mass. ABFS is a rather complicated, dense material used for applications such as railroad ballast, stabilizing roadbeds, concrete aggregate, or generally wherever a heavy, strong base is required. Expanded slag is produced using a mechanical device and relatively small amounts of cooling water, forming a lightweight dry material. Generally, it is used in light building blocks, in the making of brick, in insulation, and as an aggregate in producing light concrete.

Great efforts to use industrial waste byproducts to reduce carbon dioxide emissions and conserve natural resources have been reported over the past several decades. Concrete materials are the most widely used building construction materials, but their production generates more than 10 billion tons of carbon dioxide per year globally [49]. Environmental regulations in many countries require the removal of as much industrial waste as possible. Enforcing reuse of waste materials in the cement industry is estimated to be responsible for approximately 6-7% of all generated carbon dioxide. Since approximately one ton of carbon dioxide is released into the atmosphere for each ton of ordinary Portland cement produced, carbon dioxide emissions are important greenhouse gas emissions contributing to sustainable development.

3.2 Background of BFS

BFS, a coproduct as show in **Figure 3.1**, is an environmentally friendly construction material whose production requires a relatively small energy input and emits carbon dioxide at 120 to 160 kg/ton (less than concrete production). BFS, as a mineral admixture in concrete, significantly increases the resource efficiency of concrete production. For example, one of the goals of sustainable steelmaking is to reduce the amount of waste and material sent to landfills. In addition, BFS, which requires comparably little energy to produce, is an industrial waste byproduct of manufacturing processes. A recent study has shown that slag contaminated by toxic metals can be used safely and beneficially in concrete applications and can be immobilized into hydration products [49].

A thermochemical reduction in a blast furnace produces BFS during the manufacturing of iron [53]. The iron oxide ore is reduced to metallic iron using coke, while the silica and alumina components combine with lime and magnesia to produce a molten slag that gathers on top of the molten iron at the furnace's bottom. Some of the constituents, such as silicon, manganese, and sulfur, are decreased by iron. As a result, sulfur fractionation between iron and slag is significant. To encourage sulfur solution in the slag, which either the temperature or the lime content of the slag increased; the latter, in any case, necessitates a temperature increase to maintain fluidity. Increased magnesia concentration, within specific limitations, decreases slag viscosity and is thus preferred in current practices with low slag volumes. For economic reasons, dolomite or magnesian limestones are also employed in several areas.

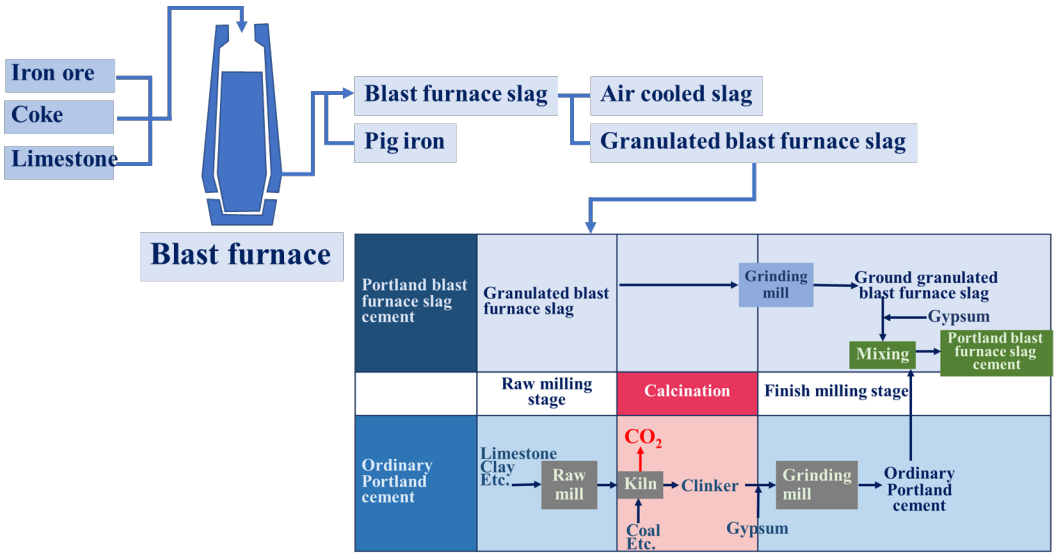

Figure 3.1 The production of Portland BFS and ordinary Portland cement [53]

BFS is a molten stream that emerges from the blast furnace at a temperature of about 1500℃. The conversion of molten slag into products appropriate for diverse purposes is dependent on further processing; widely different products are created depending on the cooling techniques utilized.

- Air-cooled blast furnace slag (ABS): When the BFS is allowed to cool slowly with air, it solidifies into a grey, crystalline, stony material, known as 'air-cooled' or crystalline blast furnace slag. The material is used in a road stone, concrete aggregate, and various cooling procedures and slag properties as an aggregate.
- BFS pellets: This material is obtained when a quick cooling with air is applied to the liquid BFS. Several fractions are obtained. The layer pellets (>10mm) occur as nodules with a porous structure that is partly crystalline. This expanded slag is suitable as a lightweight aggregate. The smaller fraction (<10 mm) is mainly in a glassy state and is used as a hydraulic constituent of blended cement.
- Blast furnace slag (GBS): The slag is cooled very rapidly and solidifies as a glassy granulated mass into a granulator. The granulated slag is poured into a significant excess of water (100 m^2/ton of slag) or subjected to spraying jets under 0.6 MPa pressure (water 3 m^2/ton of slag). After the treatment, the water content of slag (<30%) is largely eliminated in dryer mills or filter basins. Vitrified granulates (0-5mm) are obtained and used as a hydraulic binder for

cement, mortar, and concrete. After grinding separately or together with Portland cement clinker, GBS provides BFS.

3.3 Components of BFS

3.3.1 Chemical composition of iron and steel slag

Limestone (CaO) and silica (SiO_2) are the most basic components of iron and steel slag. Alumina (Al sub>$2O_3$) and magnesium oxide (MgO), as well as a residue of sulfur (S), are other components of BFS, whereas steelmaking slag contains iron oxide (FeO) and magnesium oxide (MgO). In the case of steelmaking slag, metal components (such as iron) are present in oxide form. Because the refining period is short and the amount of limestone used is significant, some of the limestone auxiliary material may stay undissolved and free (CaO) [2] . Examples of iron and steel slag compositions as show in **Table 3.1**.

Table 3.1 Examples of iron and steel slag compositions (in percentages) [2]

Type Component	BFS	Converter slag	Electric arc furnace slag		Andesite (for ref.)	Ordinary cement
			Oxidizing slag	Reducing slag		
CaO	41.7	45.8	22.8	55.1	5.8	64.2
SiO_2	33.8	11.0	12.1	18.8	59.6	22.0
T-Fe	0.4	17.4	29.5	0.3	3.1	3.0
MgO	7.4	6.5	4.8	7.3	2.8	1.5
Al_2O_3	13.4	1.9	6.8	16.5	17.3	5.5
S	0.8	0.06	0.2	0.4	-	2.0
P_2O_3	<0.1	1.7	0.3	0.1	-	-
MnO	0.3	5.3	7.9	1.0	0.2	-

The chemical composition of these components is equivalent to that of ordinary Portland cement, and they may be discovered in the natural world in places such as the Earth's crust, natural rock, and minerals. Iron and steel slag have comparable form and physical properties to crushed stone and sand. However, because of variations in chemical components and cooling methods, several kinds of slag can be produced with a wide range of distinct characteristics. When alkali stimulation occurs, for example, some kinds of slag harden. As a result, various applications based on the physical and chemical properties of slag have been discovered and utilized in various industries.

3.3.2 Dissolution characteristics

(1) **pH**: The alkalinity of iron and steel slag increases to 10-12 when it reacts with water due to the effects of the limestone it contains, indicating that it is the same as or lower than that of recycled concrete base course aggregate and cement stabilized soil. The alkali components that dissolve iron and steel slag products are absorbed and neutralized by the soil in Japan since the soil is typically acidic. Therefore, water with slag does not pass through the soil and flows straight to the outside. Therefore, actions must be taken to decrease alkalinity, same as with recycled concrete base course material and cement stabilized soil, which can involve creating a high soil embankment or neutralizing the water with carbon dioxide gas before draining it an iron and steel slag product. The manufacturer and seller ahead of time to see what water drainage measures are required during and after construction.

(2) **Heavy metals**: When iron and steel slag products are used on land, environmental safety is verified based on the Environmental Quality Standards for Soil Contamination. When the products are used in a marine environment or landfill, safety is verified based on the benthic soil standards in the Law on the Prevention of Marine Pollution and Maritime Disaster. Although the quality of iron and steel slag products is already prescribed by JIS as materials for use in civil engineering works, because there was previously no quality standard related to environmental safety, no specific environmental considerations had been prescribed for these products. Subsequently Test Methods for Chemicals in Slags (JIS K0058-1) [54] was established in 2005, and at present environmental considerations are being

added to or revised in JIS for iron and steel slag used in roads and other iron and steel slag products.

BFS is a nonmetallic product consisting essentially of silicates and alumina silicates of calcium in molten form and iron in a blast furnace, according to ASTM C 125-16 [52], which accumulate at the bottom of the blast furnace after rapidly quenching the molten slag using high-pressure water jets. Then, the molten slag is directed into pits, or ground bay solidification occurs under prevailing atmospheric conditions. BFS could be a direct replacement for between 30% and 85% of ordinary Portland cement in a structure.

BFS exhibits excellent cementitious properties and is off-white; moreover, the composition of the raw materials affects the chemical composition of BFS. The principal constituents of BFS, as presented in **Table 3.2**, are silica (SiO_2), alumina (Al_2O_3), calcium (CaO), and magnesia (MgO), which make up 95% of its composition (Iron and Steel Slag Statistics and Information 2017) [55].

The main components of slag are MgO, Al_2O_3, SiO_2, and CaO. The hydraulic activity of slag increases with increasing contents of CaO, MgO, and Al_2O_3 but decreases with increasing SiO_2. Several factors contribute to the reactivity of slag, such as the component composition, chemical composition, geometrical properties, temperature, glass structure, and alkali environment.

Table 3.2 Chemical analysis (in percentages) of BFS [56]

SiO_2	CaO	MgO	Al_2O_3	Na_2O	SO_3	MnO	TiO_2	Fe_2O_3	P_2O_3
35.09	37.79	5.50	17.54	0.30	0.66	0.83	0.68	0.70	0.37

A preliminary study [57, 58] reported factors affecting the reactivity of slag in cement, of which the chemical composition, pore solution, slag processing, and geometrical properties were the main parameters. Higher hydration temperatures increased the slag reactivity as the percentage of slag replacement was reduced; on the other hand, the reactions increased with increasing amounts of water.

Generally, when added in the right proportion, a mineral admixture improves the workability of fresh concrete. Early studies suggested that BFS increased the workability because the specific gravity of BFS was slightly lower than that of cement. As a preliminary examination [59], and prepared concrete mixes containing 0%, 40%,

and 70% BFS [60]. An earlier report found that a water-to-binder (W/B) ratio of 0.43-0.46 is needed to decrease the amount of plasticizer needed as the BFS content increases in plasticized concrete [8]. They concluded that BFS reduces the superplasticizer dosage in concrete because it acts as a super plasticizing agent replacement. In their initial study found that the more cement that is replaced by BFS and the lower the W/B ratio, the more significant the reduction in the superplasticizer dosage for high strength concrete (HSC) [61].

The delay in the setting time depends on the initial temperature of the concrete, the proportions of the blend used, the W/C material ratio, and the characteristics of the PC, and adjusting these parameters can have undesirable effects on manufacturing precast elements and executing concrete work during a low temperature period. The addition of accelerating admixtures can significantly reduce the setting time delay, thereby eliminating it as a barrier to the use of BFS.

Although the slow development of compressive strength of concrete containing BFS is disadvantageous in the early ages of concrete curing, such as its effects on the early strength of concrete, this slow development is advantageous for the later development of compressive strength to a level that is higher than the strength of OPC concrete. As a result, BFS can replace approximately 50% of the average PC concrete in ready mixed concrete production.

The fineness of BFS cement is also an important parameter affecting the strength development of slag concrete. BFS with a small specific surface area causes a decrease in strength. Therefore, BFS should typically be ground more delicately than standard PC since it reacts more slowly, especially at lower temperatures. Experimental studies have reported that the 28 days strength of concrete increased significantly as the fineness of BFS increased for an exact replacement ratio. More finely ground BFS had exceptional early strength and fineness increased from 4,080 to 6,230 cm^2/g, the 28 days strength increased significantly [62, 63].

3.3.3 Improving the durability of concrete structures

Iron and steel slag products are used in a variety of areas where their unique characteristics are put to effective use. The majority of the demand for these products comes from the field of cement. Approximately 40% of iron and steel slag products,

and 60% of BFS, are used in cement. Most of these products are used as a raw material in Portland BFS cement. Portland BFS cement has the following characteristics.

(1) It has high resistance to seawater and to chemicals, and can improve durability.
(2) It has a low chloride ion diffusion coefficient (resists rebar corrosion).
(3) It can reduce alkali aggregate reaction.
(4) Its strength increases over time.
(5) It produces little elution of hexavalent chrome when used in ground improvement.

This product is also increasingly being used in construction projects. For reasons including the generally large material cross sections, ease of ensuring concrete curing time, and the relatively large cover it provides, Portland BFS cement is suitable for use in structures such as piles, foundations, underground beams, and continuous walls. With the CASBEE evaluation system that is increasingly being instituted by local governments and under the Tokyo Metropolitan Environmental Building System, the use of Portland BFS cement adds points to the evaluation score. The Tokyo system was started in 2002, and Portland BFS cement is used in approximately 50% of the buildings that have been designated under this system.

3.4 Application on concrete industry

As a result of growing environmental awareness, iron and steel slag is highly regarded as a recycled material that can reduce impacts on the environment due to its resource conservation and energy saving effects.

3.4.1 Air-cooled BFS

This slag hardens when it reacts with water, with a hydraulic property that increases strength over time because of its large load bearing capacity, it is used in road base course material in the same way as gravel. There is no risk of alkali aggregate reaction, and this slag contains no clay or organic impurities. As a result, it is also used as a concrete aggregate in the same way as natural aggregate.

3.4.2 Granulated slag

As air-cooled blast furnace slag, this slag has a hydraulic property and there is no risk of alkali-aggregate reaction. Because of the powerful latent hydraulic property that results from fine grinding, this slag is used in products such as Portland BFS cement. When blended with cement, the BFS becomes Portland BFS cement with the same properties as ordinary Portland cement. The advantages of this BFS cement, such as increasing strength over long periods of time, low heating speed when reacting with water, and high chemical durability, are put to effective use in a broad range of fields including in the construction of ports and harbors and other large civil engineering works.

3.4.3 Steelmaking slag

Because of its hydraulic property and the large bearing capacity it can provide, steelmaking slag is used as a road base course material. With high particle density and hardness, this slag has superior wear resistance and for this reason is used as an aggregate for asphalt concrete. In addition, due to its high angle of shearing resistance, high particle density, and large weight per unit volume, it is also used as a material for civil engineering works and as a ground improvement material (i.e., material for sand compaction piles).

3.4.4 Primary characteristics and applications of iron and steel slag

The primary characteristics and applications of iron and steel slag are present in **Table 3.3**. The various applications were functional and present by the slag type as BFS and steelmaking slag while different producing method. Moreover, the characteristics were present by chemical characteristics the suggestion was suggesting the application which suitable.

Table 3.3 Primary characteristics and applications of iron and steel slag [2]

Slag	Method	Characteristics	Applications
BFS	Air-cooled slag	Hydraulic property	Road base course material
		No alkali-aggregate reaction	Coarse aggregate for concrete
		Low Na_2O and K_2O	Cement clinker raw material (replacement for clay)
		Thermal insulation and sound absorption effects when made into a fiber	Raw material for rock wool
		Fertilizer component (CaO, SiO_2)	Calcium silicate fertilizer
	Granulated slag	Strong latent hydraulic property when finely ground	Raw material for Portland BFS cement
			Blending material for Portland cement
			Concrete admixtures
		Low Na_2O and K_2O	Raw material for cement clinker (replacement for clay)
		Latent hydraulic property	Material for civil engineering works, ground improvement material (Backfill material, earth cover material, embankment material, road subgrade improvement material, sand compaction material, ground drainage layers, etc.)
		Lightweight, large angle of internal friction, large water permeability	
		Does not contain chlorides.	Fine aggregate for concrete
		No alkali-aggregate reaction	
		Fertilizer component (CaO, SiO_2)	Calcium silicate fertilizer
			Soil improvement
Steel making slag	Converter slag, electric arc furnace slag	ard, wear-resistant	Aggregate for asphalt concrete
		Hydraulic property	Base course material
		Large angle of internal friction	Material for civil engineering works, ground improvement material (Material for sand compaction piles)
		FeO, CaO, SiO_2 components	Raw material for cement clinker
		Fertilizer components (CaO, SiO_2, MgO, FeO)	Fertilizer and soil improvement

3.5 Portland blast furnace slag cement

Reducing CO_2 emissions: Expanding the use of Portland BFS cement is one measure included in the plan to achieve the targets of the Kyoto Protocol, and there are large expectations for its ability to help reduce CO_2 emissions. Under the Kyoto Protocol, Japan has committed to the world to reduce its 2008-2012 emissions of greenhouse gases by 6% from 1990 levels. The plan for achieving this public commitment includes a reduction in CO_2 emissions of 1.12 million tons resulting from a 16% increase in the production ratio of blended cement.

The majority of the blended cement that is produced in Japan is Portland BFS cement assume that Portland BFS cement accounted for all of the 16% increase in the production ratio of blended cement, this would contribute to an annual reduction in CO_2 emissions of 640,000 tons. Specifically, the use of 20% Portland BFS cement in constructing a single apartment complex would result in a per-household CO_2reduction of approximately 1,200 kg. The national government has recognized these effects, local governmental organizations, and private companies.

As a result, there is growing momentum toward stopping global warming by expanding the use of Portland BFS cement. The slag can also be added to ordinary Portland cement at 5% or used as an admixture in concrete products. The limestone and coal used production of ordinary Portland cement are reduced, and the CO_2 emitted by the decarboxylation of limestone or the incineration of coal is also reduced. By reducing the limestone and fuel used for cement production, the CO_2 generation is reduced by 320 kg/ton of cement. Portland BFS cement features excellent durability, greatly enhanced long term strength, and less chloride migration suppresses alkali aggregate reactivity and can be used with recycled aggregates. BFS cement does not require calcination, as present in **Figure 3.1** and the following **Table 3.4**, the annual reduction of CO_2 emission by Portland BFS cement production in Japan is approximately 4,000,00 tons.

Table 3.4 The comparison of cement production

CO_2 emission source	**Portland cement (i) CO_2 emission**	**BFS cement (ii) CO_2 emission**	**Reduced CO_2 emission (i)-(ii)**	**Reduction rate of CO_2 emission (%)**
Limestone	468	268	200	43
Electric power/energy	296	176	120	41
Total	764	444	320	42

*CO_2 emission per 1 ton of cement (unit: kg)

3.6 Fresh properties of mortar/concrete containing BFS

3.6.1 Workability

The mineral admixture improves the workability as a critical characteristic of fresh mortar or concrete. Incorporating mineral admixtures in concrete would generally enhance fresh concrete properties that will enhance consistency, cohesiveness, and reduction in bleeding and segregation [58]. The workability of cement pastes and mortars was increased due to improved particle dispersion and fluidity, both with and without water reducing admixtures. The specific gravity of BFS was slightly lower than that of cement, which increased the workability. However, slump, vibe, and compaction factor test results showed that the ratio of water cementitious (W/C) materials decreased to maintain the same workability of the concrete mix with 0% BFS. Slump, Vibe, and compaction factor test results showed that the W/C ratio materials decreased to maintain the same workability of the concrete mix with non BFS [59].

BFS particles have smooth and dense surfaces, which provide smooth slip planes were absorb less water than PC particles, making BFS concrete more workable. Therefore, a reduction in water content is possible for equivalent workability [64]. As a result, BFS concrete mixes had 20-50 percent higher slumps than regular concrete with the same W/C content ratio. In addition, the improving BFS ratio was an accompanying increase in the slump in non-superplasticizer concrete[44, 65].

Mineral additives such as fly ash and BFS are commonly used in manufacturing high strength and high performance concrete (HPC) due to their exceptional technical and performance properties. In addition, compared to the same concrete without any additions, these additions may increase the fluidity of the concrete and lower the amount of superplasticizer required to get a similar slump flow [66]. In plasticized concretes with 0.43-0.46 water-to-binder (W/B) ratios, the amount of water required to achieve a particular slump reduces as the BFS concentration increases [8]. The superplasticizer agent replacement, BFS, decreases the superplasticizer used in concrete. The lower the w/b ratio and the higher the cement replacement by BFS, the more significant the reduction in superplasticizer dosage for high strength concrete (HSC) [61].

The properties of fresh self compacting concrete (SCC) that added BFS by substitution to cement were found very beneficial to fresh SCC. Workability was improved up to 20% of BFS content with an optimum content of 15% when the W/B ratio and superplasticizer content were maintained constant. Furthermore, with 15% BFS content, workability retention of approximately 60 minutes was accomplished [67].

BFS had a high specific surface area between 5000 and 9000 (cm^2/g), imparting a high segregation resistance to concrete while ensuring fluidity. A previous study investigated the workability and other properties of concrete containing BFS with fineness's ranging from 1000 to 2000 cm^2/g [68]. The observed that the slump of concrete increases by BFS when the replacement ratio is about 50%, especially in a low W/C ratio. There was no significant difference between the concretes with and without BFS when the replacement ratio was 30% or below. As a result, concrete with a low fineness of BFS has improved workability than concrete without BFS. According to this hypothesis, the finer the slag is grinding, the better several properties, including strength, workability, and bonding. The finely BFS has a greater specific surface area and, as a result, a larger surface area for water reaction. They discovered that replacing cement with more than 20% by mass improved the consistency of the concrete mixture [69].

Fresh concrete containing BFS tends to require less energy for movement than comparable PC concrete, in addition to increased consistency. Pumping, placing in molds, and compacting is easier for concrete containing BFS. In addition, concretes containing BFS retain their workability for longer. The workability of concrete

incorporating BFS as a partial cement substitution is improved. Reported an increase in consistency after mixing the concrete mixture immediately and after 30 min when finely BFS was substituted at 80% and 100% for cement. BFS slows both the rate of setting and the rate of slump loss. As a result, concrete containing BFS as a partial cement substitute has a reduced slump loss during hot weather construction [69].

The fineness of BFS concerning cement affects bleeding related to the physical properties and permeability of fresh concrete. The bleeding ratio of concrete is influenced by the ratio of solid surface area to the unit volume of water. Bleeding is decreased when the BFS is more acceptable than the PC and is substituted on an equalmass basis; nevertheless, when the BFS is coarser, the bleeding rate and amount may be increased [70]. The bleeding ratio under pressure greater than 25 bar reported bleeding readings for various mix proportions at high pressures compared to BFS and cement [71]. Half of the water is drained out under high pressure in cement pastes, having a water-to-powder ratio higher than 50%. When BFS paste was utilized, however, the bleeding ratio did not reach 50%, demonstrating that bleeding increases with an increase in the initial water-to-binder ratio (W/B) or pressure and that the rates of increase of the bleeding ratio were similar in the cementitious pastes. BFS paste has a lower packing density than cement paste under the same pressure supports the finding that concrete incorporating BFS is less prone to bleeding. In general, when comparing BFS concretes to PC concretes of the same strength, BFS concretes exhibited reduced bleeding.

3.6.2 Setting time

The thorough use of cement in place of BFS generally increases the time [50, 70]. In BFS incorporated cement, there was a significant delay in the final setting time [65]. The BFS replacement ratios did not significantly affect the setting time when the temperature was 23°C, as previously disclosed. Slag may cure slower than regulate concrete at temperatures below 23°C, which has significant consequences for winter concreting [72]. The rate during which the setting time is delayed the determined by concrete's initial temperature, the proportion of the mix used, the W/C materials ratio, and the PC's properties. The final setting time of concrete is longer than OPC concrete when the ambient temperature decreases or the replacement ratio increases. It is a negative thing unless making precast elements, including doing concrete work in the

winter. Setting time delays can be considerably reduced by using accelerating admixtures. As a result, the delay in final setting times would not be a problem. At higher temperatures, though, the slower rate of setting is preferable. Slag concrete seems to have little change in setting time at higher temperatures (30°C). As a result, depending on the weather, adjusting the BFS proportions is achievable.

The previous study investigated the influence of BFS on concrete setting times [73-80]. The inclusion of BFS in the SCC, which replaced 20%, 30%, and 40% of the OPC, demonstrated that the presence of BFS prolonged the setting times of cement paste [79]. Furthermore, depending on the chemical base of the admixture, all accelerators provide a 40-50 % reduction in initial setting time. Consequently, they concluded that the C-S-H crystal seeds based additive was the most effective for cement when combined with BFS [80]. The initial and final setting times of concrete containing 60% BFS were increased by factors 2.75 and 2.27, respectively, in an experimental study [76].

3.7 Properties of hardened concrete containing BFS

3.7.1 Strength development

As a primary supplemental cementing material, BFS was used. It has cementitious as well as pozzolanic characteristics. The influence of BFS on the strength of various types of concrete and mortars. The use of BFS instead of PC results in a considerable increase in the compressive strength of the mix. In general, the ideal slag blend for the most significant strength at 28 days appears to be at 50%. The strength of slag concrete develops more slowly than that of concrete without BFS. Although this is a disadvantage for early concrete ages such as 3 or 7 days, delaying strength development is helpful for 28 days and after. Because BFS containing concrete gains strength faster than OPC concrete at later ages, the compressive strength of BFS approaches that of the control concrete between 7 and 28 days. Beyond this period, the strength of BFS exceeds that of the control concrete. Thus, BFS replaces a significant amount of standard PC concrete in ready mixed concrete production, roughly 50%. In most cases, the reasonable maximum throughput except for specific concretes, where the replacement ratio would be around 70%. In addition, for constructions with high

early strength requirements, the replacement ratio decreases to 20-30%. Too many variables as chemical composition, fineness, activity index, curing conditions, and amounts of slag utilized in concrete mixtures influence compressive strength development in concrete containing slag [44].

The investigated a superplasticizer, no entrained mix constant w/cm at a strength level of 100 MPa [81]. The percent strength of the 70 percent slag mix compared to the conventional PC control mix was 71 and 96 for 28, and 91 days ages, respectively, which discovered that the strength of slag mixtures was initially lower than that of a typical PC mix, but that after 91 days, they had caught up at all replacement levels [82].

In the case of high level BFS replacements, concrete compressive strength has been observed to be reduced. For example, the strength decreased when the amount of BFS grew to 90% [72, 83-85].

The compressive strength rate of BFS containing self compacting repair mortar was lower at younger ages. On the other hand, the compressive strength grew more robust over time, becoming more evident at 30-50 % replacement levels. As a result, the maximum limit of the BFS replacement ratio was proposed to be regulated at 50% to provide an unprecedented long term compressive strength increase [86].

The fineness of BFS cement has an impact on the strength development of slag concrete. The strength of BFS with a limited specific surface area is decreased. Although BFS reacts more slowly, especially at lower temperatures, it should be ground more acceptable than a standard PC. According to the experimental studies, the 28 days strength of concrete improved considerably as the fineness of BFS increased for the appropriate replacement ratio. More coarsely BFS exhibited early increasing strengths [62, 63].

The curing temperature affects the hydration rate of cement, which influences the strength development of concrete. The curing temperature rose, the rate of hydration increased. As a result, the response rates of BFS containing concrete are decreased. As a result, a longer curing time is required for the BFS characteristics to develop appropriately [87]. As a result, the strength values of the BFS concrete mixtures increase more than the control mixtures when the curing period is increased.

The BFS concrete mixtures had greater strength values than the control mixtures with much the same binder concentration. The BFS concrete takes longer to develop strength since the pozzolanic reaction is delayed and dependent on the availability of calcium hydroxide [88]. Compared to a water cured sample of the same BFS

replacement level, the strength of a 50 % BFS replacement mix with an initial 7 days of moist curing followed by air curing is not significantly impacted [89, 90]. The impact of curing temperature on the strength development of BFS mortars [91]. The discovered that the temperature has a significant impact on the strength development of BFS combinations that BFS mortars develop strength significantly more slowly than PC only mortars under typical curing conditions. Strength gain is significantly faster at higher temperatures, and the improvement in early age strength is more substantial at higher levels of BFS.

The BFS replacement level varies depending on the country's practice. In the United States, the percentage of BFS replacements ranges from 25% to 50% for HSC [68]. For different uses and environmental circumstances, the Slag Cement Association (SCA) recommends varied replacement rates.

The three BFS containing mixtures (25 %, 40 %, and 50 %) performed similarly to the control combination at 28 days but outperformed the control mixture at 56 days [92]. However, they found that control specimens had poorer compressive strength below 55 % cement replacement after 7 days. With an increase in BFS content at an early age, these experimental results revealed that latent hydraulic responses by BFS slowed down the strength development. However, at later ages, 28, 56, and 91 days, they discovered compressive strength similar to or slightly higher than control specimens.

The combined effect of chemical and physical processes can drive concrete to deteriorate when exposed to saltwater. However, the inclusion of SCM can enable concrete to achieve long term performance. Due to the reduced number of larger pores, concrete combining pozzolanic and cementitious ingredients such as BFS in an aggressive environment exhibits a significant increase in durability. The process is that when pozzolanic materials are introduced, calcium hydroxide ($Ca(OH)_2$) is converted into secondary calcium silicate hydrate gel, causing the pozzolanic reaction of the mineral admixtures to transform larger pores into more delicate pores.

In concrete exposed to seawater, Europeans usually use a high quality pozzolan. BFS is a pozzolan that is commonly used in concrete mixes for marine settings. BFS hardened cementitious materials enhance concrete strength while lowering permeability. Pozzolans also bind to lime chemically, producing less soluble compounds that reduce the impacts of lime leaching.

Although flexural strength is susceptible to microcracks, the replacement of BFS to concrete production is affected by changing the reaction products and pore structure in hardened concrete, improving flexural strength, particularly at later ages. Many studies have shown that BFS included concretes have the same or slightly higher flexural strength than PC concretes at ages more significant than 7 days, owing to increased paste compactness and adherence at the aggregate paste interface [93].

For 7 days or later ages, concretes including BFS exhibit equal flexural strength. Some researchers, on the other hand, found the opposite. For example, a modest decrease in flexural strength at 40% replacement level and a significant decrease at 80% replacement level [94]. The flexural strength of concrete containing 60% BFS, on the other hand, was much higher than the control mix. As a result, it indicates that a BFS replacement level of 40-60% is optimal for maximum strength growth. Although more significant percentages can be used, the specimens' strength generally decreases compared to control specimens. Ultrafine BFS has a more significant impact on the flexural strength of concrete with a lower W/C ratio [95].

3.7.2 Elastic properties

Elastic modulus can be expressed as a function of compressive strength for standard concrete. Most national and international codes are used to express the modulus of elasticity of concrete. For example, building code requirements for Structural Concrete ACI 318-11 (Eq. 3.1) and Canadian concrete code (Eq. 3.2) [96] express equations based on the compressive strength of concrete for the evaluation of the modulus of elasticity of concrete.

$$E_c = 4700\sqrt{f_c'}(\text{ACI318R-05}) \tag{3.1}$$

$$E_c = 4500\sqrt{f_c'}(\text{CSA}) \tag{3.2}$$

A few difference between the modulus of elasticity of the control concrete and concrete containing a South African origin BFS at the same strength level [97]. Furthermore, on a Japanese slag, showed no significant difference between the values of Young’s modulus of elasticity of concrete incorporating granulated slag and that of

the control concrete [43]. Thus, it is widely accepted that the effect of BFS replacement on the elastic modulus of concrete is negligible.

3.7.3 Microstructure

In relative to ordinary concrete, BFS concrete is less permeable, with capillary particles and a denser structure. Concrete with a higher BFS replacement percentage has a denser structure and is less susceptible to water penetration, making it more resistant to violent assaults, including alkali-silica reaction (ASR), corrosion, and sulfate attack. Because of the various reactions with BFS, the microstructure of BFS concrete differs from PC concrete [98, 99]. Calcium silica hydrates develop close to the cement particle when PC interacts with water. Calcium hydroxide migrates through the pore solution and forms discrete crystals that are surrounded by extensive pores. Both BFS and PC hydrate to create calcium silicate hydrates when BFS particles are present.

The BFS also interacts with excess calcium hydroxide to create a finely distributed gel covering the bigger holes. As a result, there are fewer calcium hydroxide crystals in the cured cement paste and fewer large capillary pores. Concrete becomes more chemically stable as the amount of free calcium hydroxide decreases. Furthermore, the improved pore structure reduces the potential of chemicals to infiltrate through the concrete [98]. The primary reason for slag cement paste appreciates the importance of durability is the microstructure's low permeability.

To increasing the BFS replacement percentage reduced average pore size diameter by 15%, 30%, and 47% for 10%, 30%, and 50% BFS replacement, respectively [10]. Coarse pores in BFS concrete were significantly smaller, and the pore structure of OPC concrete was greatly improved when 70% BFS was added, notably for the 60 days pore structure [100]. The investigated the hydration products in BFS concrete using a scanning electron microscope (SEM). Cement was substituted with 40% BFS, with a specific surface area of 600 m^2/kg [7].

Used SEM with 50% and 65% slag and a specific surface of 350 m^2/kg to investigate the internal microstructure of the different concretes. Researchers utilized two concrete mixes with good workability and low W/B ratios [101]. At around 6 months, the shattered pieces of concrete prisms were inspected. Continuously cured concrete in a moisture environment developed a compact and dense texture throughout

time. Pores and microcracks were consistently observed in concretes that had been subjected to a prolonged drying environment. SEM confirmed the drying environment to be the primary cause of increased porosity.

3.7.4 Porosity

The porosity of concrete affects both strength and transport characteristics, while finer SCMs influence the porosity of mortar mixes. The pore sizes visible by SEM imaging are determined mainly by image resolution, with the least detectable size being in the region of 0.2 mm, depending on equipment and setting characteristics. BFS might well be utilized to reduce pore sizes significantly and cumulative pore volume, resulting

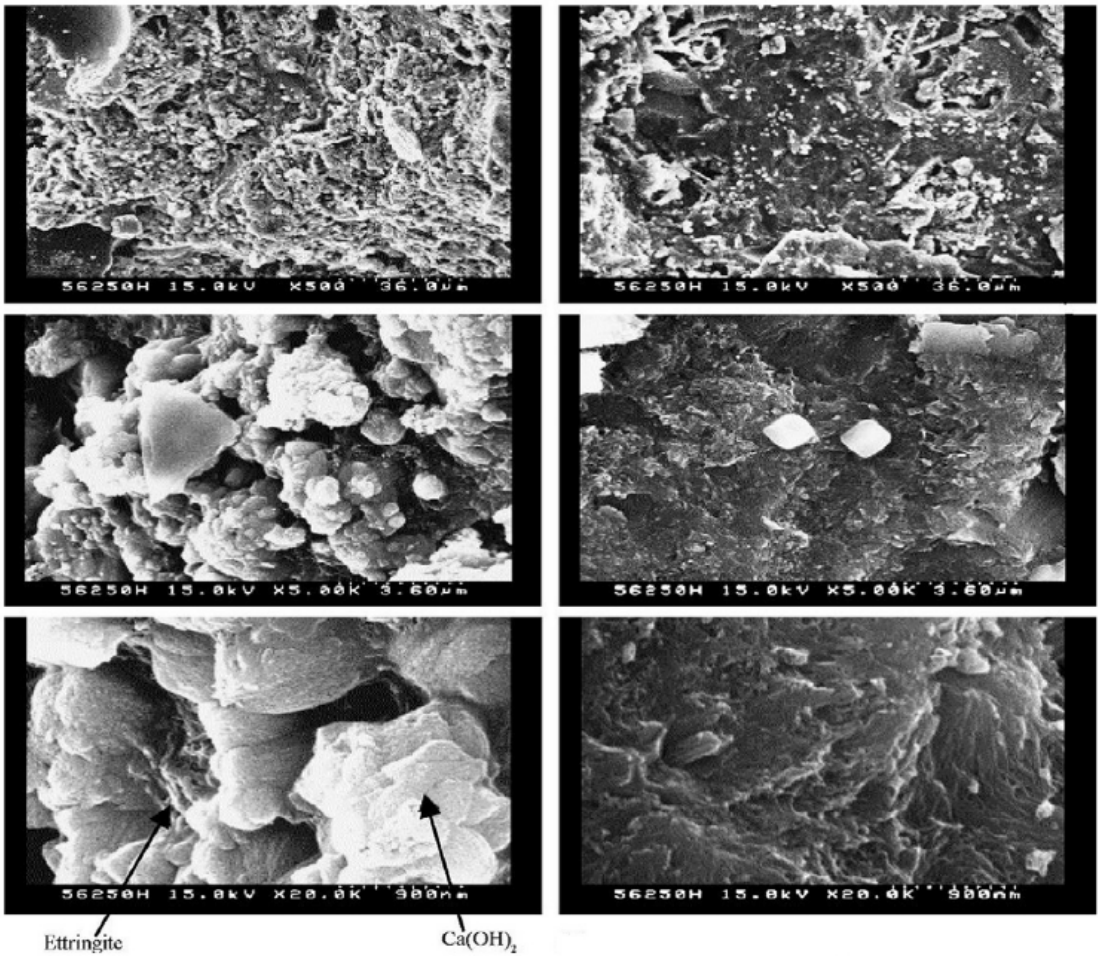

(A) OPC concrete (B) BFS (60%) concrete

Figure 3.2 SEM micrograph [1]

in more impermeable concrete [102, 103]. The porosity of slag cement is similar to that of PC at the early stages of reaction.

The volume of tiny pores in the nanoscale region increases with increasing age and during slag reaction [104]. The use of a high BFS replacement % results in a denser concrete structure that resists water penetration. In addition, BFS incorporation influences the concrete's compressive strength and shrinkage (swelling). Increased C-S-H content indicates a higher BFS replacement % and higher concrete strength and durability, resulting in a denser microstructure or reduced porosity.

Using the mercury intrusion porosimetry (MIP) test [101] , investigated pore size distribution due to slag replacement rate and curing environment. In their investigation, the BFS replacement amounts were 50% and 65%. At 28 and 180 days, the porosimetry test was performed and found that extended exposure to a drying environment increased pore volume in all sizes of pores and that this increase was increased when the slag replacement amount was set at 65%. Thus, slag concretes had a considerably more refined pore structure than OPC concretes. There is insufficient lime generated at high replacement levels to continue the reaction with the slag; this, of course, is related to a lack of moisture to enable continuous interaction between water and PC. SEM micrographs (**Figure 3.2**) of BFS (60%) concrete and OPC specimens were compared [1]. In a hardened cementitious material, BFS changes the products and pore structure. In OPC specimens, they discovered a lot of calcium hydroxides and large capillary pores (0.05-60 mm). In BFS concrete specimens, however, needle shaped ettringites were uncommon. The evaluated the impact of SCMs on the engineering characteristics of HSC with a 28 days cube compressive strength of more than 80 MPa [105]. The porosity and pore size distribution of HSC containing various SCMs was one of the studied characteristics. Porosity was measured in percent, median, and average pore sizes were calculated in nanometers using the MIP test. The BFS decreased the porosity, median, and average pore size of the high strength mortars.

In terms of pore size, the BFS had a widespread impact of reducing the mean pore size and average pore size of the high strength mortars considerably. They also discovered that BFS and other SCMs changed the high strength mortars' pore size distribution toward a more even distribution. In addition, the calcium hydroxide is converted into secondary C-S-H gel due to the pozzolanic reaction, which is thought to improve the pore structure by converting coarser pores into finer ones.

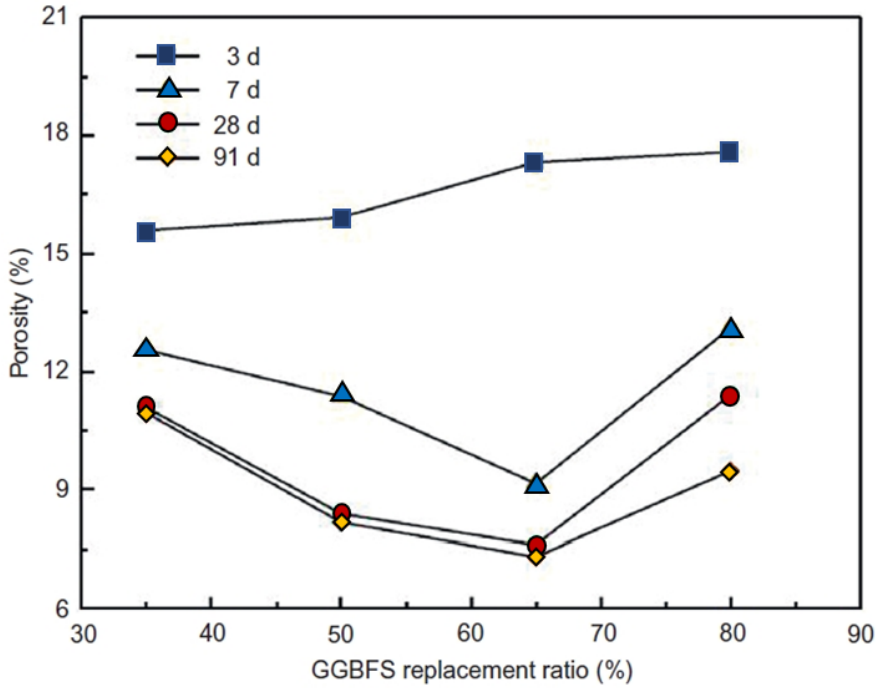

Figure 3.3 Total porosities of the specimens as a function of BFS replacement ratio [4]

The reactivity of BFS is reported to start developing 2-3 to discovered that threshold pore sizes decreased. The hydration products mainly originated from the hydration of cement particles since BFS did not actively contribute to the reaction until it was three days old [4]. However, as individuals become aged, the hydration products that are produced get more complicated. The pore blocking impact of the BFS latent hydraulic response then reduced the threshold pore diameter.

3.7.5 Water absorption

Water absorption is a good instrument for evaluating concrete's resistance to aggressive environments because the water flow in concrete has a significant impact on its durability [106]. In addition, the structural pores (interlayer C-S-H), porous paste, and aggregate interface zone are related to water absorption, especially in the early stages. To investigate the influence of slag on water absorption for roller compacted concrete (RCC) compositions and conducted a water absorption test utilizing cubic specimens 150×150×150 mm^3 in size [78].

The specimens were cured in water for 28 days before being evaluated according to ASTM C642-97 [107], which indicated that water absorption decreased as the slag

replacement ratio increased in the mix designs with 12% and 15% BFS, compared to the reference specimens. Furthermore, increasing the cementitious components from 12% to 15% decreased water absorption across the range in all mix compositions [106]. To utilized ASTM C642-97 to conduct a 365 days water absorption test on a 150 mm SCC cube [107]. Their findings show that when the proportion of iron slag (IS) in a concrete mixture grows, the percentage of water absorption reduces in all concrete mixtures and that this is also true in the case of curing age, where water absorption decreases as time passes.

Furthermore, when the IS concentration increased, water absorption reduced, indicating that the concrete became denser. To examined the characteristics of hardened concretes and mortars under sulfate attack utilizing Algerian low activity slag as a cement replacement [108]. The water capillary absorption test revealed that the coefficient decreased with curing age and W/B ratio in their experimental program. At the age of 90 days, they found a modest decrease in the sportively coefficient for concretes containing BFS, particularly for concrete mixture B50 (50 percent of cement replaced by BFS) and used CEM-I 42, 5 N to make concrete mixes and evaluated the specimens after 28 days [109]. BFS was ground to a specific surface area of 500 m^2/kg in a laboratory mill. The replacement rates for BFS were 20%, 30%, and 40%, respectively. They discovered that incorporating BFS into concrete mixes was quite efficient in reducing capillary water absorption. For example, concrete with a 40% BFS reduced capillary water absorption by 40% compared to the reference mixture.

3.8 Durability properties of concrete containing BFS

3.8.1 Permeability

The ease with which a fluid under pressure might flow through a solid is characterized as permeability. There is no use in suggesting that the size and continuity of the pores in a solid's microstructure determine its permeability [59]. Instead, it is regarded as a fundamental material characteristic controlling the durability of concrete, particularly in buildings exposed to extreme conditions [110]. Many factors influence concrete permeability, including mix proportions, compaction and curing, microcracks, and humidity cycles large pores in concrete affect compressive strength and

permeability the most. Due to the reaction of BFS with the calcium hydroxide and alkalis produced during PC hydration, BFS increases the pore diameters and significantly decreases the permeability of concrete [93].

According to the literature, BFS can reduce the permeability of ordinary concrete significantly. The significant consequence of SCMs such as BFS on the pore structure of concrete is the decrease of large pores through hydration product absorption. The conversion of continuous pores to discontinuous pores significantly impacts concrete permeability (ACI 234R-96). To examined the effect of replacing OPC with BFS in concrete specimens by 40% and 60% [111]. They discovered that as the BFS replacement values were increased, the permeability values decreased.

Furthermore, their research revealed that using replacement BFS resulted in a denser concrete construction. The decrease in chloride ion permeability of concrete containing BFS which change in the pore structure of the hydrated cementitious system according to [112]. Water permeability and chloride ion permeability of concretes, including BFS, were studied from 0% to 60% replacement ratio with a 20% increasing rate [113]. They concluded that OPC concrete had the most significant total charged discharged, which they characterized as moderate chloride ion permeable concrete. BFS comprised concretes, which reduced chloride ion permeability by 20%, 40%, and 60%, respectively. Chloride ions became less permeable with mineral admixtures, and concrete with chloride ion permeability of 20%, 40%, and 60% BFS was included. It was also discovered that using BFS reduced water penetration depth from 26 mm (which is typical of PC concrete) to 14 mm. However, they did not discover a significant difference between concrete water penetration depth and the BFS replacement level [114]. In their investigation, up to 60% of PCs were replaced with BFS, also investigating the implications of the W/B ratio. They discovered that changing the W/B ratios did not influence the gas permeability effect of BFS inclusion. The gas permeability coefficient increased by 30% when BFS was replaced with cement at a W/B ratio of 0.30. To use a preconditioned cylindrical specimen with a diameter of 150 mm and a length of 50 mm to determine the nitrogen permeability of various concrete mixes after 90 days [108].

At the ages of 28 and 90 days, the gas permeability of concrete mixes with a W/B ratio of 0.65 rises with increasing BFS content as cement replacement. The gas permeability coefficients of concrete mixes containing 15% and 30% BFS were comparable. The inclusion of 50% BFS, on the other hand, lowered the gas permeability

somewhat. Compared to OPC paste without BFS, the pore size of cement matrices containing 50-65% BFS was significantly reduced [101].

When utilized in binary systems, BFS decreased the water penetration depth compared to the reference mixture [115]. However, when combined with silica fume (SF) and class C, it performed much better. They observed that at both ages, all of the mixes, including BFS and other SCMs, had lower water penetration depths than the reference mixtures.

The implications of BFS on RCC durability were investigated as water absorption, permeability, and freeze-thaw cycles were all taken into consideration. For the minimal permeability of RCC, they suggested a 40% replacement ratio. Even when the air content of concrete is as low as 1.7%, concrete containing BFS and BFS has a high resistance to freeze and thaw [78].

3.8.2 Sulfate resistance

Sulfates are one of the most damaging environmental agents to concrete's long-term durability. Sulfates include sodium sulfate (Na_2SO_4), potassium sulfate (K_2SO_4), magnesium sulfate ($MgSO_4$), and calcium sulfate ($CaSO_4$), all of which are highly soluble salts. Sulfate salts are harmful to concrete whether they are present in high concentrations of a specific threshold level >1000 ppm. The development of expansive ettringite (AFt-phase) and gypsum is generally attributed to the sulfate attack [116]. Ettringite eventually transforms into C_4ASH_{18} monosulfate hydrate, which forms hexagonal-plate crystals in OPC pastes. Due to the apparent presence of monosulfate hydrate in PC concrete, it is resistant to sulfate attack. The rate of sulfate attack is determined by the quantity of calcium hydroxide and reactive alumina phases present, as well as permeability [117]. Sulfate resistance is affected mainly by C_3A, although C_4AF and CH can also influence sulfate resistance in low C_3A PCs [113].

In acidic sulfate conditions, gypsum formation produces expansion, spalling, and a loss of strength. The acidic environment aid in the progressive elimination of CH from the cement paste until it is completely depleted, encouraging C-S-H decomposition. On the $MgSO_4$ attack, Mg^{2+} and SO_4^{2-} react with CH on the surface to produce gypsum and brucite, producing a double layer. The decrease in alkalinity caused by $Mg(OH)_2$ insolubility causes more CA^{2+} to be released from C-S-H, resulting

in increased gypsum production and, eventually, C-S-H breakdown to non-cementitious MSH [118].

When sulfate attack proceeds, the disintegration of C-S-H in cement paste occurs more rapidly in cold environments, and it is more damaging when sulfates are associated with Mg^{2+} and low pH, since both contribute to C-S-H decomposition [119]. In addition, this attack produces a progressive softening of the concrete's surface and a slow inward migration. Finally, cement paste degrades into a non-cohesive material, resulting in particle loss [120]. As a result, sulfate assaults in concrete buildings can cause expansion, cracking, loss of strength, and disintegration. Sulfate attack in PC mortar and concrete can be reduced by decreasing mono-sulfur aluminate and calcium aluminate hydrates. In three ways, adding BFS to PC decreases sulfate attack:

1) BFS contains no C_3A; thus, adding it to concrete decreases the total amount of C_3A in the mix.
2) BFS interactions with $Ca(OH)_2$ in the concrete drastically diminish its presence, leaving significantly less $Ca(OH)_2$ to react and create ettringite.
3) BFS concrete has a considerably decreased permeability [106].

Many studies have shown that partially replacing PC with BFS improves the sulfate resistance of concrete considerably. The following paragraphs provide an overview of some of these studies.

The development of ettringite is the primary cause of sulfate deterioration in concrete, and the decreased level of calcium hydroxide produced by blended cement, including mineral additive, increases sulfate resistance [121]. Furthermore, the pore-blocking action of BFS hydration results in increased strength and decreased permeability, which, in addition to better binding and absorptive effects, improves BFS concrete's resistance to sulfate diffusion [122].

When BFS is used to replace PC partially, concrete's resistance to sulfate attack improves [123]. The impact of early curing conditions on the sulfate resistance of OPC concrete with BFS as a partial cement substitute [124]. BFS was used to replace 80 percent of the cement. Extensometers were used to obtain initial measurements for the specimens across each face after being cured in water for 28 days. The specimens were then immersed in a sulfate solution (7% Na_2SO_4 + 3%$MgSO_4$ by weight). Expand measurements were obtained after 47, 83, 152, 207, 337, 502, and 660 days in the sulfate solution.

SEM has been used to analyze cube specimens preserved in Na_2SO_4 or $MgSO_4$ solutions. For example, used a cement mixture that included 31% PC and 69% BFS [125]. They observed that sulfate attack induced the materials containing slag cement to crack and disintegrate rather than expand.

The investigated the sulfate resistance of FA, BFS, and SF mixed cement with four different PCs. Mortar cubes with a W/B ratio of 0.6 and a sand-to-binder ratio of 2.75 were produced [126]. After a 7 days soaking in water, specimens were submerged in three different solutions: 5% Na_2SO_4 solution, and 10% H_2SO_4. Their results reveal that cementitious materials' sulfate resistance was influenced by their composition and the pH of the external environment. BFS mixed cement showed improvement throughout a wide pH range when the replacement percentage was more than 60%.

Under tropical environment conditions [116], evaluated the progressive deterioration of concrete mixes containing various proportions of BFS and SF due to sulfate attack. Experimental variables have included w/b ratio (0.40 and 0.50), moisture curing duration (3, 7, and 28 days), and Blaine fineness of BFS (4500, 6000, and 8000 cm^2/g). The specimens were immersed in a 5%Na_2SO_4 solution for 32 weeks after a specified curing period (3, 7, or 28 days). Every two weeks, linear expansion measurements were taken. They employed concrete specimens produced with OPC and sulfate resistant PC as a reference. Regardless of the moist curing duration, the concrete mixes with a W/B of 0.50, including BFS (75% and 85%), exhibited increased resistance to sulfate attack than the control mixture. They also observed that the linear thermal expansion data and the reported flexural strength were strongly associated. The greater the complete expansion, the higher the reduced flexural strength, and vice versa.

The investigated the effect of a tiny proportion of calcium carbonate or calcium sulfate on the sulfate resistance of concrete containing BFS [127]. A W/B ratio of 0.5 was used to produce various concrete mixes. Over 6 years, wear rating, strength loss, and expansions were measured on specimens immersed in $MgSO_4$ (containing 1.5 percent SO_3 and Na_2SO_4 solutions (containing 1.5% and 2.4% SO_3). After 6 years in Na_2SO_4, the reference concrete (without BFS) had practically decomposed. At a higher amount of calcium sulfate addition, the severity of the assault was decreased. A similar situation was observed when calcium carbonate was introduced. The performance of BFS concretes in the magnesium solution was not as good as in the sodium solution. 70% of BFS concretes, on the other hand, were more resistant than 60%.

Furthermore, increasing the amount of calcium sulfate and decreasing the amount of calcium carbonate reduced the degree of the attack. In all solutions, rapid expansion was seen on PC concrete specimens. The 70% BFS and specimens containing calcium sulfate or carbonate in sodium sulfate solutions showed modest expansions. Magnesium sulfate, on the other hand, showed more rapid and severe expansions.

Concretes produced with 70% BFS and 30% PC and low-quality carbonate aggregates performed poorly at both 5 °C and 20 °C sulfate solution temperatures. However, conventional sulfate assault and the thaumasite type of sulfate attack improve with an initial air cure. In addition, they discovered that air-cured concretes containing 70% BFS exhibited no attack after 6 years, even when exposed to the highest sulfate solution [127].

The developed blended cement containing 10%, 20%, and 30% BFS and investigated compressive strength changes in concrete specimens prepared with this blended cement during immersion in a 5% sodium sulfate solution [128]. In the sulfate environment, the mixed cement performed better than the control PCs. Furthermore, the decrease in strength attributable to sulfate action was reduced as the mineral admixture utilized increased.

The investigated the influence of Algerian low activity slag as a substitute for cement on the durability of mortars subjected to sulfate assault in an experimental investigation. They used mortar specimens submerged in 5% Na_2SO_4 and 5% $MgSO_4$ solutions to assess expansion. The binder consisted of OPC cement and various rates of BFS, and the W/B ratio was 0.5 (0 %, 10 %, 20 %, 30 %, 50 %, and 60 %). The expansion of mortars maintained in the two sulfate solutions is reduced when BFS is included in the cement. In addition, when the replacement ratio of low reactivity BFS is greater than 30%, the mortar's efficiency against sulfate assaults is significantly improved. In the magnesium sulfate solution, slag cement resistance was lower than in the sodium sulfate solution [108].

3.8.3 Alkali-silica reaction

ASR is a chemical reaction that occurs in concrete between the alkali pore fluids in the concrete and siliceous components of the aggregate particles. ASR forms a hydrophilic gel. The amount of gel depends on the amount and type of reactive silica and the alkali hydroxide concentration in the concrete pore solution. Reaction products

from ASR have an excellent affinity for moisture. As it absorbs moisture, it increases in volume, thus generating pressures sufficient to disrupt the fabric of the concrete. Once the pressure is larger than the tensile strength of concrete, cracks occur and lead to additional water permeation through migration and gel swelling. The reaction may be considered to progress according to the following idealized equations [129]:

$$4SiO_2 + 2NaOH = Na_2SiO_4O_9 + H_2O \quad (3.3)$$

$$SiO_2 + 2NaOH = Na_2Si_3O_9 + H_2O \quad (3.4)$$

The ASR cannot proceed in concrete if the alkali concentration is below a particular threshold value. In order to assess the total alkalis, present in cement or concrete, it has become a standard practice to express the alkali content in terms of "sodium equivalent" [130]. The great majority of concrete structures reported as showing deterioration due to ASR were made using high-alkali cement. OPC will generally contain a small proportion of sodium and potassium present as sulfates and double sulfates $(K,Na)SO_4$, which tend to coat other clinker minerals and as minor constituents in the other cement minerals [131]. Therefore, BFS could be very useful in controlling ASR. The ASR restraining effect of BFS is considered mainly due to the dilution of alkalis, the fixation of alkalis by slag hydrate, and the slowdown of moving speeds of water and alkali ions by an increase in density of the structure of hydrate [42, 99].

The possibility of an alkali-aggregate reaction (AAR) is much higher than conventional concrete because of the high-alkali content in HSC. The effect of BFS on the AAR in HSC. Alkali-aggregate reactivity test on aggregate and alkali-aggregate reactivity test using concrete were conducted to investigate the inhibiting effect of BFS for HSC [132]. Three types of BFS with a fineness of 4000, 6000, and 8000 cm^2/g were used. These were used in 0%, 30%, 45%, or 60% of cement. They observed that while the replacement ratio is increasing, expansion coefficients are decreasing. This result indicates inhibiting effect of BFS. Also, the fineness of BFS had a significant effect on this inhabitation.

Some researchers mentioned parameters such as the nature of the BFS, the alkali content of cement, and the reactivity of aggregate greatly influencing ASR expansions [133, 134]. For instance, to tested both concrete and mortar bar specimens containing

up to 65% BFS for the efficiency of ASR expansion control. They found that BFS effectively delayed the final expansion at 2 years in concrete specimens, including alkali-silica reactive aggregates. They also found that the ASR expansions depended on the amount of alkali and the nature of the aggregate. On the other hand, there was no significant difference in behavior irrespective of aggregate type or alkali load, indicating that the alkali level of the slag was not a contributory factor at the 50% replacement level [135].

The literature suggests that up to a 50% replacement of standard PC is required to counteract the effects of ASR depending on aggregate reactivity. This requirement was confirmed by ASTM C1260 accelerated mortar bar tests performed on Millar's Pit aggregates, where 50% slag mixture did not exceed 0.10% even after 49 days [136]. The amount of slag required to mitigate ASR for slag cement depends on the reactivity of the aggregate and the alkali contributed by the PC. The amount of slag required with a particular reactive aggregate can be determined by testing various slag aggregate combinations in the accelerated mortar bar or concrete prism tests. SCA generally recommends the ranges from 30% to 60% by mass of total cementitious material. The ACI guide [137] indicates that a minimum of 40% cement replacement with BFS is needed to control ASR. In total, 50% is suggested as the minimum amount of slag to mitigate ASR with higher alkali cement [138]. However, it was stated in a project report prepared by Delaware Center for Transportation [139] that a 50% level could present construction difficulties concerning low early strength.

The investigated the ASR of concrete containing 50% and 65% slag [101]. They used a high alkali PC with 1% sodium oxide and slag with 0.53% sodium oxide equivalent. According to test results, continued exposure to a hot and humid regime resulted in increasing expansion. The concrete incorporating 50% slag showed higher expansions than the concrete incorporating 65% slag at corresponding ages. However, concretes with 65% slag replacement reached higher expansion than concretes with 50% slag in case of subsequent exposure to the hot and humid environment.

To realize an outdoor exposure demonstration to show the long term effectiveness of a variety of SCMs at deleterious expansion with a highly alkali silica reactive aggregate and to provide a correlation between short term laboratory tests and long term performance [136].

3.8.4 Corrosion and chloride binding capacity

The corrosion of reinforcement in concrete adversely affects the structural response of buildings and other structural systems. Its principal effects are decreases in load bearing capacity of members due to loss in diameter of reinforcement steel, impairment of bond between rebar and surrounding concrete, the modification of the constitutive relationship of the corroded reinforcement in terms of stress strain relationship and fatigue resistance, and anchorage of reinforcement steel bars. The most severe deterioration mechanism is the penetration of chloride ions into concrete, leading to rebar corrosion. Corrosion can impair the structural performance of an RC structure essentially. At ultimate conditions, corrosion, other than reducing the load bearing capacity, could also be responsible for modifications to the collapse mechanism [68, 140]. Previous studies have shown that cement replacement materials such as SF, FA, and BFS may reduce the rebar corrosion probability significantly. Since a high volume of BFS concrete can reduce chloride ingress, many coastal and marine structures were constructed from BFS concrete in the world [50, 92, 141-143].

The small pore size decreases the penetration and diffusion of chloride ions in concrete. BFS makes the cement matrix denser and diminishes the pore size. The average pore size of OPC concrete was 1.57-2 times larger than that of BFS concrete [144].

The critical chloride content can be defined as the chloride content required for the de passivation of the steel. There is still a debate on determining the critical chloride content in terms of free or total chlorides [145]. According to Glass and Reddy's work [35, 146, 147], total chloride content should be considered because bound chlorides present a corrosion risk acting as a reservoir of chloride that might dissolve at altered pH conditions. The difference between the quantity of total chloride and free chloride is referred to as bound chloride. Chloride binding by cement based materials is very complex and influenced by many factors. SCMs are one of the factors of them. The chloride binding capacity strongly depends on the amount of C-S-H gel in the concrete [148]. Slag cement enhances the formation of more gel, thereby offering a larger surface area available for adsorption. The formation of Friedel's salt plays a significant role in chloride binding in OPC concrete [87]. In addition, chloride binding capacity depends on the pH value or OH_2 concentration in the pore solution of concrete.

The much lower chloride ion concentration can be achieved according to accelerated chloride ion diffusion test results if higher volumes of BFS are added [92]. They compared Type I cement with Type V cement and Type I cement, showing a lower diffusion coefficient. Type I cement containing 9.5% C_3A by weight binds almost 1.6 times more chloride than the cement that contains 2.8% C_3A. Therefore, the resistance to rebar corrosion is better in Type I cement with a higher amount of BFS.

The ability of BFS to protect against chloride induced corrosion is attributed to the effective binding of free chloride ions [149]. BFS pastes have a higher chloride binding capacity than the PC control, and the difference increases with increasing BFS replacement level [150]. As the replacement level increases, the chloride binding capacity also increases for all chloride concentrations. For a BFS replacement level of 66.7%, the chloride binding capacity is around 5 times that of the PC control for the case of 5 mol/L exposure concentration. The high aluminate levels present in BFS are most likely to be responsible for its good binding characteristics. There is generally a good correlation between C_3A content and chloride binding capacity. One mechanism of chloride binding is known to be the formation of Friedel's salt due to a relatively sizeable Al_2O_3 content in the BFS. The attributed this capability to the increased formation of Friedel's salt due to the alumina present in the slag [150]. The second mechanism of chloride binding: the formation of hydrotalcite responsible for the superior chloride binding ability of BFS concrete [149].

Hydrotalcite belongs to the family of layered double hydroxide and is known as anionic clay capable of adsorbing chloride ions from surrounding environments due to its distinctive anion exchange property [151]. The formation of hydrotalcite during hydration is due primarily to a significant amount of magnesia in BFS. They concluded that the hydrotalcite adsorbs many chloride ions, and its structure remained unchanged when it adsorbs chloride ions. Hydrotalcite is the most abundant of the crystalline phases [149], and its crystalline proportion is more than five times that of Friedel's salt in alkali activated BFS [151]. The hydrotalcite is the most likely hydration development in BFS responsible for the remarkable improvement in chloride binding. They also concluded that free chloride content in BFS pastes significantly reduced compared with its content in an OPC paste [152]. Accordingly, the admixed chlorides are most likely attached to the interlayers of hydration products, and these attached chlorides are not readily available to be dissolved if the conditions for such dissolution existed.

The results show that the resistivity of concrete increases with the increasing content of cement replacement materials such as BFS at a 60% replacement level. Also, they concluded that the replacement of cement by up to 40% BFS has no significant influence on rebar corrosion. However, some researchers found high corrosion resistance in replacement ratios lower than 40% [153-155].

3.8.5 Pore size distribution

BFS can be effectively used to considerably reduce the pore size and cumulative pore volume, leading to more impermeable concrete [102, 103]. A high BFS replacement percentage results in a denser concrete structure, preventing water from penetrating concrete. The compressive strength and shrinkage/swelling of concrete are also affected by BFS inclusion. A denser microstructure or lower porosity results from a higher calcium-silicate-hydrate (C-S-H) content, corresponding to a higher BFS replacement percentage and higher strength and durability of concrete. The effects of the slag replacement level and the curing environment on the pore size distribution by mercury intrusion porosimetry (MIP) [101]. The BFS replacement levels used in their study were 50% and 65%. In the porosimetry test, prolonged exposure to a drying environment increased the volume of pores of all sizes, and BFS enhanced this increase at a 65% slag replacement level.

The intruded pore volume per volume of paste in the mortar increases as the replacement level increases because a small pore size decreases the penetration and diffusion of chloride ions in concrete. Thus, the results confirmed that the immobilization performance could be significantly improved by increasing the basicity. Furthermore, the pore distribution impacted by this testing might consist of pores in only the paste, with impacts on the water ratio, fissures, and bond cracks at the aggregate paste interface [6, 9].

Moisture in concrete significantly affects the durability of concrete as it relates to structural pores in areas such as the C-S-H gel, porous paste, and aggregate interface zone, especially in the initial stage of curing. Additionally, physical adsorption of chloride resulting from C-S-H gel can also contribute to chloride immobilization [106].

Friedel's salt formation from the reaction of monosulfate (AFm) with chloride ions is the mechanism of concrete degradation due to chloride ion ingress and carbonation. In addition, the dissolution of chloride ions immobilized in Friedel's salt

into the pore solution and an increase in the concentration of chloride ions in the pore solution resulted in the further ingress of chloride ions into the concrete through concentration and diffusion cycles.

Friedel's salt (FS) and Kuzel's salt (KS) are produced from chemically bound chloride ions, whereas physical adsorption mainly consists of chloride adsorption on the surface of C-S-H gel via electrical double layers. Moreover, migration resistance achieved by refining the pore structure to block the channel is another way to hinder chloride ion transport. Therefore, the mechanism of chloride immobilization can be defined as chemical binding, physical adsorption, and migration resistance [156-160].

3.8.6 Penetration property

The alkali-silica reaction (ASR) in concrete forms a hydrophilic gel depending on the amount and type of reactive silica, and the alkali hydroxide concentration in the concrete pore solution may progress according to the following idealized equations [129]:

$$H_4SiO_4 + 2Na(OH) \rightarrow Na_2H_2SiO_4 + 2H_2O \quad (3.5)$$

The effect of BFS as an ASR limiter has been considered to mainly involve alkalis, the fixation of alkalis by slag hydrate, and the retardation of water and alkali ion movement by an increase in the density of the hydrate structure [42, 99]. The probability of an ASR occurring is much higher in BFS containing concrete than in conventional concrete because of the high alkali content in HSC. The effect of BFS on the ASR in HSCs. Alkali-aggregate reactivity tests using concrete were conducted to investigate the inhibitory effect of BFS on HSC [132]. Three types of BFS with a fineness of 4000, 6000, and 8000 cm^2/g were used to replace 0%, 30%, 45%, or 60% of the cement. They observed that as the replacement ratio increased, the expansion coefficients decreased. This result indicates the inhibitory effect of BFS. Additionally, the fineness of BFS had a significant effect on this inhibition. A preliminary review [133, 134] mentioned that parameters such as the nature of the BFS, the alkali content of cement, and the aggregate reactivity greatly influence ASR expansions.

The most severe deterioration is from the penetration of chloride ions into concrete, leading to rebar corrosion. Corrosion could essentially impair the structural performance of an RC structure. A few studies [50, 92, 141-143] have discussed that

using cement replacement materials such as SF, FA, and BFS may significantly reduce the rebar corrosion probability. The small pore size decreases the penetration and diffusion of chloride ions in concrete, chloride binding capacity strongly depends on the amount of C-S-H gel in the concrete [148]. The significant effect of the formation of Friedel's salt on the chloride binding in OPC concrete depends on the pH or OH_2 concentration in the pore solution of concrete [87].

The performed accelerated chloride ion diffusion tests and found that a much lower chloride ion concentration can be achieved if higher volumes of BFS are added. One mechanism of chloride binding is the formation of Friedel's salt via the Al_2O_3 in BFS [92]. The attributed this binding to the increased formation of Friedel's salt from the alumina present in the slag [150].

The crystallinity of concrete is more than five times that of Friedel's salt in alkali activated BFS, and abundant crystalline phases can be found in hydrotalcite [151, 152, 161]. Therefore, increases in the chloride resistance of concrete increase the compressive strength of concrete. The modification of hydrates and pore structures, the formation of dense transition zones surrounding aggregate particles, and filler effects are possible mechanisms for improving the chloride resistance of BFS containing concrete.

3.9 Summary of durability against chloride attach

A literature review reveals many studies of BFS containing concrete in various countries. However, few studies have examined its use in reducing chloride ion permeability as the main factor of corrosion reactions. Thus, this study utilizes BFS as cement to investigate the performance of concrete in terms of delaying chloride ion penetration, which affects corrosion reactions.

Furthermore, an experiment was conducted to examine improvements in the performance of an alternative concrete using BFS as cement replacement, focusing on chloride diffusion on concrete with BFS. This study aims to develop products for use in the precast concrete industry toward extending the life of concrete structures, especially reinforced concrete structures, in marine environments.

Chapter 4

Methodology

4.1 Introduction

The properties of concrete using BFS as a binder are investigated in this study. The experiments focused on the properties of concrete, such as compressive strength and diffusion of chloride ions, and resistance to chloride ions. The experimental results show that when BFS is used in concrete, it improves the durability properties of concrete.

4.2 Materials used and Proportions

The cement used in this experiment was OPC, which is denoted as N with a density of 3.16 g/cm^3 and Blaine size of 3300 cm^2/g, as shown in **Table 4.1**. Material properties include fine aggregate, river sand (density in saturated surface dry condition: 2.64 g/cm^3, water absorption: 1.98%), BFS. N contained 2.41% of SO_3. By contrast, BFS does not contain SO_3, so it was added in amounts equivalent to N. The purpose of the replacement was to unify the initial strength to allow for the hydration reaction to occur (to prevent false condensation), as the amount of SO_3 was more extensive, which supported early strength and decreased shrinkage. In addition, this study used BFS with a fineness of 3000, 4000, and 6000 cm^2/g, (density of 2.91 g/cm^3) to replace OPC at 22.5% and 45% by weight. The proportion of cement mortar with water binder ratio (W/B) of 0.50 was prepared. **Table 4.2** shows the mixed proportions of mortar as the 7 symbols should be explained by 6 symbols' 3000-22.5', '3000-45', '4000-22.5', '4000-45', '6000-22.5', and '6000-45' mean as 3 different conditions of Blaine value of BFS by 2 different condition of cement replacement and 'N' for Normal concrete as reference. For example, 3000-22.5 was the mean for which specimen used BFS by 6000 Blaine value, and cement replacement was 22.5%. The testing was for general mechanical properties by the compressive strength was used in 3 specimens; moreover, the other testing was conducted by 2 specimens for each experiment.

Table 4.1 Material properties

Abbreviations	**Properties**		**Density (g/cm^3)**
OPC	Ordinary Portland cement		3.16
BFS	Blast furnace slag		2.90
	Commercial name	Actual Blaine value	
	3000	3,090cm^2/g	
	4000	4,350cm^2/g	
	6000	6,490cm^2/g	
S	Sand		2.64
AG	Anhydrous gypsum (Sulfur trioxide: 56.5%)		2.91
W	Water		1.00

Table 4.2 Mixed proportions

Symbol	**W/B**	**Unit Weight (kg/m^3)**						
		W	**OPC**	**BFS (Blaine Value)**			**AG**	**S**
				3000	**4000**	**6000**		
N	50%	318	636					1272
3000-22.5			493	143			6.2	
3000-45.0			350	268			12.4	
4000-22.5			493		143		6.2	
4000-45.0			350		268		12.4	
6000-22.5			493			143	6.2	
6000-45.0			350			268	12.4	

* W/B: water binder ratio

Several studies have shown that decreasing the W/B ratio and incorporating various pozzolanic minerals can increase compressive strength, durability, and

permeability [17]. Lowering the W/B decreases the porosity and chloride penetration by as much as 25% throughout the exposure period [18]. Silica fume (SF), including some of the mineral admixtures used, significantly decreased the chloride penetration into concrete in maritime conditions [19]. The influence of SF on concrete microstructure has been widely published.

4.3 Mixing method

Mixing was performed according to JIS R 5201, "Physical testing methods of cement" [162, 163]. The mixer used in this study, Hobart-type mixer, and method are shown in **Figure 4.1**.

First, cement and fine aggregate were mixed at low speed (low speed: 110 r/min) for 30 sec. Next, admixture and water were added and mixed at low speed for 60 sec and high speed (high speed: 230 r/min) for 30 sec, as shown in **Figure 4.1**.

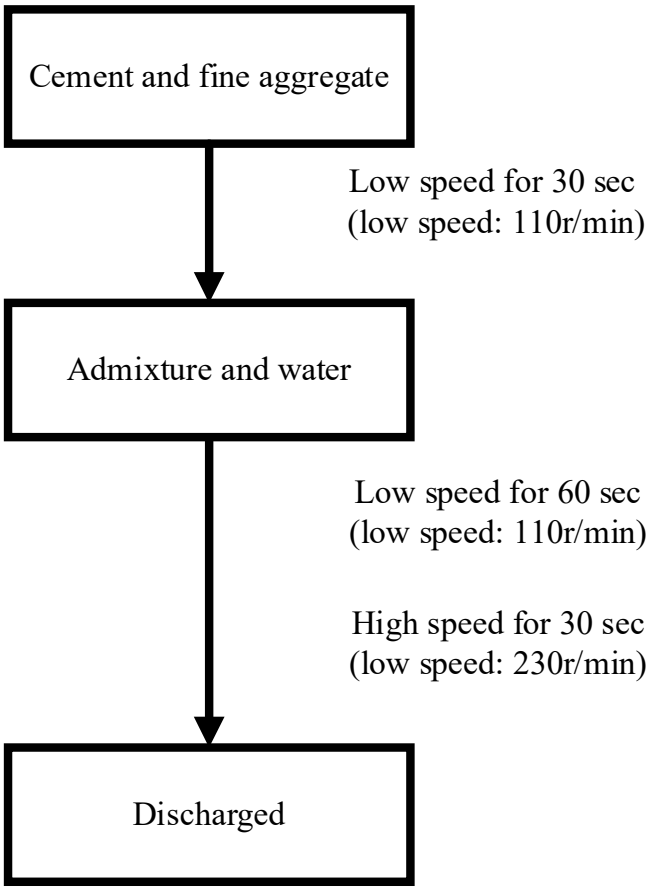

Figure 4.1 Mixing method

4.4 Curing conditions

Two different curing conditions were used: water curing and steam curing.

4.4.1 Water curing condition

Water curing was conducted in the water tank for 28 days after demolding, conducted at 7, 14, and 28 days. Curing was carried out in air under a constant 20 ℃ and 60% humidity.

4.4.2 Steam curing condition

Steam precuring was performed 2 hrs. in advance. The temperature was raised at 20 ℃/hr, held at 60 ℃ for 2 hrs, then lowered to 20 ℃ at 10 ℃/hr, as shown in **Figure 4.2**: (A) precuring time, 2 hrs. before steam curing; (B) temperature raised to 60 ℃ at 20 ℃/hr.; (℃) temperature was held at 60 ℃ for 2 hrs.; (D) temperature was lowered

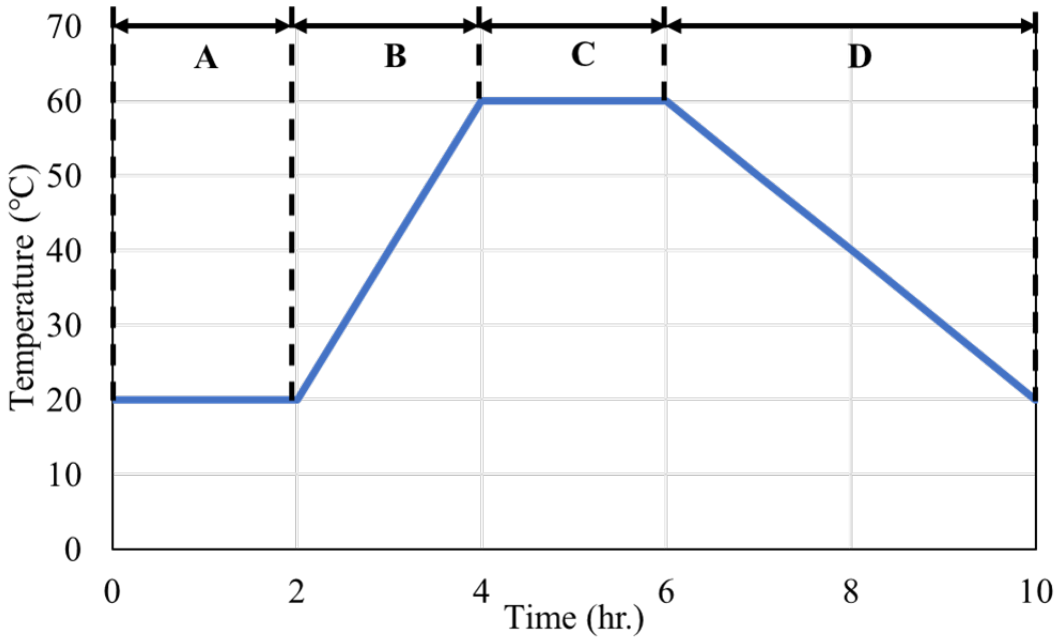

Figure 4.2 Diagram for steam curing 1st condition

to 20 ℃ at 10 ℃/hr., and was carried out for 28 days a constant 20 ℃ and 60% humidity. Curing was carried out in air under a constant 20 ℃ and 60% humidity. The sample was prepared with steam curing at 1, 7, 14, and 28 days.

The steam curing in another condition was different pre-preparation times as 0.5 and 3.0 hrs., and the temperature was maintained at a maximum temperature of 65℃ for 2 hrs., respectively. In addition, the de-mold was 24 hrs., and atmosphere curing was performed for 28 days in an environment at a temperature of 20℃ and a humidity of 60% as shown in **Figure 4.3**.

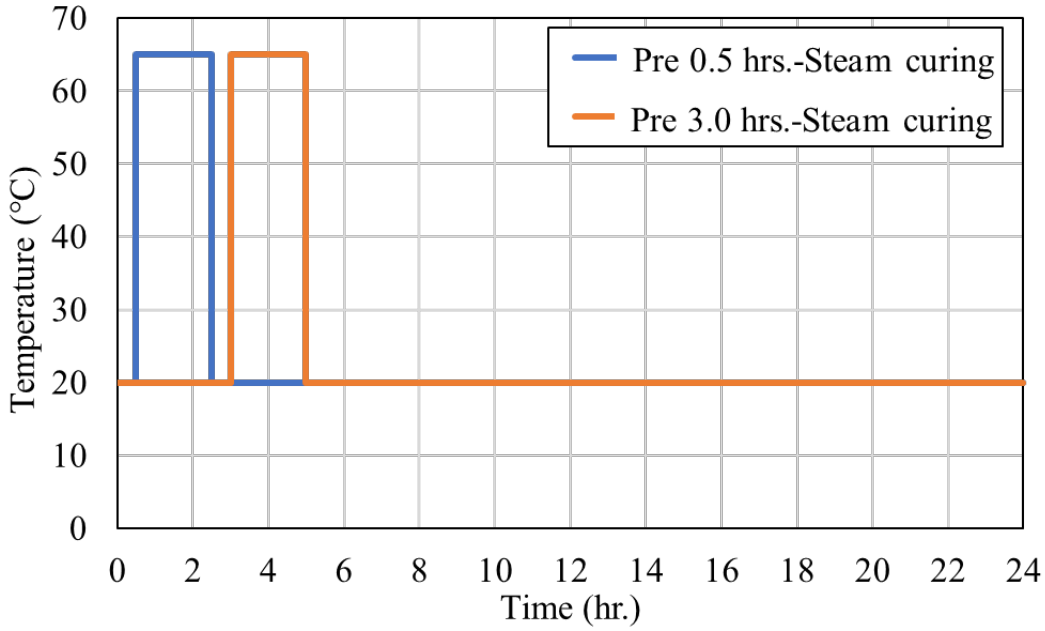

On the different pre-preparation times as 0.5 and 3.0 hrs

Figure 4.3 Diagram for steam curing 2nd condition

4.5 Performance testing of concrete

4.5.1 General mechanical properties

4.5.1.1 Hydration speed: Initial setting time testing

The setting time test is carried out by measuring the beginning and ending times of a standard soft cement paste in a mold at 20℃ and relative humidity of 90% or more. The starting time and ending time are measured by the Vicat needle device or automatic setting tester, and the cement paste is made by kneading machine, compressed into a mold, and the starting time and ending time are measured by Vicat needle device or automatic setting tester. The beginning time shows that the cement begins to harden

due to the hydration reaction, and the finishing time indicates that the hardening has progressed and the fluidity has vanished. The methodology as shown in **Figure 4.4.**

4.5.1.2 Compressive strength

Compressive strength test method. A 50×100 mm^2 summit mold was used for compressive strength testing. This concrete is poured into the mold and appropriately tempered so as not to have any voids. After 24 hrs., molds are removed. Since the sample was de-molded until the age of 28, the curing condition was done. The top surface of these specimen should be made even and smooth. The testing is done by placing cement paste and spreading smoothly on the whole area of the specimen. A compression testing machine tests these specimens after one day, seven days curing and 28 days curing. Load should be applied gradually at 13.7293 N/mm^2 per minute until

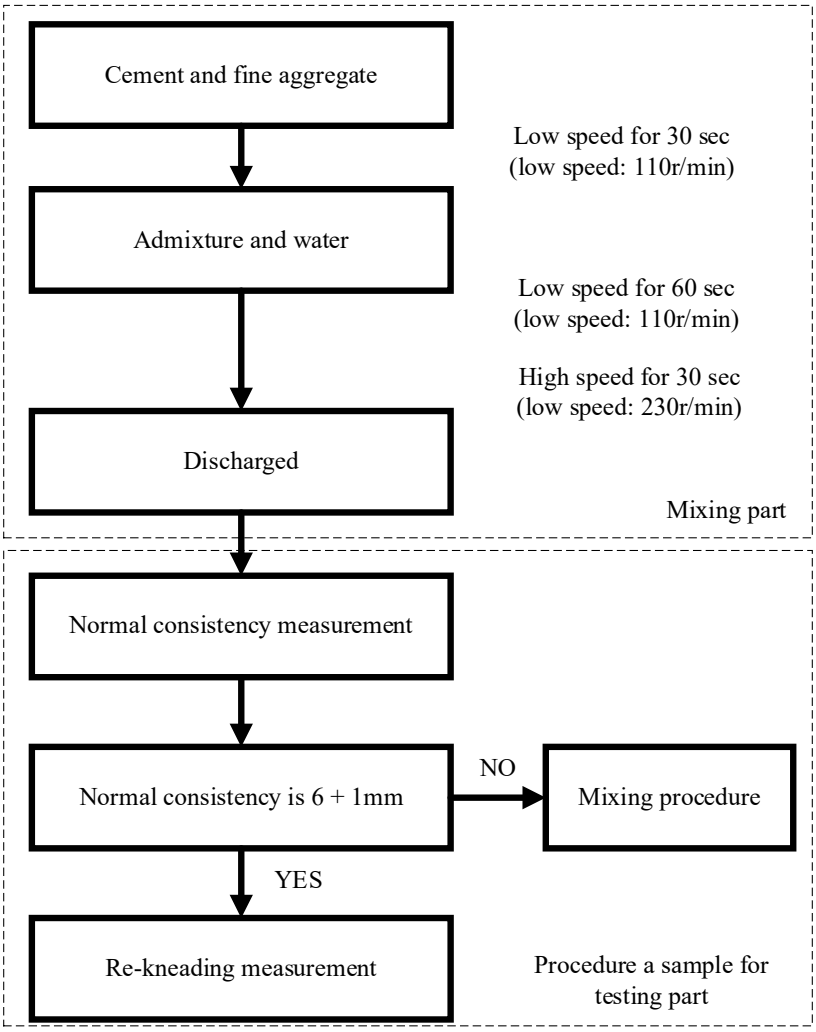

Figure 4.4 Initial setting time testing method

the specimens fail. Load at the failure divided by area of specimen gives the compressive strength of concrete.

4.5.1.3 Mercury Injection Porosimetry (MIP)

Mercury Injection Porosimetry (MIP) is used to evaluate the porosity, pore size distribution, and pore volume of various concrete and powder materials. The technique involves the intrusion of a high pressure, non wetting liquid (often mercury) into the material using an instrument known as a porosimeter. The device uses a pressurized chamber to force the mercury into the voids of a porous substrate. As pressure is applied, the mercury initially fills the large pores. As the pressure increases, the filling proceeds into increasingly smaller pores. Both interparticle pores (between individual particles) and intraparticle pores (within the particles themselves) could be characterized using this technique. To determine the pore size based on the external pressure required to push the liquid into the pores against the liquid's surface tension's opposite force. Since this technique is usually performed in a vacuum, the initial gas pressure is zero. Since mercury's contact angle with most solids is between 135℃ and 142℃, the method could take an average of 140℃ without significant error. The surface tension of mercury at 20℃ under vacuum is 480 mN/m. As the pressure increases, the cumulative pore volume also increases. It can find the pressure and pore size from the cumulative pore volume, which gives the median pore size by adding 50% of the total volume.

A measurement method with a wide pore measurement range was common to use the integrated pore volume distribution and $\frac{dV}{d \log D}$ with the horizontal axis on a logarithmic scale. However, when looking at the pore distribution in an incredibly narrow range, use the integrated pore volume distribution and $\frac{dV}{dD}$ with the abscissa on a linear scale to obtain a distribution when the specific surface area is essential shown in the result.

4.5.2 Durability against chloride ion attack

4.5.2.1 The rapid chloride ion penetration test (RCPT)

A protracted study period was required a standard salt damage penetration test determined the chloride ion diffusion coefficient. Therefore, retrenching the study time has become an issue, so chloride ions were measured by the rapid chloride ion

penetration test (RCPT). The significant diffusion coefficient was calculated as the chloride ion effective diffusion coefficient of mortar was based on the Japan Society of Civil Engineers standard in concrete by electrophoresis. The effective diffusion coefficient test method for chloride ions according to JSCE-G571-2003 measured [164].

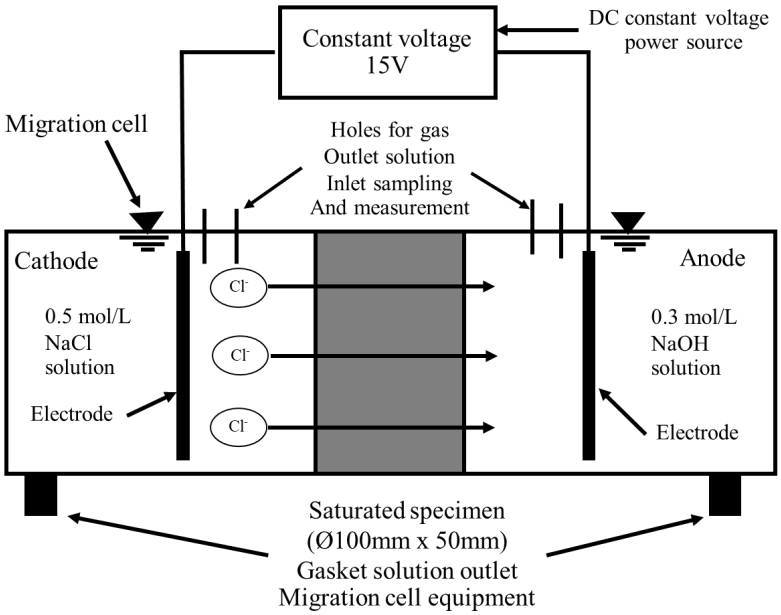

Figure 4.5 A typical schematic diagram of a migration test [3]

- Test Equipment

  The equipment used for migration testing (1) is as follows:

  Note (1): **Figure 4.5** gives a typical schematic diagram of a migration test.

a) The migration cell shall be manufactured of materials (3) resistant to the solution used in the test. A concrete specimen prepared according to the method given in Clause 6 (Test Specimens) of this standard shall separate the cathode and anode sections. The volume of the anode and cathode sections is approximately 1 liter. **Figure 4.6** give shape and size of a typical migration cell.

   Note (3): Transparent acrylic material is recommended.

b) The starting solution in the anode section shall be 0.5 mol/L of NaCl solution and in the cathode section 0.3 mol/L of NaOH solution, respectively (3).

   Note (3): The NaCl and NaOH shall be of quality similar to that specified in JIS K 8150 and JIS K 8576, respectively.

c) The DC constant voltage power supply shall be capable of applying a constant DC voltage with a precision of ±0.1V (4).

Note (4): The DC constant voltage power supply should have a 1 Amp rating.

The anode and cathode electrodes in the migration cell shall remain electrochemically stable for the duration of the test. The electrode material must not affect the experimental results. The electrodes shall be either circular or rectangular in

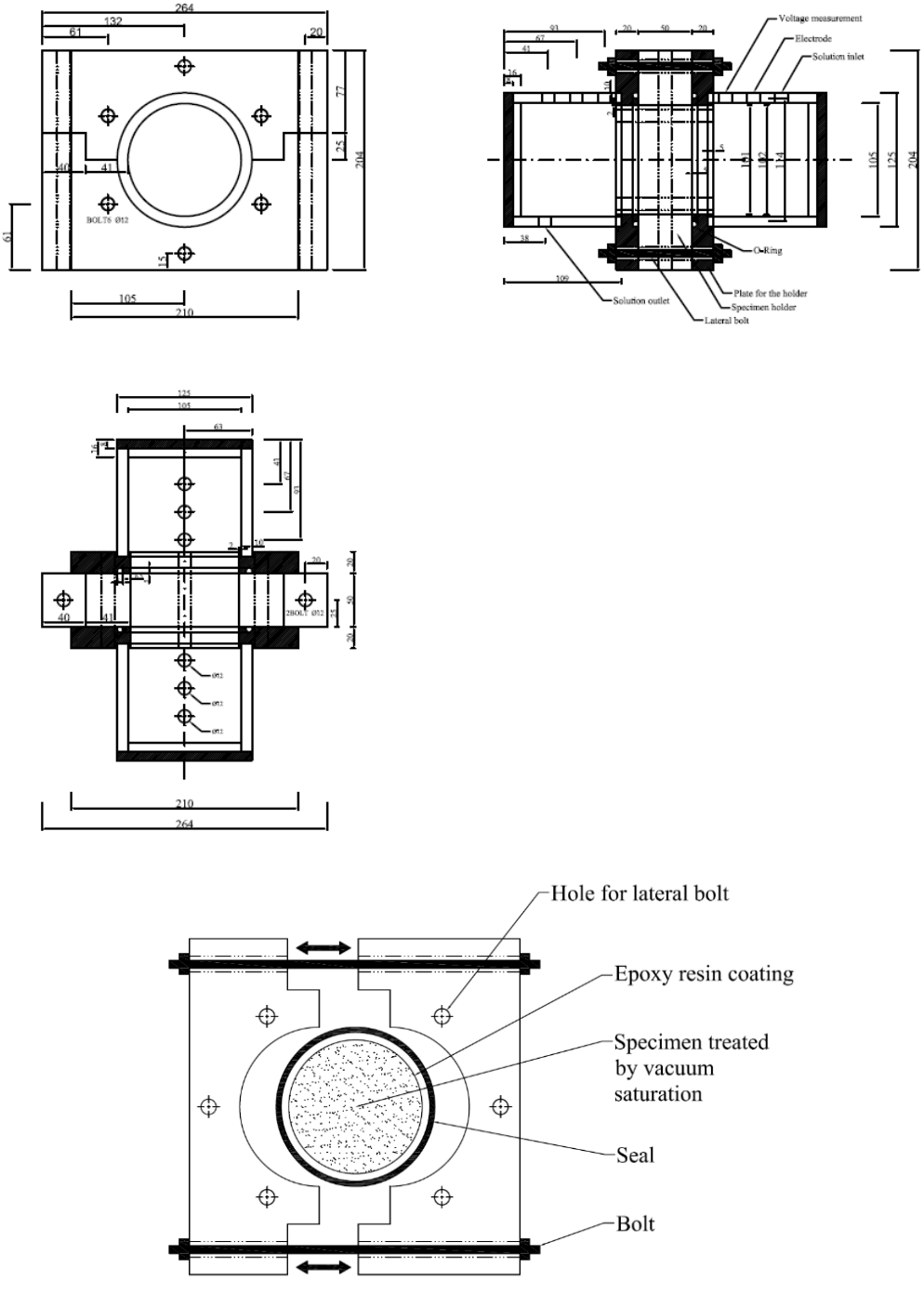

Figure 4.6 A shape and size of a typical migration cell [3]

shape, and their cross sectional area shall be at least 60% of the cross sectional area of concrete exposed to the cell solution.

Note (5): Stainless steel may be used for the cathode, while a carbon plate, titanium plate, or platinum plate is suitable for the anode. Carbon is consumed with the passage of time and therefore shall be renewed after a number of tests.

d) The thermocouple used to monitor temperature changes in the solution shall be watertight and resistant to the cell solution. It shall have a measurement range of approximately -10°C to ±110°C with a precision of ±1°C.

e) The potentiometer used to measure the actual potential gradient between the two concrete surfaces shall have a range of 0 to 99.9 V with precision of ±1%.

The electrophoresis test used a 0.5 mol/L sodium chloride solution and a stainless steel electrode on the cathode side, as shown in **Figure 4.6.**

The apparatus, a 0.3 mol/L sodium hydroxide solution, and a titanium electrode were used, and the specimen was placed between the electrodes. A DC constant voltage of 15 V was applied between the electrodes, and the solution on the cathode side had chloride ions below 0.45 mol/L. The solution was appropriately exchanged on the anode side so that chloride ions did not exceed 0.3 mmol/L. The specimen's shape was a cylinder with a 100 mm diameter and a thickness of 50 mm. When chloride ions on the cathode side penetrated the sample and reached the anode side, the number was the lead time.

Seven levels of specimens with different physical properties of BFS were prepared with different curing conditions. Production, water curing was 28 days, and steam curing was aerially curing for up to 28 days. Vacuum and wet inside after making the specimen, after vacuuming the inside of the sample using an aspirator, moisture treatment with distilled water energization applies DC constant voltage of 15 V measurement measure the chloride ion concentration of the cathode and anode every three days as show in **Figure 4.7**.

This study method assumes that the porosity in concrete is an electric field, and an external voltage applied causes chloride ions to have a negative charge to be electrically continuously transferred to the anode. Furthermore, the number of chloride ions that moved to the pole side and the penetrated chloride ions to the anode side were

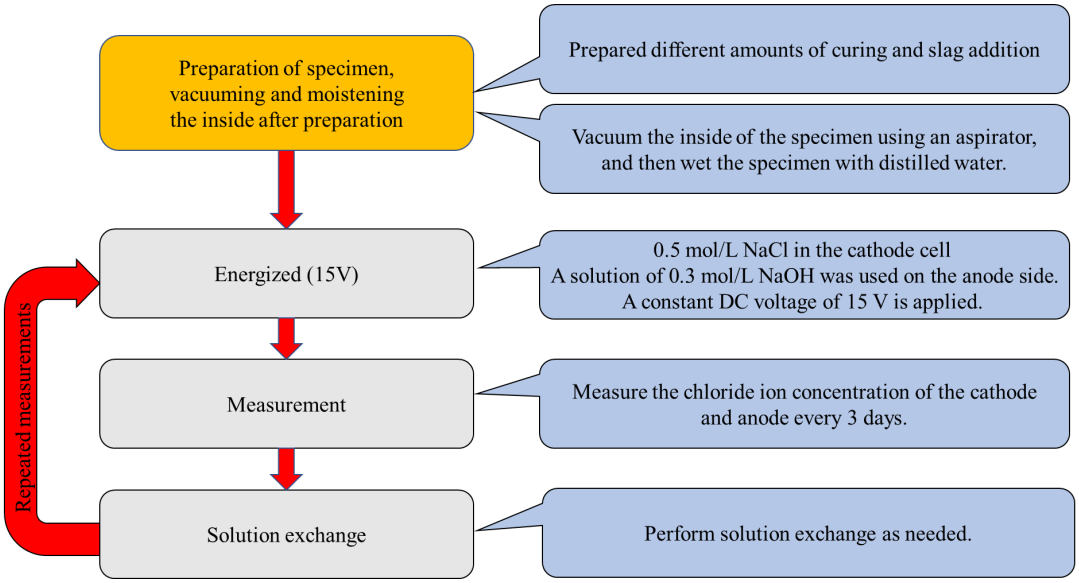

Figure 4.7 RCPT loop testing

steady. The flux of chloride ions, when considered, has to reach a state (ion per unit time and unit area). The amount of movement was used to calculate the diffusion coefficient. The steady state assumes that immobilization factors that affect electrophoresis can be excluded. Steady state judgment was made when the increasing rate of the chloride ion concentration on the anode side became constant with time. Additionally, chloride ions penetrating the steady state were required for the significant diffusion coefficient calculation.

Calculation of chloride ion flux.

The flux of chloride ions in the steady state is calculated using the following equation, and the value obtained is rounded to three significant digits.

$$J_{Cl} = \frac{V^{II}}{A} \frac{\Delta c_{Cl}^{II}}{\Delta t} \tag{4.1}$$

where

J_{Cl}: Flux of chloride ions in steady state (mol/(cm^{2}year))

V^{II}: Volume of anode solution (L)

A: Cross section of specimen (cm^2)

$\frac{\Delta c_{Cl}^{II}}{\Delta t}$: Rate of increase in chloride ion concentration on anode side ((mol/L)/year)

Effective diffusion coefficient of chloride ion

The effective diffusion coefficient of chloride ions in concrete is calculated using the following equation, and the result is rounded to three significant digits:

$$D_e = \frac{J_{Cl}RTL}{|Z_{Cl}|FC_{Cl}(\Delta E-\Delta E_c)} \times 100 \quad (4.2)$$

where

D_e: Effective diffusion coefficient (cm^2/year))

R: Gas constant (8.31 J/(mol K))

T: Absolute temperature (K)

Z_{Cl}: Charge of chloride ion (-1)

F: Faraday constant (96,500 C/mol)

C_{Cl}: Measured chloride ion concentration on the cathode side (mol/L)

$\Delta E-\Delta E_c$: Electrical potential difference between specimen surfaces (V)

L: Length of the specimen (mm)

The chloride diffusion coefficient

During the last years, chloride ingress into concrete has increasingly been characterized by measuring a diffusion coefficient considered the rate determining parameter of the whole process [5, 165, 166]. Assuming a constant external concentration, Cs, the chloride ingress is a non evolutive process with a constant diffusion coefficient. However, chloride profiles analyzed from natural structures [167,

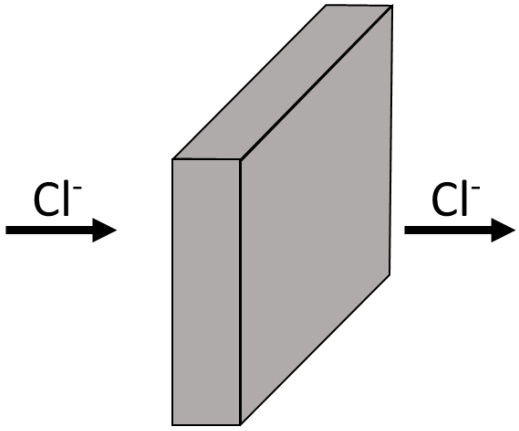

Figure 4.8 Unit section for defining chloride flow

168] show that chloride ingress seems to be a very complex phenomenon, not well characterized yet.

The present paper shows that the whole phenomenon is more complex than expected, but the diffusion coefficient is not a unique concept that results in defining several D values. The different circumstances are described, and a proposal for naming the different D values is presented.

Definition of the diffusion coefficient

Following Crank [169], the diffusion coefficient is defined (**Figure 4.8**) as the rate of transfer of the diffusing substance across a unit area of a section divided by the spatial gradient of concentration at the section.

$$D(cm^2/s) = \frac{F}{\frac{\partial c}{\partial t}} \tag{4.3}$$

Where

F: flow in $mol/cm^2 \cdot s$

$\frac{\partial c}{\partial t}$: the gradient of concentration.

For this definition to be applied, the total volume should remain constant on either side of the section unit as diffusion proceeds, and the same unit of length has to be used in measuring the volume which appears in the definition of concentration.

This definition draws attention to the importance of the units of D and their coherence in the whole expression. Thus, **Figure 4.9** shows that in concrete, the units used for expressing chloride concentration [170]:

- refer to the concrete: in % or kg/m^3 of concrete.
- refer to the cement content: in % or kg/kg cement
- refer to the pore solution: in g or mol Cl/l of solution

Usually, the so called steady state diffusion coefficient, Ds, refers to the pore solution concentration and expresses the movement of water soluble chlorides. However, the non steady state and DNS are expressed by volume of concrete or mass of cement and refers to the number of chlorides in the sample.

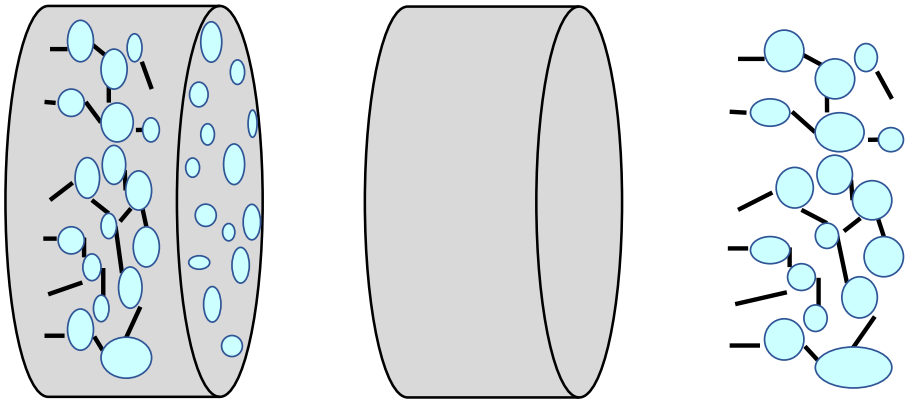

Units of chloride concentration referring to the substantial weight, the cement weight, or the amount of evaporable water in the pores.

Figure 4.9 Chloride concentration

Attending the units of chloride concentration

The chloride ions can refer to the total amount of the sample (concrete or cement) or the pore solution content. Both possibilities aim at different D values that, when compared, should be transformed into coherent units.

Part of the chlorides that penetrate is combined with the cement phases, making the process dependent on the transport only (**Figure 4.10**) and the proportion of bound chlorides. The binding or reaction of chlorides depends on many factors: type of cement, the composition of pore solution, temperature, etc.

Atkinson and Nickerson [170] in 1984 gave expressions for calculating the proportion of the total, bound and free chloride concentration assuming a linear binding:

$$C_t = P \cdot C_f t\ (1\text{-}P)C_b \qquad (4.4)$$

where

C_t : total chloride content

C_f : free chlorides

C_b : bound chlorides

P : concrete porosity

The relation between the diffusion coefficient referring to the pore solution and that referring to the total volume of concrete is:

$$\frac{D_e}{D_a} = P + (1\text{-}P)\,\frac{C_b}{C_f} \tag{4.5}$$

where

D_e : the effective D referring to the pore solution

D_a: apparent D referring to the volume of the sample.

$$C_b = \frac{\alpha C_f}{1+\beta C_f} \tag{4.6}$$

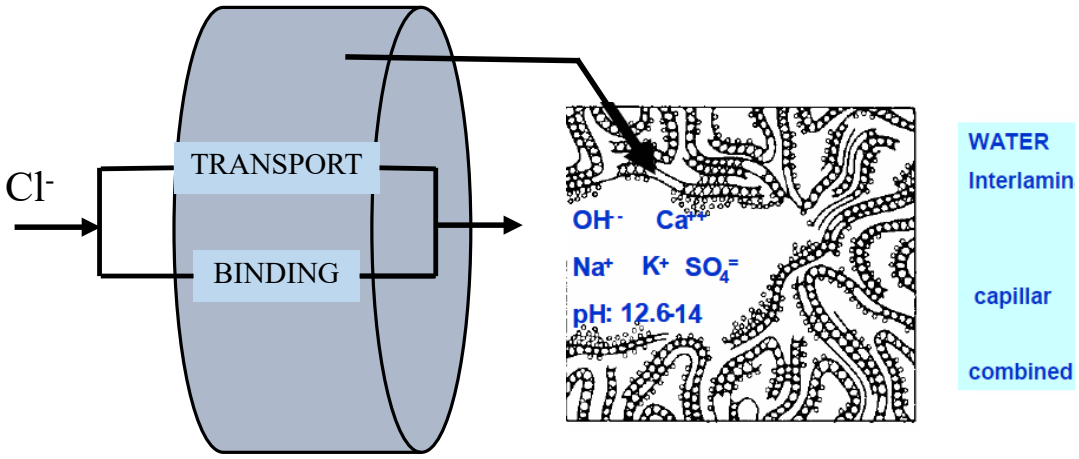

Ttransport and binding with cement phases.

Figure 4.10 Chloride ingress induces two simultaneous processes

Concerning the effect of the application of an electrical field (migration experiments) on the ability of chloride binding from cement phases, the isotherm of [171] calculated from a diffusion experiment and that of [172] made from a migration one. It is worth noting that there is opposite behavior between diffusion and migration when the chloride concentration is low. Thus, while in diffusion, there is binding from when small quantities of chlorides are present, however in migration, only for chloride amounts higher than 20-30 gr/L reaction with cement phases starts to be significant, and only the isotherms equal when the external testing solution is 1 M in NaCl (0.5% by substantial weight in the sample).

This observation is significant, as migration tests using external solutions with chloride concentrations <1M. NaCl will not aim into the full binding and therefore cannot be used for obtaining a D_{ns}. That is the case of the Rapid Chloride Permeability test (RCPT) [173], now modified by Tang and Nilsson to obtain a D_{ns} [174]. The results of this last test have been reported [175] to agree reasonably well with resistivity values taken from the current measured and potential applied. This agreement between resistivity and the D_{ns} calculated from the T&N test confirms that this migration test does not account for chloride binding, as resistivity can only Figure out the porosity and the connectivity of pores [176]

Attending the diffusion regime

The sample thickness is finite, the chlorides can permeate through it in a reasonable time, and the diffusion coefficient can be calculated from a steady state regime when the chlorides emerge in the downstream chamber of a diffusion cell. Thus, **Figure 4.11a** is shown the typical diffusion cell in which one chamber contains a chloride solution and the other is free from them. After a specific time when the chlorides penetrate the sample and react with the cement phases, they appear in the chloride free chamber. The increase in chloride concentration constantly results with time if the reaction in the sample has been completed. A D_s value is calculated from the slope of the graph chloride concentration time (4.7) (4.8). Notice that the chlorides refer to the volume of solution in the chambers, and therefore, they represent the movement of free chlorides. J denotes the chloride flow.

$$J = -D\frac{dc}{dx} \tag{4.7}$$

However, the time to appear in the downstream chamber is related to both free and combined chlorides. This time is known as “time lag” and enables the calculation of a non steady state D, D_{ns} from the expression [169].

$$t = \frac{l^2}{6D_{ns}} \tag{4.8}$$

where

t: time lag

l: sample thickness.

When the test is made in a cylindrical specimen with a pond (**Figure 4.11b**), the D_{ns} is calculated by fitting the solution of Fick's second law assuming semi-infinite media and constant surface concentration [5]:

$$C_x = C_s\left(1\text{-erf}\,\frac{x}{2\sqrt{D_{ns}\,t}}\right) \tag{4.9}$$

C_x: chloride concentration at depth x and time t

C_s: surface concentration

The values of D_{ns} seem more representative of natural conditions as they do consider the binding. However, on the other hand, the natural driven forces for chloride ingress are not the chlorides immobilized but the free chlorides. Free chlorides as well are those able to D_e passivate the steel.

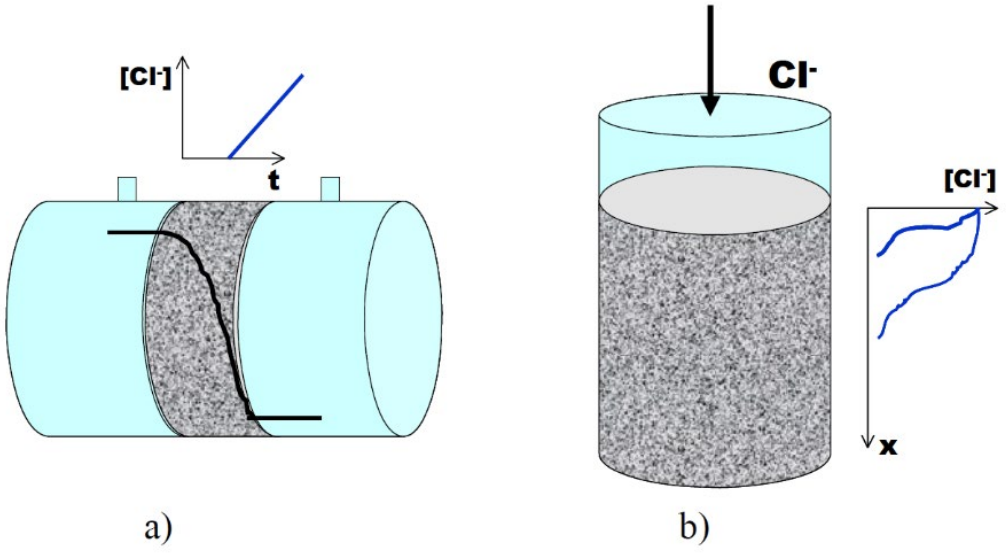

a) Typical diffusion cell in which D_s is calculated from the slope of the graph [Cl^-] – time

b) Typical ponding test where D_{ns} value is obtained from the chloride – cover depth profile

Figure 4.11 Cylindrical specimen

4.5.2.2 The effect of physical characteristics on the amount of Friedel's salt production by X-ray Powder Diffraction (XRD)

X-ray Powder Diffraction (XRD) is a technique used to define the quantification of cementitious materials. XRD analysis is conducted with an X-ray source of Cu–Ka radiation (X = 1.5406 A), in which the Bragg–Brentano method is used to analyze and

identify crystalline compounds. Different parameters such as scan step size, collection time, range, X-ray tube voltage, and current should be fixed on the basis of the specimen requirements for analysis. For a diverse variety of crystalline phases in concrete specimens, the XRD pattern uses phase identification [25].

In addition, for specimens that had been pulverized and immersed in 3% salt water to simulate seawater, the Friedel's salt intensity significantly increased after immersion. The effect before and after immersion in saltwater on the products was measured using X-ray diffraction, and quantitative analysis was performed. In quantitative analysis, the integrated strength obtained by calculating the integrated strength of each product was compared as the amount of production. In addition, the impact of saltwater immersion was measured using XRD, and quantitative analysis was performed before and after immersion in saltwater. Measurements were carried out by using the D8 discover machine. In this study, we measured the formation of Friedel's salt, which affects salt immobilization mainly measured Friedel's salt, which affects salt fixation, and Kuzel's salt, which is related to the formation of Friedel's salt. The chemical formula and reflection angles are shown in **Table 4.3**.

Table 4.3 Formula of each product and X-ray angle.

Product Material	**Chemical Formula**	**Angle of Reflection**
Kuzel's salt	$C_3A \cdot (0.5\ CaSO_4 \cdot 0.5CaCl_2) \cdot 10H_2O$	10.6
Friedel's salt	$C_3A \cdot CaCl_2 \cdot 10H_2O$	11.3
Aluminum oxide	Al_2O_3	25.55

Chapter 5

Results

5.1 Introduction

Concrete has generally been the primary material for civil infrastructure systems, including those in the maritime environment. Unfortunately, bacteria react with hydrogen sulfate in these facilities, generating sulfuric acid, which causes the concrete to degrade rapidly. There are several ways to protect concrete from this impact, including oxygen injection, which prevents the formation of hydrogen sulfate or applying a substance to the concrete's surface that comes into direct contact with sulfuric acid.

Although these procedures are successful, they are primarily utilized to defend the structure's most vulnerable regions. Developing concrete with an inherent resistance to chloride ion degradation is the most efficient technique to extend the concrete's integrity.

In this study, BFS as a cement replacement improves the resistance to chloride ions. This study shows that the Blaine value rate significantly affects compressive strength. However, in addition to enhancing the BFS replacement rate, a more significant change was discovered, confirming the influence of the Blaine value. This study utilizes BFS as cement to investigate the performance of concrete in terms of delaying chloride ion penetration, which affects corrosion reactions. In addition, the experiment was conducted to examine improvements in the performance of an alternative concrete using BFS as cement replacement, focusing on chloride diffusion on concrete with BFS.

Finally, this study evaluates and compares the salt prevention properties of mortar prepared by either steam curing or water curing. The study revealed the factors significantly impacted by basicity that influence the salt preventive properties of mortar in the examined specimens, such as the lead time and diffusion coefficient. Furthermore, these factors were also significantly affected by differences in curing conditions and other physical properties.

5.2 General mechanical properties

5.2.1 Hydration speed

Using BFS as an admixture for the mortar to following findings was obtained within the scope of the effects of differences in the physical properties of BFS with different basicity's setting time as shown in **Figure 5.1**. The hydration reaction rate was delayed in the BFS 4000 Blaine value by 45% replacement, and the BFS 4000 Blaine value by 22.5% replacement with increased basicity had a delayed hydration reaction rate compared to the other three types. The result confirms that the hydration reaction rate was increased by simply changing the crushing method, but the hydration reaction rate was delayed by increasing the replacement ratio.

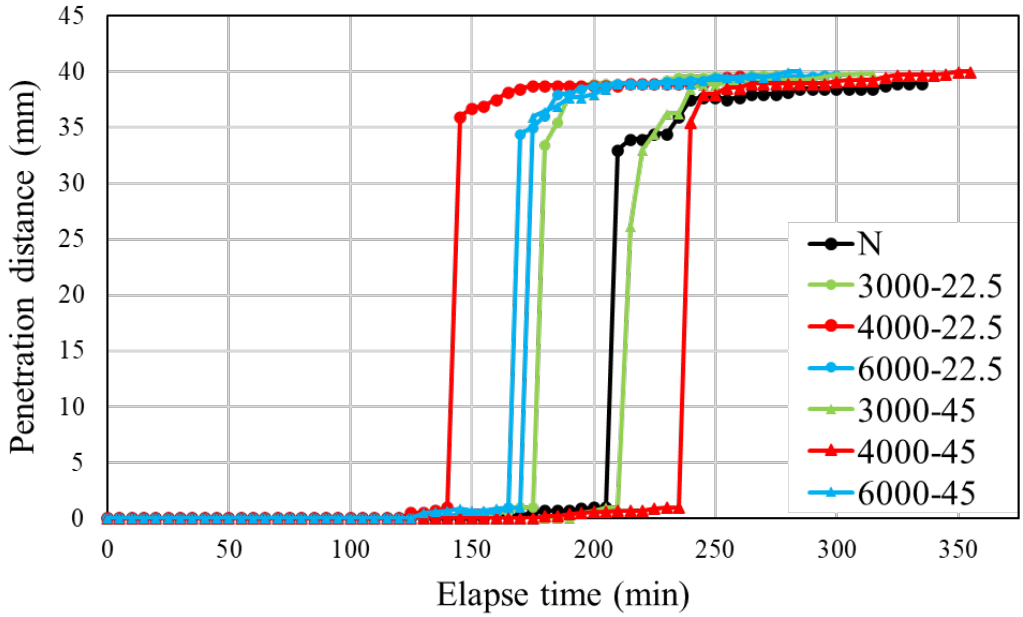

Figure 5.1 The penetration setting time tests

5.2.2 Compressive strength

The compressive strength test for all specimens in the two curing conditions is shown in **Figures 5.2 and 5.3** The compressive strength of the concrete increased significantly between 7 days and 28 days under standard curing conditions and steam curing conditions. These resulting curing conditions found that the steam curing

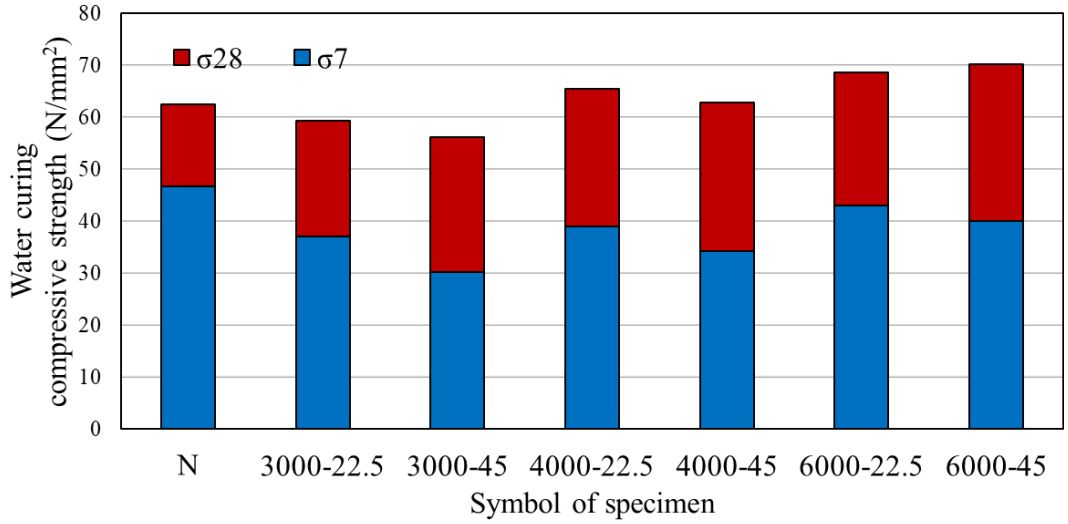

Figure 5.2 The compressive strength test water curing conditions

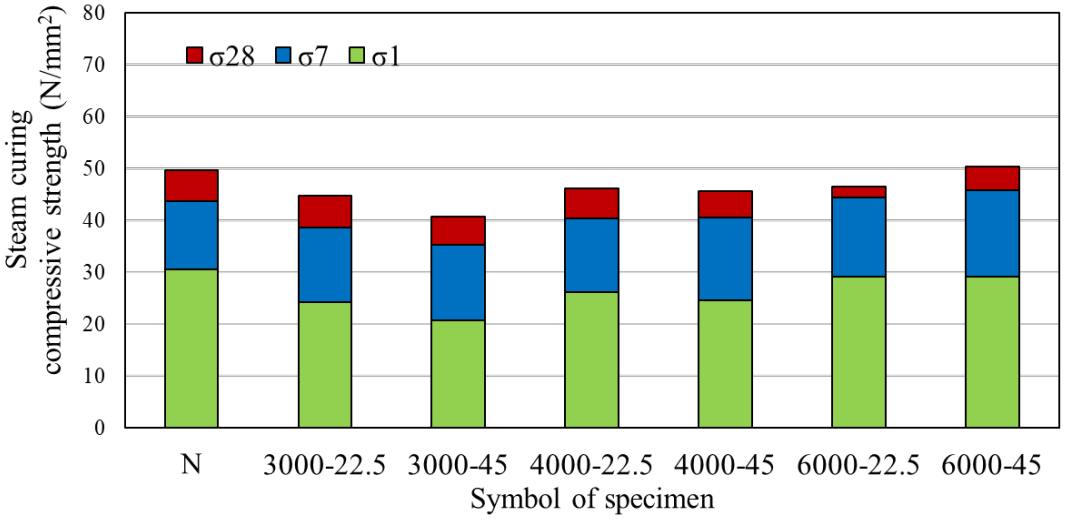

Figure 5.3 The compressive strength test steam curing conditions

condition was affected regardless of physical properties. The comparison results under the water curing condition showed a high early strength, as shown in **Figure 5.3**, and the result showed that the non replacement BFS had a high early strength; on the other hand, after 28 days of curing, the 6000 Blaine value added had the highest strength. The steam curing produced showed that the difference in compressive strength measured was not a significant effect of confirmation.

Comparing the test in which specimens added different Blaine values at the overall substitution rate showed 22.5%. The condensation's significant difference in the

compressive strength of the cured product at age 28 confirmed that a highly fine black BFS with a Blaine value of 6000 influenced the strength.

5.2.3 Marcury Injection Porsimetry

The pore structure of BFS with different mix proportions after 28 days of curing as two conditions is discussed. The cumulative intrusion pore volume versus pore diameter curves in **Figure 5.4** and the differential intrudes volume versus pore diameter curves as shown in **Figure 5.5**, which was (a) water curing; replacement rate 22.5%, (b) steam curing; replacement rate 22.5%, (c) water curing; replacement rate 45% and (d) steam curing; replacement rate 45% described both Figures. The graph in **Figure 5.4** represents the amount of pore volume that was increased by using water curing condition, and the pore diameter was influenced to a BFS replacement level of 45%, as shown in **Figure 5.5**.

The threshold radius is assumed to be the initial intergranular spacing at the setting time; the result has influenced the higher BFS replacement cement ratio, the curing condition, and the replacement level to generate a higher threshold radius. As replacement volume concentration increases, the threshold region tends to flatten out, and the threshold radius increases progressively, which could be attributed to the replacement level effect of the reorientation of the pore system of mortar.

The MIP test data indicate a threshold radius below which there is a relatively little intrusion and immediately above where rapid intrusion commences, which corresponds to the inflection region, following an almost horizontal portion of cumulative intrusion curves. The test results also indicate that the threshold radius increases with different curing conditions and BFS replacement percentages.

According to the aim of the study to improve the durability of the pore size distribution of cement, the existing models of the pore size distribution of cement based materials have been reviewed and compared with test results in this investigation. Although too many parameters are included in the model, the compound lognormal distribution is excellent for simulating the experimental pore size distributions.

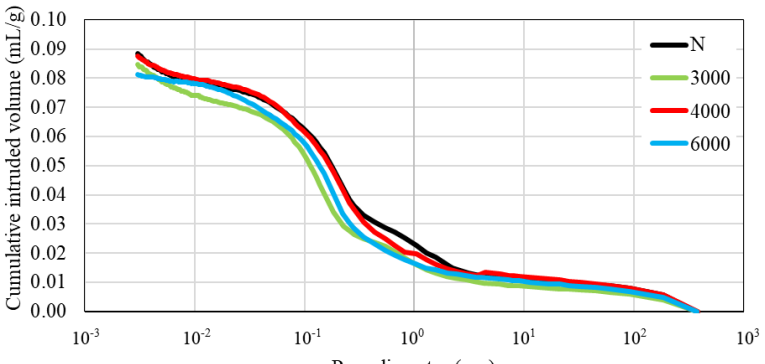

a) Cumulative intruded pore volume versus pore diameter
(steam curing ; addition rate 22.5%)

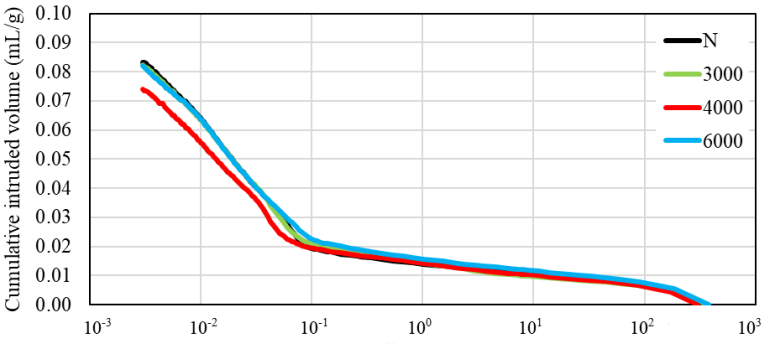

b) Cumulative intruded pore volume versus pore diameter
(water curing ; addition rate 22.5%)

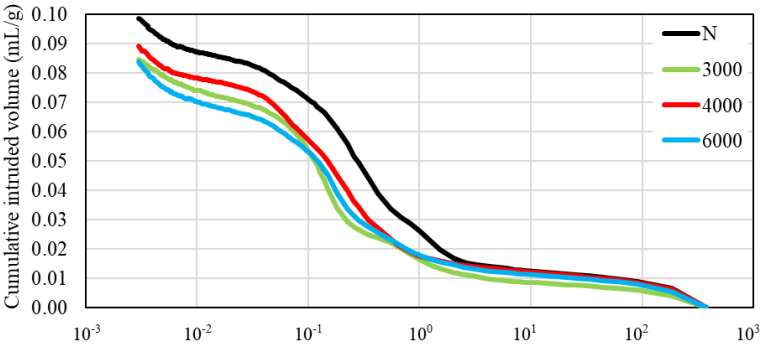

c) Cumulative intruded pore volume versus pore diameter
(stream curing ; addition rate 45%)

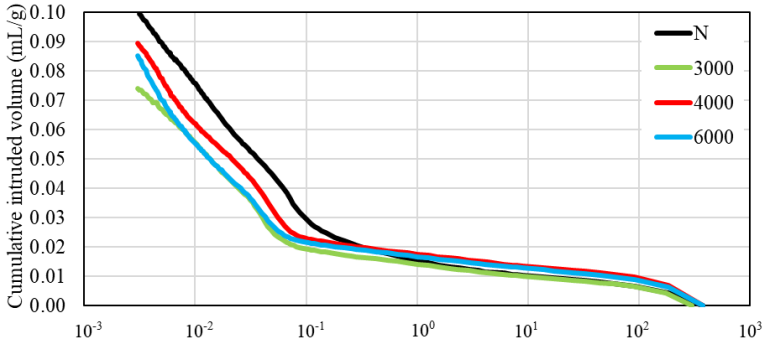

d) Cumulative intruded pore volume versus pore diameter
(water curing ; addition rate 45%)

Figure 5.4 Cumulative intruded pore volume versus pore diameter

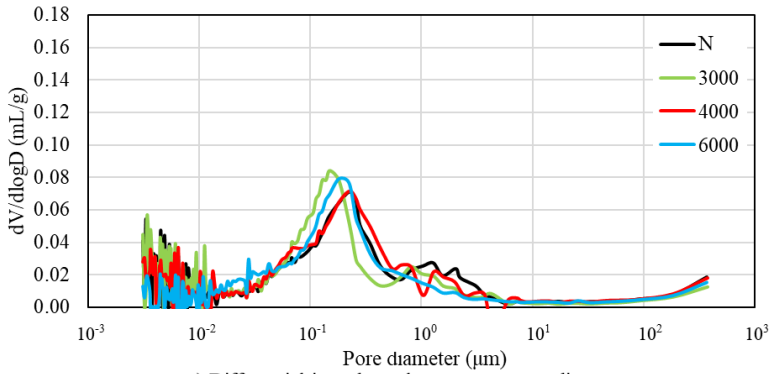

a) Differential intrudes volume versus pore diameter
(steam curing ; addition rate 22.5%)

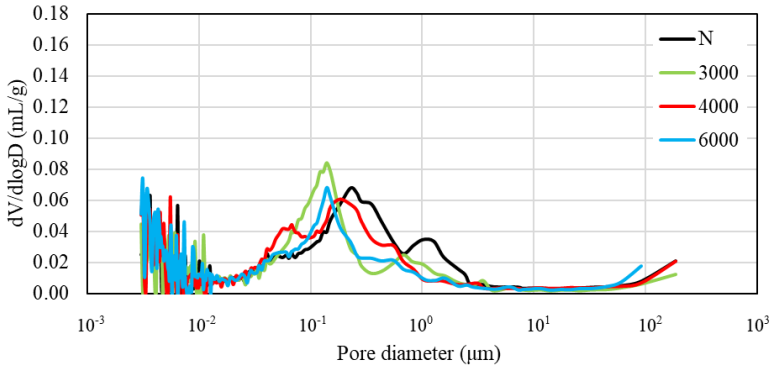

b) Differential intrudes volume versus pore diameter
(steam curing ; addition rate 45%)

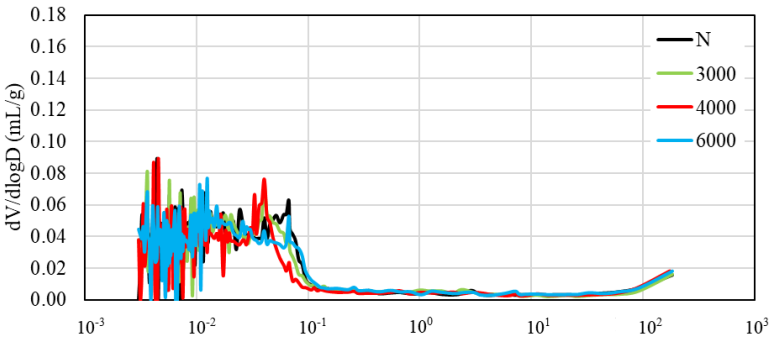

c) Differential intrudes volume versus pore diameter
(water curing ; addition rate 22.5%)

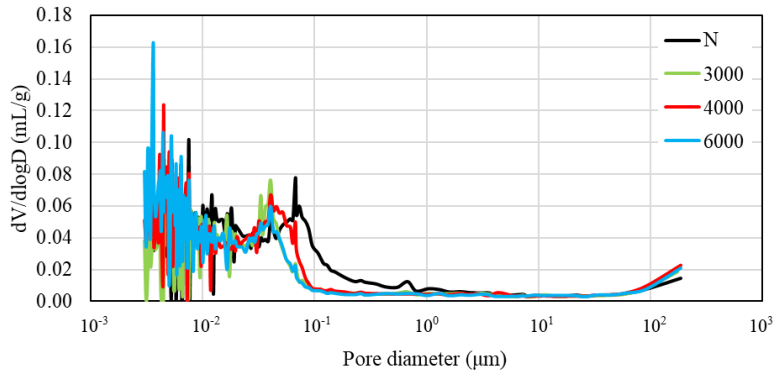

d) Differential intrudes volume versus pore diameter
(water curing ; addition rate 45%)

Figure 5.5 Differential intrudes volume versus pore diameter

Porosity and mean diameter were considered, which clearly explains the relationship between pore structure and curing condition, as shown in the result are following :

1) It was found that the curing condition affects the pore volume and pore diameter.
2) It was confirmed that the pore volume was greatly affected by the level of Blaine value.
3) The effects as mentioned earlier are remarkable in 45% of BFS cement replacement and the case of water curing, which is a replacement condition and a curing method for general precast products.

Studies show that increasing the value of BFS by cement replacement was affected by reduced pore properties, and curing conditions were affected to value of pore, which has a beneficial effect on the development of concrete properties. However, intruded pore volume per volume of paste in the mortar increases with increasing replacement level concentration.

5.3 Durability against chloride attack

5.3.1 Rapid chloride ion penetration test

5.3.1.1 The effective diffusion coefficient (De)

The effective diffusion coefficient and concentration were established to verify the salt preventive properties, whereby chloride ions on the cathode side penetrate the specimen in the electrophoresis test and permeate to the anode side. This study shows the effective diffusion coefficient results in both curing conditions in **Figures 5.6** and **5.7**. The concentration rate was increased by water curing conditions and featured high salt damage resistance by suppressing the penetration of chloride ions. The effective diffusion coefficient and the salt preventive property were increased by the BFS Blaine value and water-curing condition. On the other hand, the result of the effective diffusion coefficient by RCPT was not affected by the steam curing condition and Blaine value.

Comparing the BFS replacement rate ratio confirmed that 45% BFS cement replacement of both steam curing and water curing increased the rate of salt preventive properties. The BFS replacement rate ratio of no replacement and 22.5% were of no

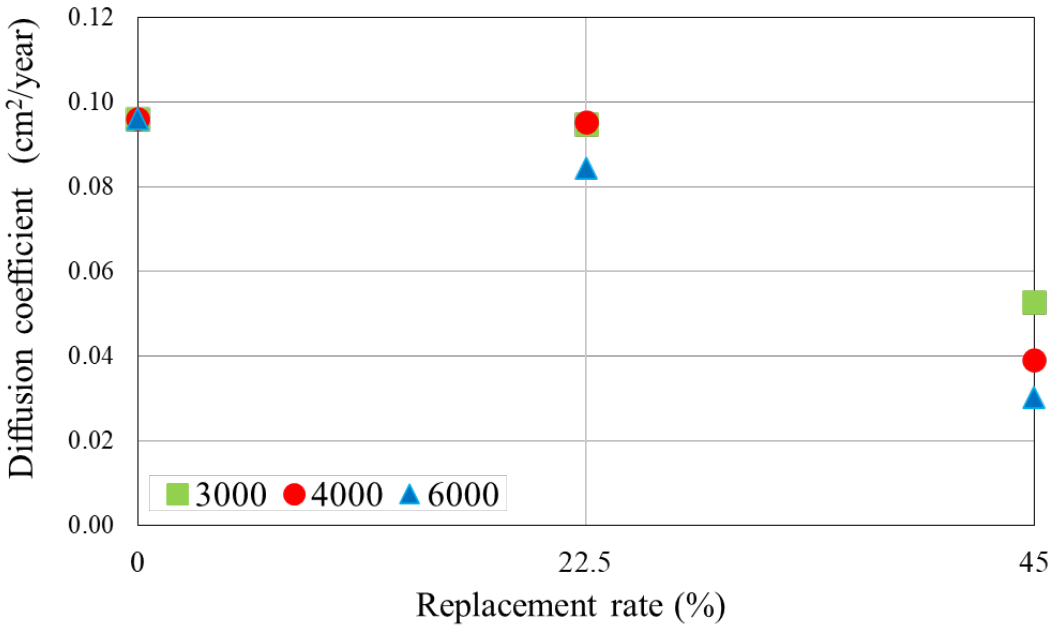

Figure 5.6 Diffusion coefficient by water curing

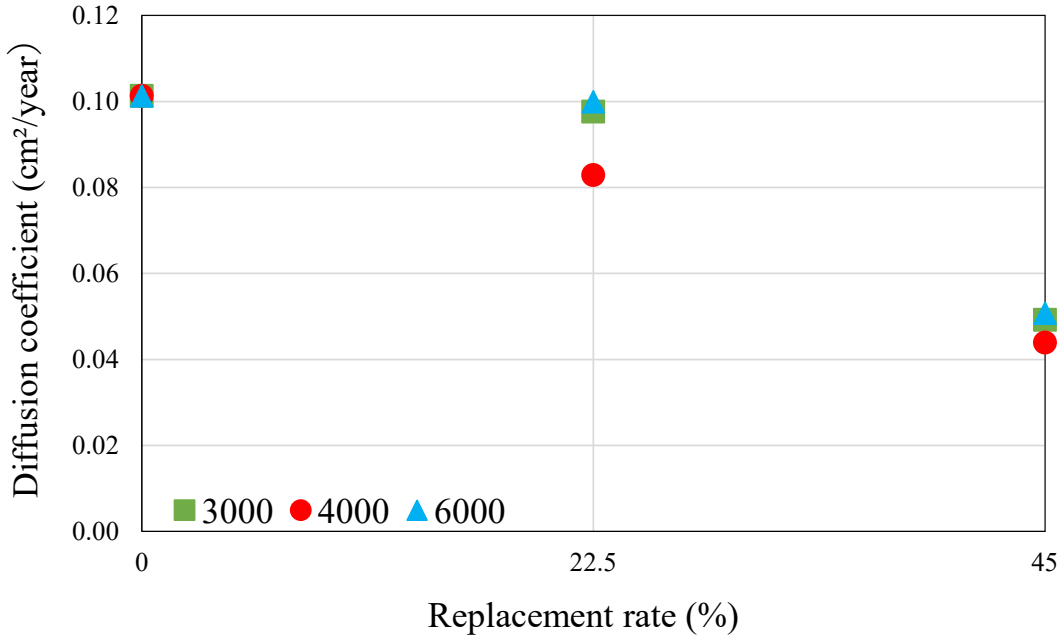

Figure 5.7 Diffusion coefficient by steam curing

significance to the salt preventive property, which might have been caused by the effect of voids and pore structure. **Figures 5.8** and **5.9** show the concentrations for water curing, and this is shown for steam curing in **Figures 5.10** and **5.11**. Therefore, the increase in BFS replacement rate ratio might have been affected by the chloride concentration and the salt preventive property in both curing conditions. In water curing, the higher the Blaine value, the lower the ion concentration, whereas no

correlation was observed in steam curing. Therefore, when comparing the curing methods, water curing tended to increase salt preventive properties. However, this study also considered the Blaine value, which might increase the volume of voids due to steam.

A comparison of the effective diffusion coefficient (D_e) of chloride ions in this study found that increasing the BFS replacement level might decrease D_e. Water curing

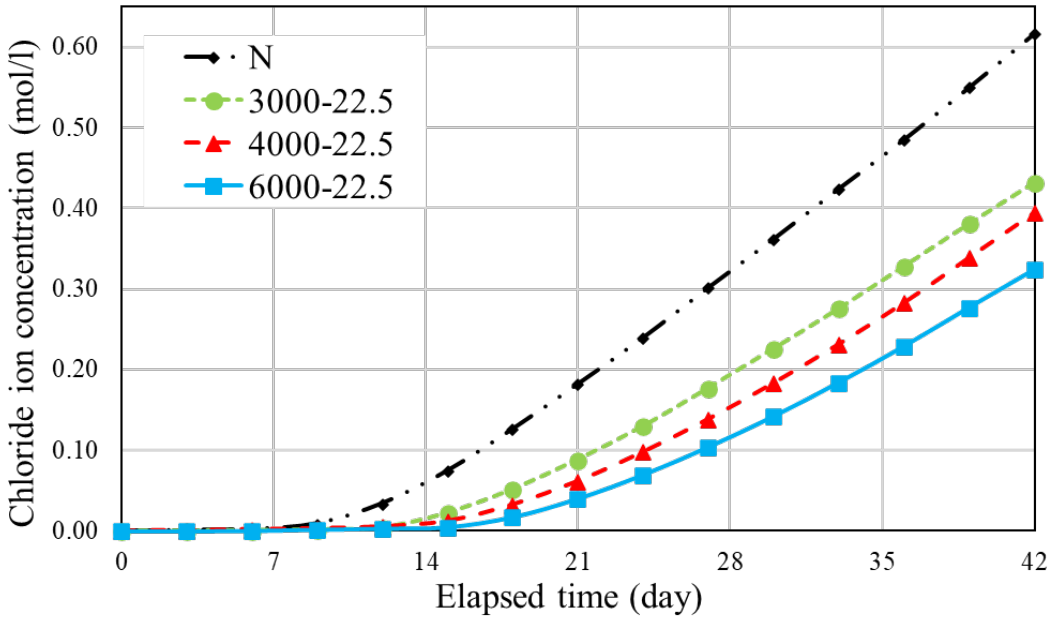

Figure 5.8 Chloride ion concentration in water curing (22.5% replacement rate)

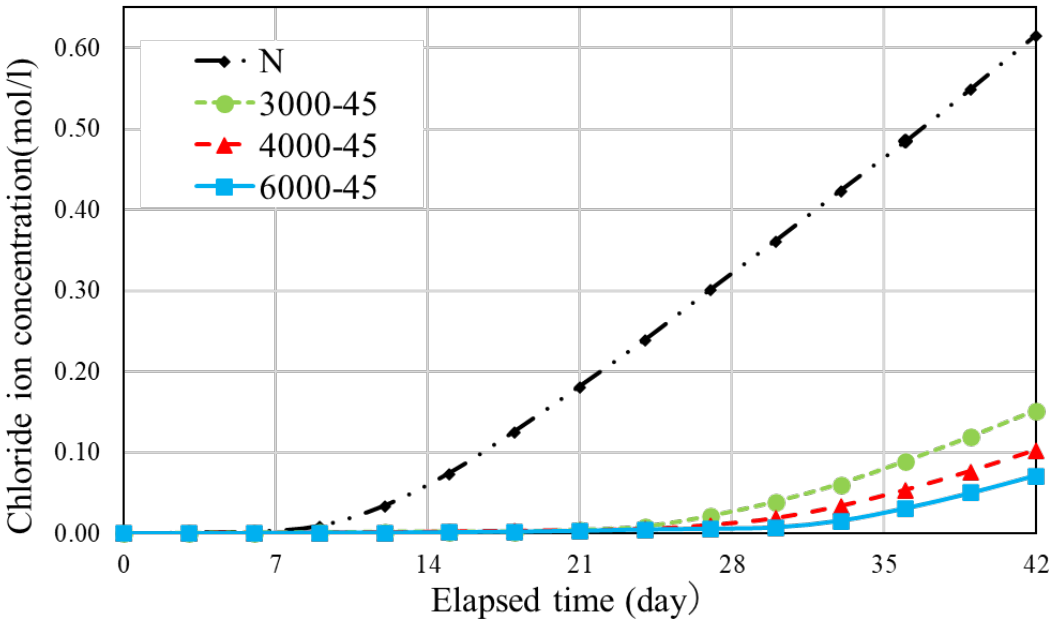

Figure 5.9 Chloride ion concentration in water curing (45% replacement rate).

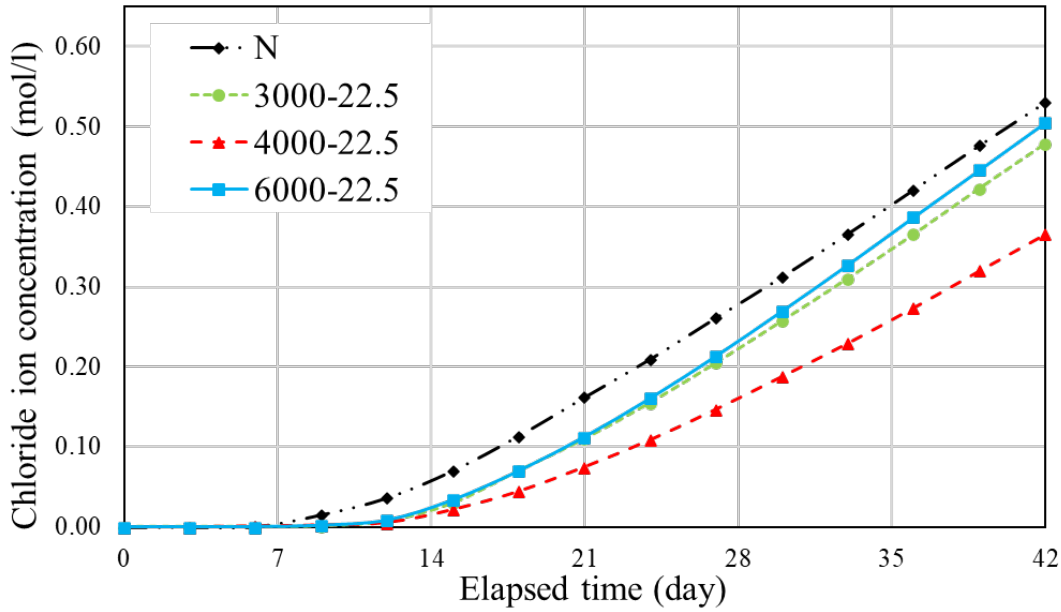

Figure 5.10 Chloride ion concentration in steam curing (22.5% replacement rate)

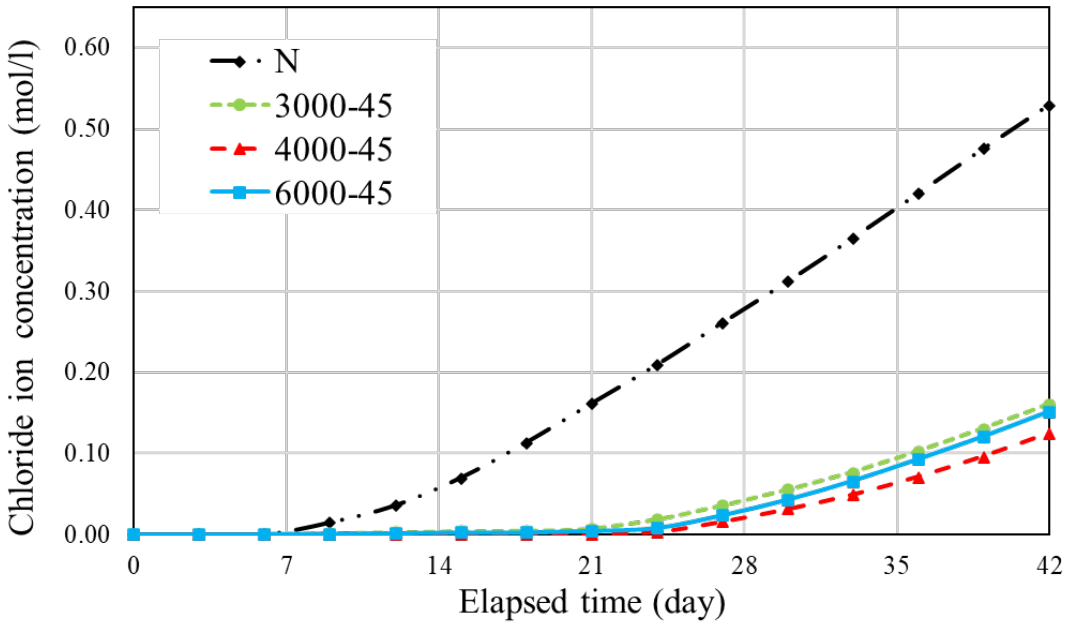

Figure 5.11 Chloride ion concentration in steam curing (45% replacement rate)

conditions at 22.5% BFS replacement D_e this study showed that curing conditions significantly affected the effective diffusion coefficient. In contrast, the Blaine value conditions did not influence the effective diffusion coefficient.

A lower diffusion coefficient indicates that chloride insertion into the structure decreases with increased service life due to chloride diffusion. The greater concentration enters the structure with lower chloride concentrations and decreases when the chloride concentrations in the two conditions are approximately the same. The increased concrete strength and the effect of the reduction in the diffusion coefficient are due to factors that increase the strength of the concrete, such as the amount of cement. In addition to giving the concrete higher strength, it also contributes to the lower porosity of the concrete increasing the chloride binding capacity in the hydration product, thereby increasing the diffusion coefficient of the chloride into the structure is

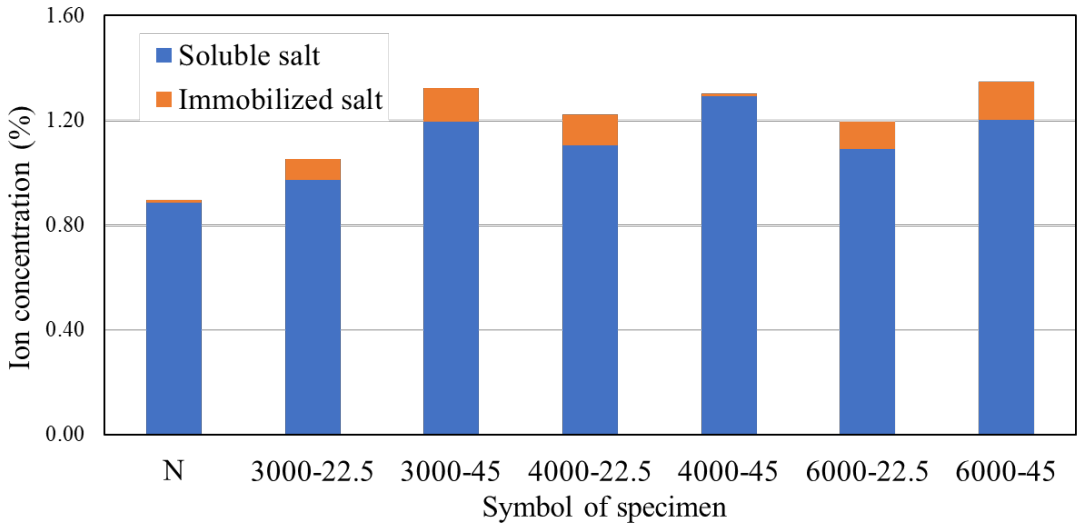

Figure 5.12 The chloride immobilization concentration (water curing)

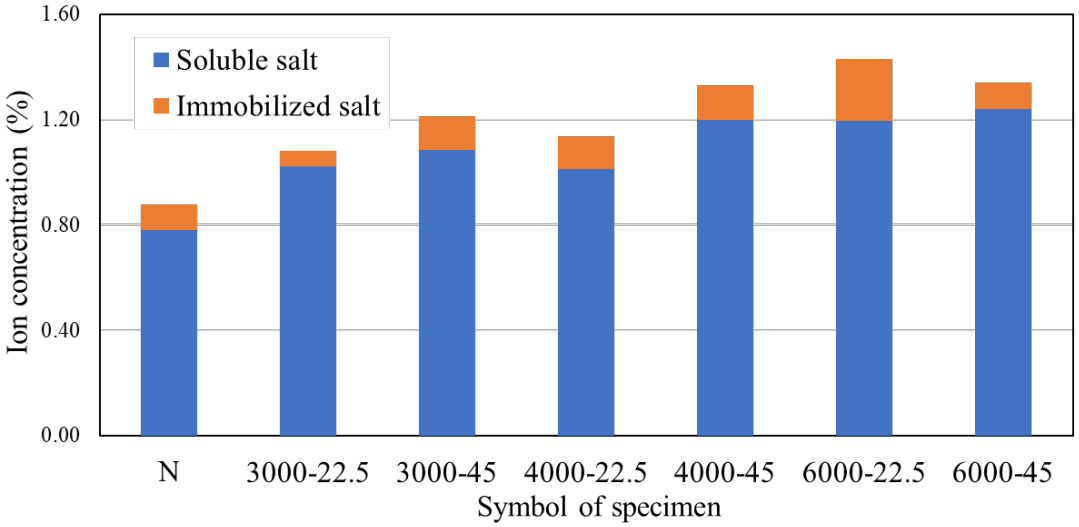

Figure 5.13 The chloride immobilization concentration (Steam curing)

reduced in which the diffusion coefficient of chloride was compared with the structure age.

5.3.1.2 The chloride immobilization

Previous studies mentioned above and the combination of cement and water produce a hydration reaction resulting in exothermic energy, C-S-H products, and calcium hydroxide (CH). The BFS used as a mineral admixture was a reaction with a hydration reaction, which resulted in Friedel's salt being produced using the fomular:

$$3CaO \cdot Al_2O_3 \cdot CaCl_2 \cdot 10H_2O$$

The ion chromatography testing result can determine chloride immobilization to explain the delay of chloride ion properties in which chloride immobilization increased. An internal reaction suppresses the conduction of the reaction, causing corrosion. Studies have shown that the BFS replacement level significantly affects chloride immobilization. Chloride immobilization increased due to the influence of the Blaine value level, as the study showed that high Blaine levels were affected. The percentage of BFS replacement significantly affected the immobilization of all curing conditions described by the components of BFS. From the increased BFS cement replacement study, chemical components more significantly supported the reaction to used chloride to produce Friedel's salt.

A graph of chloride ions in water curing and steam curing is shown in **Figure 5.12** and **5.13**. It was found that when the replacement rate of BFS was increased with the same degree of powder, most of them tended to have a more significant amount of immobilization. It was also found that when the degree of powder was changed at the same replacement rate, the higher the degree of powder, the more the chloride ions were immobilized. To compare curing conditions as steam curing had a more significant amount of chloride ion immobilization, albeit slightly. In the other condition with different basicity, the result shows that the immobilization capacity is significantly influenced by the basicity of BFS, especially in water curing was increased by 50% of the percentage amount of immobilization by an increase of basicity as show in **Figure 5.14**. On the other hand, the maximum temperature of steam curing affected the percentage amount of immobilization capacity.

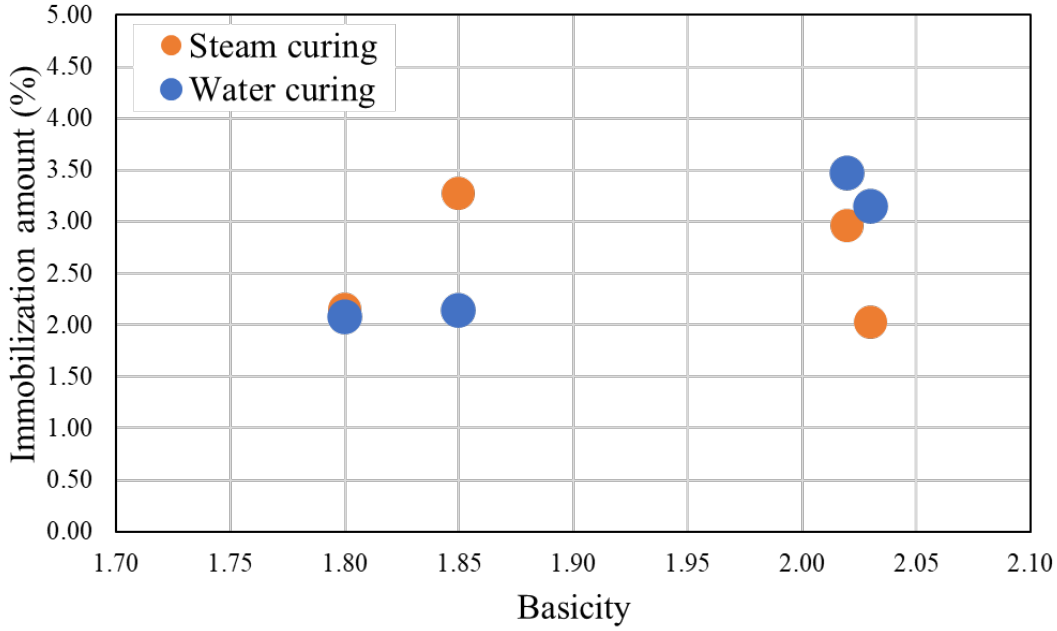

Basicity = $(CaO+Al_2O_3+MgO)/SiO_2$

Figure 5.14 The chloride immobilization on different basicity

5.3.1.3 The chloride immobilization for prediction

The above study shows that replacing the BFS material to cement the process leads to the development of properties that affect chloride permeability as an advantage in product development. Furthermore, diffusion coefficient values could result from a study to determine the prediction time from the concept of Fick's second law. The first is the conventional macroeconomic diffusion theory, which is based on Fick's law. On a microscopic level, the second is based on electrochemistry theory. The diffusion model, which is based on Fick's second law, is used in this investigation. This diffusion model could be used to predict how long it will take for chloride to reach and initiate corrosion at a depth of the reinforcing steel.

For one dimensional diffusion into a semi infinite medium, an error function solution is usually used as follows [158]:

$$C_x = C_s\left(1\text{-erf}\,\frac{x}{2\sqrt{D_{ns}\,t}}\right) \tag{5.1}$$

The uncertainty analysis started with a study into the diffusion coefficient in the series analytical solution that affected the variability of effective diffusivity adjusted

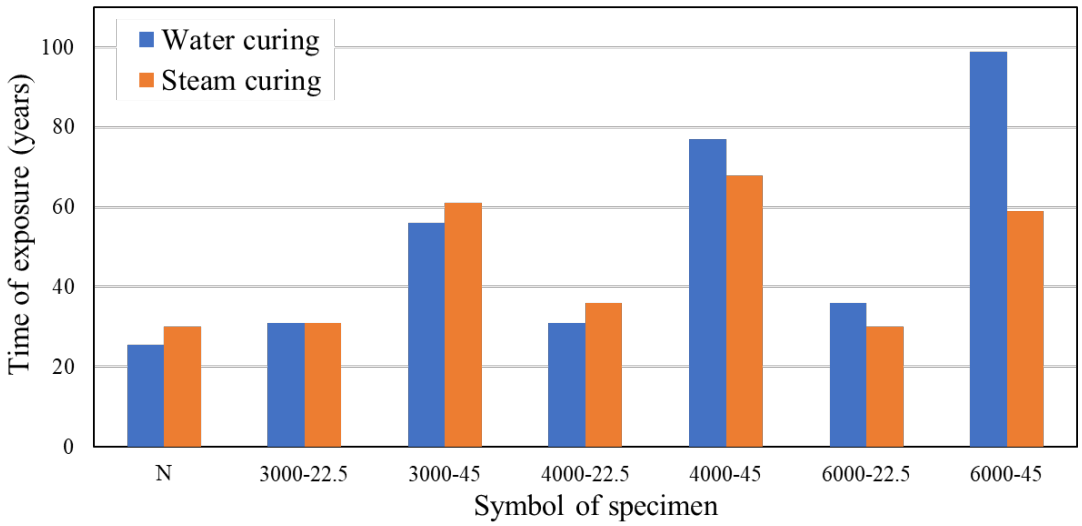

Figure 5.15 Calculation of corrosion prediction time based on Fick's second law

for each data set. The calculation of corrosion prediction time is based on Fick's second law as the equation mention above. **Figure 5.15** presents these results for both curing conditions and various Blaine values obtained for each value of effective diffusivity. The water curing has influenced chloride diffusion properties as the study shows that 6000 Blaine of BFS by 45% cement replacement delayed chloride diffusion. Thus, extending the time to product corrosion reaction while the 22.5% replacement rate has significantly decreased chloride diffusion.

5.3.2 The effect of physical characteristics on the amount of Friedel's salt production by X-ray Powder Diffraction (XRD)

This study compares the result of X-ray diffraction data of cement paste partially replace with BFS at ages of 28 days. The results were compared before and after 28 days of the specimen's immersion in saltwater, indicating that Friedel's salt was formed. The experiment with different Blaine values and intensity counting for chemical product materials in **Figure 5.16** shows nonreplacement, and replacement with BFS with 3000, 4000, and 6000 Blaine values, respectively, where the X-axis is the angle of reflection and the Y axis is count intensity. The area of the diffraction peak was obtained by functionally fitting the diffraction peak by the method of least squares and calculating the intensity.

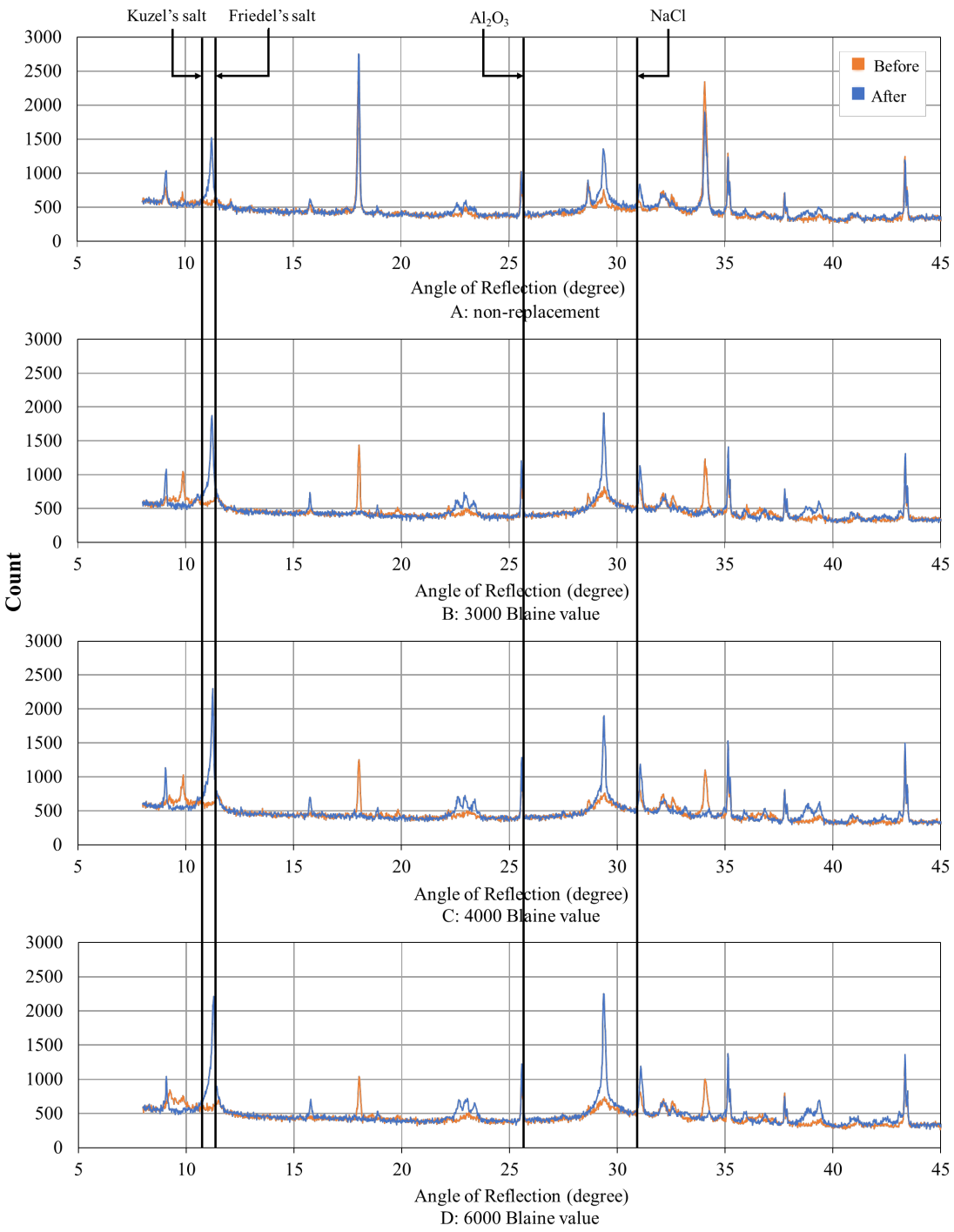

Figure 5.16 X-ray diffraction patterns

Chloride intensity determined from the XRD experiment is shown in **Table 5.1**, compared with aluminum oxide as standard material. When calculating Friedel's salt, an indicator of delay penetration, there was an increase in Friedel's salt over time, as shown in **Table 5.1**, which obtained Friedel's Salt correction calculation. When

Friedel's salt substance intensity (Counts) and aluminum oxide (α-Al_2O_3) substance intensity (counts) obtained from the XRD experiment were added to equation (5.1), the results were shown that the replacement with BFS had a significant effect on the formation of Friedel's salt stages.

$$\text{Friedel's Salt Correction Calculation} = \frac{\text{Friedel's Salt Substance Intensity (Counts)}}{\text{Aluminum Oxide } (\alpha\text{-}Al_2O_3) \text{ Substance Intensity (Counts)}} \times \text{diffraction peak} \quad (5.2)$$

Table 5.1 The formula of each product and x-ray angle

Blaine value	**Friedel's salt substance intensity (Counts)**	**Aluminum oxide substance Intensity (Counts)**	**Friedel's salt correction calculation**
Non	1523	1021	1796
3000	1875	1204	1875
4000	2302	1288	2151
6000	2214	1225	2176

From the results, the replacement with BFS had a considerable impact on the appearance of Friedel's salt stages. For non-replacement, the Friedel's Salt was 1796, adjusting by equation (5.2), whereas the value increased when looking at the sample with substitution. The higher the Blaine, the higher the rate of Friedel's Salt, such as 6000 Blaine value is 2176 adjusting by equation (5.2), which is a significant difference.

Thus, the Blaine value was investigated, as the amount of Friedel's salt that had emerged was confirmed as affecting the immobilization capacity of chloride ions. Immersion for BFS with Blaine value 6000 had the highest Friedel's salt of all the BFS samples of other Blaine values. Thus, the result confirmed that increasing the Blaine value of BFS was responsible for the increasing immobilization capacity of chloride ions.

On the other hand, while focusing on pre-curing time in the second condition, the **Figure 5.17** show the relationship between the pre-preparation time and the amount of immobilization for 28 days of immersion. Regardless of the number of days of immersion and curing conditions, it was confirmed that the amount of chloride ion immobilization tended to increase as the fineness increased. It is considered that the amount of reaction with chloride ion increased as the degree of Blaine increased, and

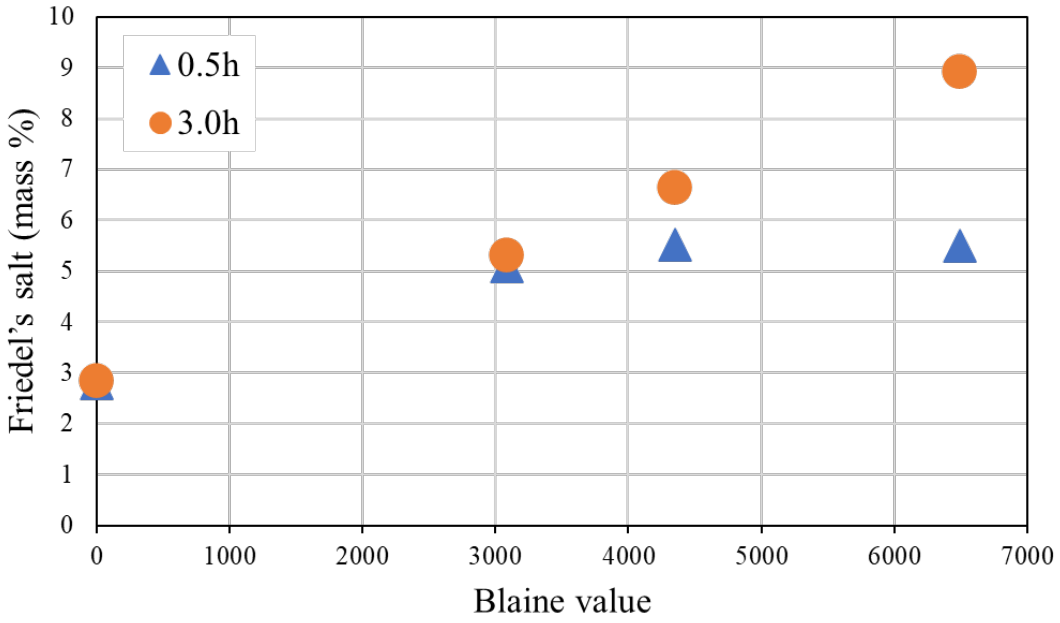

Figure 5.17 Relationship between the pre-preparation time of 28 days of immersion and the amount of immobilization

the amount of immobilization also increased. When comparing the pre-preparation time at 28 days of immersion due to a reaction between the unhydrate and chloride ion in the early stages. It was confirmed that the longer the pre-preparation time, the more significant the amount of immobilization. It is considered that the longer the pre-preparation time, the more the hydration reaction was promoted, and the long term reaction between the hydration product and chloride ion increased the amount of immobilization.

5.4 Summary

The following findings were obtained within the scope of this chapter as the effects of differences in the physical properties of BFS, which uses BFS as an admixture for mortar and has different curing conditions and basicity on salt preventive properties. Comparing steam curing and underwater curing as the effect on the salt preventive properties of mortar, the specimens subjected to underwater curing tended to be higher. Comparing the differences in the physical properties of BFS with different Blaine values on the salt preventive properties of mortar, it was found that the basicity affects the lead time and effective diffusivity. As for the difference in curing conditions and physical properties on the effective diffusion coefficient, the same result as the lead

time was confirmed. It was confirmed that the difference in physical properties is greatly affected by steam curing. From this result, it is remarkable in the case of steam curing, which is a curing method for precast products.

Chapter 6

Conclusion

6.1 Introduction

Concrete is more widely used than any manufactured material and has been a construction staple for centuries [1]. However, several theories on the deterioration of reinforced concrete (RC) show that direct current tends to corrode steel reinforcement, and chlorides are chemically bound by the cement paste (tricalcium aluminate, C_3A) [2].

In marine environments, a significant reason for the collapse of RC structures is the corrosion of steel reinforcements, which creates a course for the penetration of chloride through the concrete surface, which comes into contact with internal reinforcement, leading to rebar oxidation and corrosion. Therefore, chloride induced reinforcement corrosion is considered the leading cause of concrete deterioration. In addition, rust occupies volume and creates tensile stresses in the concrete, resulting in spalling and cracking [3].

Steel corrosion in concrete can be reinforced by oxygen starvation, especially when oxygen is only at the cathodic areas of steel in solution at the anode [4]. According to [5], carbonation and chloride diffusion processes require several years to reach the reinforcing steel in concrete during corrosion initiation. Equations for Fick's law of diffusion may be used to numerically predict the time it takes for chloride diffusion or carbonation to pass through the concrete covering and initiate corrosion in the RC structure. Covering thickness, quality of concrete, and the environment are possible factors that affect the structure's initial properties and age. Chloride levels at various depths in concrete and carbonate depth are another possible reason. The passive layer is damaged from the point of corrosion initiation to the first signs of corrosion damage. Therefore, the corrosion period can be estimated using modeled equations that calculate the corrosion time and rate, which determine the deterioration of RC in a given environment. For example, corrosion of a concrete infrastructure due to seawater reduces the ultimate service life of an RC structure.

The durability of concrete constructions is intimately connected to the durability of the component concrete material. Therefore, the environmental effect is increased

with Portland cement, which causes the expansion and deterioration of concrete. The leading chemical causes of concrete deterioration are alkali-silica reactions, alkali–carbonate reactions, carbonation, sulfate attacks, chloride attacks, and steel corrosion. A combination of various factors also frequently causes the deterioration of concrete structures. In addition to those given above, acting alone or in combination, other factors such as high structural, thermal shrinkage, poor quality of materials, and inadequate maintenance may exacerbate the situation [3].

One of the significant factors contributing to the corrosion of marine RC structures is the chloride induced corrosion of steel reinforcements, which substantially impacts structural service life [6] and has been intensively researched for decades, prompted by the rising maintenance costs resulting from the impacts of seawater exposure on coastal structures [7]. Although concrete is the ideal material to protect steel reinforcement due to increased alkalinity, RC marine structures are highly vulnerable to corrosion due to chloride attacks. The attack's severity depends on climatic conditions, among other factors [8].

Moreover, the pore solution reduces alkalinity in concrete to catch large amounts of chloride. Therefore, using high C_3A cement is good chloride corrosion resistance. On the other hand, sulfate corrosion resistance requires cement with low C_3A, which is a contradiction [9].

The mechanism of concrete deterioration caused by chloride ion infiltration and carbonation is as follows: (1) Friedel's salt is formed when monosulfate (AFm) reacts with chloride ions; (2) Friedel's salt is carbonated; (3) chloride ions immobilized in Friedel's salt dissolve into the pore solution; (4) there is an increase in chloride ion concentration in the pore solution, resulting in increased chloride ion penetration into the concrete through concentrating and diffusion cycles. Due to the acidity of HCl, the alkalinity of the concrete slightly decreases from 12.5-13.5 to in grades 11, 10, and 9, respectively. The film's destroyed area has a negative electric potential in an electrolysis reaction. "Anodic reaction" refers to this type of reaction [9]. BFS is a byproduct of pig iron manufacturing, and features high latent hydraulic property. BFS is used as an admixture in Portland BFS cement at 40% to 45%. The advantage of Portland BFS cement is that its long term strength is enhanced, and it has a higher resistance to seawater and chemicals. In addition, the diffusion coefficient of chloride ions makes the cement suitable for offshore structures. Furthermore, alkali-aggregate reactivity is

suppressed, the cement can be used with recycled aggregates, and a lower heat release rate effectively suppresses thermal cracking [13].

Chloride damage resistance is required when BFS is used. The hardened concrete is denser than ordinary Portland cement [13], as it has a solid capability for incorporating chloride ions [14].

A previous study [13] focused on the mechanisms of chloride penetrated in concrete and reinforcing steel corrosion, which developed corrosion protection, repair strategies, and detection techniques to develop reliable and practical design approaches for durability and corrosion protection for concrete reinforcing steel. To develop mechanistic and practical models (deterministic or probabilistic), the study [13] was shown to design durable concrete structures. Furthermore, it can be used to predict the deterioration and maintenance optimization of existing concrete structures to achieve a specified design life [13].

BFS can improve the resistance of cementitious materials to sulfuric acid attack as the influence of concrete quality on diffusion coefficients is related to the concrete pore structure. The time dependence is due to the hydration of cement particles and chemical reactions of seawater ions with hydration products, which reduce the pore structure. Therefore, when BFS is used, sulfuric acid has a negligible effect on erosion; instead, the high strength concrete or mortar becomes more durable, owing to the enhanced capacity to withstand sulfuric acid. Furthermore, BFS can suppress the penetration of chloride ions, inhibit steel corrosion, and reduce time dependent strains [9,10].

BFS was used as the aggregate to investigate corrosion initiation on RC structures in one study. That study focused on the physical and chemical attacks on RC structures during their service life and investigated whether any protections might be placed to mitigate the degeneration caused by these attacks. It was found that the concrete performance may be improved by including mineral additives in cement, such as silica fume, BFS, and fly ash [16].

A literature review reveals many studies of BFS containing concrete in various countries. However, few studies have examined its use in reducing chloride ion permeability as the main factor of corrosion reactions. Thus, this study utilizes BFS as cement to investigate the performance of concrete in terms of delaying chloride ion penetration, which affects corrosion reactions. Furthermore, an experiment was conducted to examine improvements in the performance of an alternative concrete

using BFS as cement replacement, focusing on chloride diffusion on concrete with BFS. This study aims to develop products for use in the precast concrete industry toward extending the life of concrete structures, especially reinforced concrete structures, in marine environments.

This study experimented with followed study utilizing BFS as cement to investigate the performance of concrete in delaying chloride ion penetration, which affects corrosion reactions, and examine improvements in the performance of an alternative concrete using BFS as cement replacement, focusing on chloride diffusion on concrete with BFS. Therefore, the specimen evaluated chloride ion adsorption into cement based on the diffusion coefficient by RCPT, which, in turn, predicted the chloride ion diffusion characteristics of the specimen. The following conclusions inferred from the test results can be separated into two parts: general mechanical property and durability against chloride attack.

6.2 Mechanical characteristics

Regarding general mechanical properties of concrete containing BFS were improved. The development of the compressive strength of concrete with BFS is the same as that of standard concrete. However, the progression of carbonation in concrete is slower due to producing a more robust and dense reaction product of BFS. This study showed the following:

- 6000 Blaine of BFS had increased compressive strength while 3000 Blaine of BFS had decreased compressive strength.
- The dosage of the cement replacement ratio influences compressive strength, as a high dosage ratio might increase strength while a low dosage ratio decreases strength.
- The steam curing is preferred for accelerated rapid hardening of concrete, high early age strength, and improving construction speed.
- The compressive strength was considerable when steam curing was applied, which affects conditions on compressive strength.
- The compressive strength increased by performing sufficient water curing, confirming that the compressive strength was greatly affected.

By measuring the pore size distribution by injecting mercury, it was confirmed that the structure became denser as the powderiness (Blaine value) and substitution rate

increased. In particular, it was confirmed that the one using 6000 Bline had almost no decrease in strength due to slag replacement concerning the plain product (non-replacement product).

6.3 Durability against chloride attack

Blaine's values of fineness affect the immobilization performance of chloride ions. A replacement of 45% of the binder with BFS exhibits the maximum efficacy in the resistance to chloride ion of cement paste. Using BFS in concrete significantly improves the resistance to chloride ions in concrete. The most effective replacement ratio of BFS in the binder is 45% of cement when BFS is the replacement. The appearance of de-molded concrete products is generally the same as standard concrete products. This study showed the following:

6.3.1 Durability 1: Effective diffusion coefficient of chloride ion

- The higher the Blaine value, the smaller the effective diffusion coefficient. It was confirmed that the 6000 Blaine 45% replacement product was halved compared to the non-replacement product.
- The above effect is in the case of 45% replacement, but it is confirmed that the difference from the non-replacement product is slight at half the replacement rate, and it is necessary to set a replacement rate of more than 22.5% in order to improve durability.
- There was almost no significant difference between 0.5 hrs. and 3.0 hrs. in terms of the effect of the pre-preparation time of steam curing.
- It was confirmed that steam curing increased the effective diffusion coefficient by about 9.4% compared to the standard curing product, which hindered the improvement of salt damage resistance.
- It was confirmed that the service period of the structure can be extended by about 30% by replacing the blast furnace slag 6000 Blaine product by 45%.

6.3.2 Durability 2: Chloride ion immobilization performance

- It was found that the greater the degree of Blaine and the substitution rate, the increased the immobilization performance. It was confirmed that 6000 Blaine

45% substitution increased by about 65.4% concerning the non-replacement product.

- Although the effect of slag basicity on durability has not been seen so far, in this study, it was found that the immobilization ability was increased by 1.5 times by slightly increasing the basicity (1.8 → 2.0).
- Regarding the effect of the pre-preparation time of steam curing, the amount of immobilization increases for 3.0 hrs. compared to 0.5 hrs., unlike the result of the effective diffusion coefficient. Furthermore, it was found that the effect became more pronounced as the Blaine value increased.
- In addition to the effect of reducing the effective diffusion coefficient, further extension of the life of the structure is expected, given the immobilization capacity.

The results reveal the effects of combining BFS with various Blaine values and ratio affecting properties on mortar. In addition, the results show increased durabilities against chloride attack, and mechanical properties for precast manufacturing industrial applications were successfully developed. Thus, resulting was confirmed that the Blaine value of BFS has affected the immobilization capacity of chloride ions. Furthermore, BFS replacement was used to affect the high early-age strength during the long term effects on physical properties.

In conclusion, Chloride immobilization increased due to the influence of the Blaine value, as the study showed that high Blaine values showed a tendency to increase durability. The percentage of BFS replacement significantly affected the immobilization of all curing conditions described by the components of BFS. From the increased BFS cement replacement study, chemical components more significantly supported the reaction to used chloride to produce Friedel's salt. Moreover, Blaine's fineness values affect chloride ions' immobilization performance while the most effective replacement ratio of BFS in the binder is 45% of cement of the binder with BFS exhibits the maximum efficacy in resisting chloride ions. Using BFS in concrete significantly improves the resistance to chloride ions in concrete. Water curing conditions, high Blaine value, high cement replacement ratio, and W/B tended to improve the general mechanical property performance and durability against chloride ion attack.

From the study, diffusion coefficient values could result from a study to determine the prediction time from the concept of Fick's second law. Furthermore, this relationship could predict the exposure time as the service life of concrete structures in a realistic working environment is determined by referring to an exposure test of known mortar specimens. Thus, resulting was confirmed that the Blaine value of BFS has affected the immobilization capacity of chloride ions.

In conclusion, the outcome of this study is the development of concrete materials that decrease durability against chloride attack and improve mechanical properties for precast manufacturer industrial applications. In this study, water curing conditions, high Blaine value, high cement replacement ratio, and W/B tend to improve the general mechanical property performance and durability against chloride ion attack.

Moreover, the use of BFS gives concrete more outstanding durability. In addition, the use of by-products such as BFS reduces the environmental impact of concrete production by reducing CO_2 emissions. Furthermore, Coastal areas should use this study's suggestion to use these data appropriately for products with suitable production properties, such as flow properties, or when environmental risks affect the coastal area.

6.4 Further study

Further study should involve experimenting with thermal simulation absorption and adding a chemical admixture to develop the product’s performance and investigate the combination’s effect, supporting various kinds of concrete industry.

Reference

1. Daube, J. and R. Bakker, *Portland blast-furnace slag cement: a review.* Blended Cements, 1986.
2. Solomon, C., *Slag-Iron and Steel.* Annual Report, US Department of the Interlor, Bureau of Mines, 1992.
3. Subpa-asa, P., et al., *Evaluation of the Prediction and Durability on the Chloride Penetration in Cementitious Materials with Blast Furnace Slag as Cement Addition.* Construction Materials, 2022. **2**(1): p. 53-69.
4. Choi, Y.C., J. Kim, and S. Choi, *Mercury intrusion porosimetry characterization of micropore structures of high-strength cement pastes incorporating high volume ground granulated blast-furnace slag.* Construction and Building Materials, 2017. **137**: p. 96-103.
5. Tuutti, K., *Corrosion of steel in concrete*. 1982, Lund University.
6. Subpa-Asa, P., Y. Ta, and H. Matsunaga. *Basic Study on the Durability of Mortar Containing Blast Furnace Slag Fine Powder with Different Basicity*. in *Key Engineering Materials*. 2021. Trans Tech Publ.
7. Gao, J., et al., *ITZ microstructure of concrete containing GGBS.* Cement and concrete research, 2005. **35**(7): p. 1299-1304.
8. Nishibayashi, S., et al., *Study on Superplasticized Concrete Containing High Volumes of Blast-Furnace Slag.* Special Publication, 1989. **119**: p. 445-456.
9. Subpa-asa, P., et al. *Influence of both Blaine value and curing condition on pore sizes distribution of mortar with using blast furnace slag*. in *AIP Conference Proceedings*. 2021. AIP Publishing LLC.
10. Divsholi, B.S., T.Y.D. Lim, and S. Teng, *Durability properties and microstructure of ground granulated blast furnace slag cement concrete.* International Journal of Concrete Structures and Materials, 2014. **8**(2): p. 157-164.
11. JARIYATHITIPONG, P., et al., *RESISTANCE TO FREEZING AND THAWING ON CONCRETE WITH BLAST FURNACE SLAG UNDER CHLORIDE ATTACK ENVIRONMENT.* Cement Science and Concrete Technology, 2013. **67**(1).
12. Castro-Borges, P., et al., *Concrete under Severe Conditions*. 2010: CRC Press [Imprint].
13. Melchers, R.E. *Observations about the corrosion of reinforcement in marine environments*. in *Proceedings of the XII DBMC, International Conference on Durability of Building Materials and Components, Porto, Portugal*. 2011.
14. Angst, U., et al., *Concrete cover cracking owing to reinforcement corrosion–theoretical considerations and practical experience.* Materials and corrosion, 2012. **63**(12): p. 1069-1077.
15. Melchers, R.E. and I.A. Chaves, *A comparative study of chlorides and longer‐term reinforcement corrosion.* Materials and Corrosion, 2017. **68**(6): p. 613-621.

16. Melchers, R., C.Q. Li, and M. Davison, *Observations and analysis of a 63-year-old reinforced concrete promenade railing exposed to the North Sea.* Magazine of Concrete Research, 2009. **61**(4): p. 233-243.
17. Melchers, R.E., et al., *Long-term durability of reinforced concrete piles from the Hornibrook Highway bridge.* Australian journal of structural engineering, 2017. **18**(1): p. 41-57.
18. Melchers, R.E. and C.M. Howlett. *Reinforcement corrosion of the Phoenix caissons after 75 years of marine exposure*. in *Proceedings of the Institution of Civil Engineers-Maritime Engineering*. 2021. Thomas Telford Ltd.
19. Richardson, M.G., *Fundamentals of durable reinforced concrete*. 2002: CRC Press.
20. Angst, U., et al., *Critical chloride content in reinforced concrete—A review.* Cement and concrete research, 2009. **39**(12): p. 1122-1138.
21. Hadley, H.M., *Concrete in Sea Water: A Revised Viewpoint Needed.* Transactions of the American Society of Civil Engineers, 1942. **107**(1): p. 345-358.
22. Wranglen, G., *Pitting and sulphide inclusions in steel.* Corrosion science, 1974. **14**(5): p. 331-349.
23. Jones, D., *The technology and evaluation of corrosion.* Principles and Prevention of Corrosion, 2nd ed.; Prentice-Hall: Upper Saddle River, NJ, USA, 1996.
24. Lins, V.F., R.B. Soares, and E.A. Alvarenga, *Corrosion behaviour of experimental copper–antimony–molybdenum carbon steels in industrial and marine atmospheres and in a sulphuric acid aqueous solution.* Corrosion Engineering, Science and Technology, 2017. **52**(5): p. 397-403.
25. Stratmann, M., K. Bohnenkamp, and H.-J. Engell, *An electrochemical study of phase-transitions in rust layers.* Corrosion Science, 1983. **23**(9): p. 969-985.
26. Heyn, E. and O. Bauer, *Ueber den Angriff des Eisens durch Wasser und wässerige Losungen.* Stahl Eisen, 1908. **28**(44): p. 1564-1573.
27. Melchers, R.E. and B.B. Chernov, *Corrosion of mild steel in elevated temperature hard freshwater.* Corrosion engineering, science and technology, 2013. **48**(2): p. 130-135.
28. Melchers, R. and R. Jeffrey, *Influence of water velocity on marine immersion corrosion of mild steel.* Corrosion, 2004. **60**(01).
29. Kelly, R.G., et al., *Electrochemical techniques in corrosion science and engineering*. 2002: CRC Press.
30. Broomfield, J., *Corrosion of steel in concrete: understanding, investigation and repair*. 2003: Crc Press.
31. Gjørv, O.E., *Durability design of concrete structures in severe environments*. 2009: CRC Press.
32. Pourbaix, M., *Significance of protection potential in pitting and intergranular corrosion.* Corrosion, 1970. **26**(10): p. 431-438.
33. Deby, F., M. Carcassès, and A. Sellier, *Probabilistic approach for durability design of reinforced concrete in marine environment.* Cement and Concrete Research, 2009. **39**(5): p. 466-471.
34. Alonso, C., M. Castellote, and C. Andrade, *Chloride threshold dependence of pitting potential of reinforcements.* Electrochimica Acta, 2002. **47**(21): p. 3469-3481.
35. Glass, G.K. and N.R. Buenfeld, *The presentation of the chloride threshold level for corrosion of steel in concrete.* Corrosion science, 1997. **39**(5): p. 1001-1013.

36. Melchers, R.E. and I.A. Chaves, *Reinforcement corrosion in marine concretes-1: initiation.* ACI Materials Journal, 2019. **116**(5): p. 57-66.
37. Francois, R. and G. Arliguie, *Effect of microcracking and cracking on the development of corrosion in reinforced concrete members.* Magazine of Concrete Research, 1999. **51**(2): p. 143-150.
38. Yu, L., et al., *Development of chloride-induced corrosion in pre-cracked RC beams under sustained loading: Effect of load-induced cracks, concrete cover, and exposure conditions.* Cement and Concrete Research, 2015. **67**: p. 246-258.
39. Nawy, E.G., *Concrete construction engineering handbook*. 2008: CRC press.
40. Du, X., L. Jin, and R. Zhang, *Modeling the cracking of cover concrete due to non-uniform corrosion of reinforcement.* Corrosion Science, 2014. **89**: p. 189-202.
41. Li, C.-Q., et al., *Concrete delamination caused by steel reinforcement corrosion.* Journal of Materials in Civil Engineering, 2007. **19**(7): p. 591-600.
42. Maeda, Y., *Slag cement-related products which utilized a property of the Ground Granulated Blast Furnace Slag.* Nippo Steel Sumitomo Metal Tech. Rep, 2015. **109**: p. 114-118.
43. Nakamura, N., et al., *Properties of High-Strength Concrete Incorporating Very Finely Ground Granulated Blast Furnace Slag.* Special Publication, 1986. **91**: p. 1361-1380.
44. Hogan, F. and J. Meusel, *Evaluation for durability and strength development of a ground granulated blast furnace slag.* Cement, Concrete and Aggregates, 1981. **3**(1): p. 40-52.
45. Eguchi, K. and K. Teranishi, *Prediction equation of drying shrinkage of concrete based on composite model.* Cement and Concrete Research, 2005. **35**(3): p. 483-493.
46. Imamura, A., et al., *Uplift behavior of spread foundation structures on sand and clay deposit, Architectural Institute of Japan.* J. Struct. Constr. Eng, 2013. **692**: p. 1759-1768.
47. Subpa-asa, P., et al. *Study on the Influence of Blast Furnace Slag on Chloride Ion Penetration Property*. in *IOP Conference Series: Materials Science and Engineering*. 2020. IOP Publishing.
48. Satou, M., et al., *A STUDY ON THE CHLORIDE RESI STIVITY OF FLY ASH CONCRETE.* Journal of Japan Society of Civil Engineers, Ser. E2 (Materials and Concrete Structures), 2011. **67**(2): p. 309-321.
49. Meyer, C., *The greening of the concrete industry.* Cement and concrete composites, 2009. **31**(8): p. 601-605.
50. Ramezanianpour, A.A., *Cement replacement materials.* Springer Geochemistry/Mineralogy, DOI, 2014. **10**: p. 978-3.
51. Meyer, C., *Concrete and sustainable development.* ACI Special Publications, 2002. **206**: p. 501-512.
52. ASTM, *ASTM C125-Standard Terminology Relating to Concrete and Concrete Aggregates*. 2018, ASTM International West Conshohocken.
53. Moranville-Regourd, M., *Cements made from blastfurnace slag.* Lea's chemistry of cement and concrete, 1998. **4**: p. 633-674.
54. 日本工業規格, *スラグ類の化学物質試験方法-第 1 部: 溶出量試験方法.* JIS K 0058-1, 2005.
55. Kennedy, A.M. and M. Arias-Paić, *Application of powdered steel slag for more sustainable removal of metals from impaired waters.* Journal of Water Process Engineering, 2020. **38**: p. 101599.

56. Yuksel, I. and T. Bilir, *Usage of industrial by-products to produce plain concrete elements.* Constr Build Mater, 2007. **21**(3): p. 686-694.
57. Chen, W. and H. Brouwers. *The reaction of slag in cement: theory and computer modelling*. in *Proceedings 16th Ibausil, International Conference on Building Materials (Internationale Baustofftagung), Weimar*. 2006.
58. Escalante, J., et al., *Reactivity of blast-furnace slag in Portland cement blends hydrated under different conditions.* Cement and Concrete Research, 2001. **31**(10): p. 1403-1409.
59. Mehta, P.K., *Pozzolanic and cementitious byproducts as mineral admixtures for concrete-a critical review.* Special Publication, 1983. **79**: p. 1-46.
60. Osborne, G., *Carbonation and permeability of blastfurnace slag cement concretes from field structures.* Special Publication, 1989. **114**: p. 1209-1238.
61. Soutsos, M., et al., *Fast track construction with high-strength concrete mixes containing ground granulated blast furnace slag.* Special Publication, 2005. **228**: p. 255-270.
62. Lim, S. and T. Wee, *Autogenous shrinkage of ground-granulated blast-furnace slag concrete.* Materials Journal, 2000. **97**(5): p. 587-593.
63. Hamling, J.W. and R.W. Kriner, *Evaluation of granulated blast furnace slag as a cementitious admixture—A case study.* Cement, concrete and aggregates, 1992. **14**(1): p. 13-20.
64. Richardson, A.E., *Compressive strength of concrete with polypropylene fibre additions.* Structural survey, 2006.
65. Duos, C. and J. Eggers, *Evaluation of ground granulated Blast Furnace Slag in concrete (Grade 120)*. 1999.
66. Sonebi, M., *Medium strength self-compacting concrete containing fly ash: Modelling using factorial experimental plans.* Cement and Concrete research, 2004. **34**(7): p. 1199-1208.
67. Boukendakdji, O., et al., *Effect of slag on the rheology of fresh self-compacted concrete.* Construction and Building Materials, 2009. **23**(7): p. 2593-2598.
68. Yuksel, I., *Blast-furnace slag*, in *Waste and Supplementary Cementitious Materials in Concrete*. 2018, Elsevier. p. 361-415.
69. Václavík, V., et al., *The use of blast furnace slag.* Metalurgija, 2012. **51**(4): p. 461-464.
70. Singh, J., H. Singh, and R. Singh, *Portland Slag Cement Using Ground Granulated Blast Furnace Slag (GGBFS).* IJREAS, 2015. **5**(11): p. 47-53.
71. Yim, H.J., et al., *Influence of Portland cement and ground-granulated blast-furnace slag on bleeding of fresh mix.* Construction and Building Materials, 2015. **80**: p. 132-140.
72. Malhotra, V. and E. Nawy, *Mineral admixtures.* Concrete Construction Engineering Handbook, Nawy Edward G. CRC Press, New York, 1997: p. 27-36.
73. Naik, T.R. and B.W. Ramme, *Effects of high-lime fly ash content on water demand, time of set, and compressive strength of concrete.* Materials Journal, 1990. **87**(6): p. 619-626.
74. Brooks, J., M.M. Johari, and M. Mazloom, *Effect of admixtures on the setting times of high-strength concrete.* Cement and concrete Composites, 2000. **22**(4): p. 293-301.
75. Nehdi, M. and J. Summer, *Optimization of ternary cementitious mortar blends using factorial experimental plans.* Materials and Structures, 2002. **35**(8): p. 495-503.

76. Gesoğlu, M. and E. Özbay, *Effects of mineral admixtures on fresh and hardened properties of self-compacting concretes: binary, ternary and quaternary systems.* Materials and Structures, 2007. **40**(9): p. 923-937.
77. Robeyst, N., et al., *Monitoring the setting of concrete containing blast-furnace slag by measuring the ultrasonic p-wave velocity.* Cement and Concrete research, 2008. **38**(10): p. 1169-1176.
78. Aghaeipour, A. and M. Madhkhan, *Effect of ground granulated blast furnace slag (GGBFS) on RCCP durability.* Construction and Building Materials, 2017. **141**: p. 533-541.
79. Zhao, H., et al., *The properties of the self-compacting concrete with fly ash and ground granulated blast furnace slag mineral admixtures.* Journal of Cleaner Production, 2015. **95**: p. 66-74.
80. Pizoń, J., P. Miera, and B. Łaźniewska-Piekarczyk, *Influence of hardening accelerating admixtures on properties of cement with ground granulated blast furnace slag.* Procedia engineering, 2016. **161**: p. 1070-1075.
81. Sanjayan, J.G. and B. Sioulas, *Strength of slag-cement concrete cured in place and in other conditions.* Materials Journal, 2000. **97**(5): p. 603-611.
82. Tomisawa, T. and M. Fujll, *Effects of high fineness and large amounts of ground granulated blast furnace slag on properties and microstructure of slag cements.* Special Publication, 1995. **153**: p. 951-974.
83. Sivasundaram, V. and V. Malhotra, *Properties of concrete incorporating low quantity of cement and high volumes of ground granulated slag.* Materials Journal, 1992. **89**(6): p. 554-563.
84. Li, C., A. Yoda, and T. Yokomur, *Pore structure, strength and carbonation of cement pastes containing ground granulated blast-furnace slag.* Special Publication, 1998. **178**: p. 875-892.
85. Zhang, M.-H., et al., *Concrete incorporating supplementary cementing materials: effect on compressive strength and resistance to chloride-ion penetration.* ACI Materials Journal, 1999. **96**: p. 181-189.
86. Lim, S.K., T.C. Ling, and M.W. Hussin, *Strength properties of self-compacting mortar mixed with GGBFS.* Proceedings of the Institution of Civil Engineers-Construction Materials, 2012. **165**(2): p. 87-98.
87. Neville, A., *Suggestions of research areas likely to improve concrete.* Concrete International, 1996. **18**(5): p. 44-49.
88. Oner, A. and S. Akyuz, *An experimental study on optimum usage of GGBS for the compressive strength of concrete.* Cement and concrete composites, 2007. **29**(6): p. 505-514.
89. Meeks, K.W. and N.J. Carino, *Curing of high-performance concrete: Report of the state-of-the-art*. 1999: US Department of Commerce, Technology Administration, National Institute of ….
90. Leung, P.W. and H. Wong, *Final Report on durability and strength development of ground granulated blast furnace slag concrete.* Geotechnical Engineering office, Civil Engineering and, 2010.
91. Barnett, S., et al., *Strength development of mortars containing ground granulated blast-furnace slag: Effect of curing temperature and determination of apparent activation energies.* Cement and Concrete Research, 2006. **36**(3): p. 434-440.
92. Yeau, K.Y. and E.K. Kim, *An experimental study on corrosion resistance of concrete with ground granulate blast-furnace slag.* Cement and Concrete Research, 2005. **35**(7): p. 1391-1399.

93. Özbay, E., M. Erdemir, and H.İ. Durmuş, *Utilization and efficiency of ground granulated blast furnace slag on concrete properties–A review.* Construction and Building Materials, 2016. **105**: p. 423-434.
94. Khatib, J. and J. Hibbert, *Selected engineering properties of concrete incorporating slag and metakaolin.* Construction and building materials, 2005. **19**(6): p. 460-472.
95. Teng, S., T.Y.D. Lim, and B.S. Divsholi, *Durability and mechanical properties of high strength concrete incorporating ultra fine ground granulated blast-furnace slag.* Construction and Building Materials, 2013. **40**: p. 875-881.
96. CSA, *Design of concrete structures.* CSA Standard A23. 3-04, 2004.
97. Stutterheim, N. *Properties and uses of high-magnesia portland slag cement concretes*. in *Journal Proceedings*. 1960.
98. Suresh, D. and K. Nagaraju, *Ground granulated blast slag (GGBS) in concrete–a review.* IOSR journal of mechanical and civil engineering, 2015. **12**(4): p. 76-82.
99. Siddique, R. and M.I. Khan, *Supplementary cementing materials*. 2011: Springer Science & Business Media.
100. Luo, R., et al., *Study of chloride binding and diffusion in GGBS concrete.* Cement and Concrete Research, 2003. **33**(1): p. 1-7.
101. Bouikni, A., R. Swamy, and A. Bali, *Durability properties of concrete containing 50% and 65% slag.* Construction and Building Materials, 2009. **23**(8): p. 2836-2845.
102. Basheer, P., et al., *Monitoring electrical resistance of concretes containing alternative cementitious materials to assess their resistance to chloride penetration.* Cement and Concrete Composites, 2002. **24**(5): p. 437-449.
103. Song, H.-W. and V. Saraswathy, *Studies on the corrosion resistance of reinforced steel in concrete with ground granulated blast-furnace slag—An overview.* Journal of Hazardous materials, 2006. **138**(2): p. 226-233.
104. Feldman, R., *Pore structure, permeability and diffusivity as related to durability*. 1986: National Research Council Canada, Institute for Research in Construction.
105. Johari, M.M., et al., *Influence of supplementary cementitious materials on engineering properties of high strength concrete.* Construction and Building Materials, 2011. **25**(5): p. 2639-2648.
106. Singh, G. and R. Siddique, *Effect of iron slag as partial replacement of fine aggregates on the durability characteristics of self-compacting concrete.* Construction and Building Materials, 2016. **128**: p. 88-95.
107. ASTM, C., *ASTM standards.* Philadelphia: American Society for Testing Materials, 1958.
108. Hadjsadok, A., et al., *Durability of mortar and concretes containing slag with low hydraulic activity.* Cement and Concrete Composites, 2012. **34**(5): p. 671-677.
109. Deboucha, W., et al., *Effect of incorporating blast furnace slag and natural pozzolana on compressive strength and capillary water absorption of concrete.* Procedia Engineering, 2015. **108**: p. 254-261.
110. Binici, H., et al., *Performance of ground blast furnace slag and ground basaltic pumice concrete against seawater attack.* Construction and Building Materials, 2008. **22**(7): p. 1515-1526.

111. Cheng, A., et al., *Influence of GGBS on durability and corrosion behavior of reinforced concrete.* Materials Chemistry and Physics, 2005. **93**(2-3): p. 404-411.
112. Güneyisi, E. and M. Gesoğlu, *A study on durability properties of high-performance concretes incorporating high replacement levels of slag.* Materials and Structures, 2008. **41**(3): p. 479-493.
113. González, M. and E. Irassar, *Effect of limestone filler on the sulfate resistance of low C3A Portland cement.* Cement and Concrete Research, 1998. **28**(11): p. 1655-1667.
114. Shi, H.-s., B.-w. Xu, and X.-c. Zhou, *Influence of mineral admixtures on compressive strength, gas permeability and carbonation of high performance concrete.* Construction and Building Materials, 2009. **23**(5): p. 1980-1985.
115. Ahari, R.S., T.K. Erdem, and K. Ramyar, *Permeability properties of self-consolidating concrete containing various supplementary cementitious materials.* Construction and Building Materials, 2015. **79**: p. 326-336.
116. Wee, T., et al., *Sulfate resistance of concrete containing mineral admixtures.* Materials Journal, 2000. **97**(5): p. 536-549.
117. Taylor, W.H., *CONCRETE TECHNOLOGY AND PRACTICE, 4/E.* 1967.
118. Irassar, E., *Sulfate attack on cementitious materials containing limestone filler—A review.* Cement and Concrete Research, 2009. **39**(3): p. 241-254.
119. Bensted, J., *Thaumasite—background and nature in deterioration of cements, mortars and concretes.* Cement and Concrete Composites, 1999. **21**(2): p. 117-121.
120. Crammond, N., *The thaumasite form of sulfate attack in the UK.* Cement and Concrete Composites, 2003. **25**(8): p. 809-818.
121. Al-Saadoun, S., A. Al-Gahtani, and F. Dakhil, *Effect of tricalcium aluminate content of cement on corrosion of reinforcing steel in concrete.* Cement and Concrete Research, 1990. **20**(5): p. 723-738.
122. Moon, H.-Y., et al., *Experimental Study on the Sulfate Resistance of Concrete Blended Ground Granulated Blast-furnace Slag for Recycling.* Geosystem Engineering, 2002. **5**(3): p. 67-73.
123. Higgins, D. and M. Uren, *The effect of GGBS on the durability of concrete.* Concrete, 1991. **25**(6).
124. Mangat, P. and J. El-Khatib, *Influence of initial curing on sulphate resistance of blended cement concrete.* Cement and Concrete Research, 1992. **22**(6): p. 1089-1100.
125. Gollop, R. and H. Taylor, *Microstructural and microanalytical studies of sulfate attack. IV. Reactions of a slag cement paste with sodium and magnesium sulfate solutions.* Cement and Concrete Research, 1996. **26**(7): p. 1013-1028.
126. Cao, H., et al., *The effect of cement composition and pH of environment on sulfate resistance of Portland cements and blended cements.* Cement and Concrete Composites, 1997. **19**(2): p. 161-171.
127. Higgins, D. and N. Crammond, *Resistance of concrete containing ggbs to the thaumasite form of sulfate attack.* cement and concrete Composites, 2003. **25**(8): p. 921-929.
128. Binici, H., et al., *The effect of particle size distribution on the properties of blended cements incorporating GGBFS and natural pozzolan (NP).* Powder Technology, 2007. **177**(3): p. 140-147.

129. Hanson, W. *Studies Relating To the Mechanism by Which the Alkali-Aggregate Reaction Produces EXPANSION IN CONCRETE*. in *Journal Proceedings*. 1944.
130. Swamy, R.N., *The alkali-silica reaction in concrete*. 1992: Blackie Glasgow.
131. Skalny, J. and W. Klemm, *Alkalis in clinker: origin, chemistry, effects.* National Building Research Institutes, Pretoria, South Africa, 1981.
132. Kwon, Y.-j., *A study on the alkali-aggregate reaction in high-strength concrete with particular respect to the ground granulated blast-furnace slag effect.* Cement and concrete research, 2005. **35**(7): p. 1305-1313.
133. Thomas, M.D., *Review of the effect of fly ash and slag on alkali-aggregate reaction in concrete.* 1996.
134. Thomas, M. and F. Innis, *Effect of slag on expansion due to alkali aggregate reaction in concrete.* Materials Journal, 1998. **95**(6): p. 716-724.
135. Hester, D., C. McNally, and M. Richardson, *A study of the influence of slag alkali level on the alkali–silica reactivity of slag concrete.* Construction and Building Materials, 2005. **19**(9): p. 661-665.
136. Hooton, D., et al. *An Assessment of the Effectiveness of Blast Furnace Slag in Counteracting the Effects of Alkali Silica Reaction*. in *11 th International Conference on Alkali Aggregate Reaction, Québec City, Canada*. 2000.
137. Meyer, C., *Recycled materials in concrete.* Developments in the Formulation and Reinforcement of Concrete, 2008: p. 208-230.
138. Lane, D. and C. Ozyildirim, *Preventive measures for alkali-silica reactions (binary and ternary systems).* Cement and concrete research, 1999. **29**(8): p. 1281-1288.
139. Attoh-Okine, N. and F. Atique, *Service life assessment of concrete with ASR and possible mitigation.* Delaware Center for Transportation, Newark, Delaware, 2006.
140. Andrade, C., et al., *Estimating corrosion attack in reinforced concrete by means of crack opening.* Structural Concrete, 2016. **17**(4): p. 533-540.
141. Osborne, G., *Durability of Portland blast-furnace slag cement concrete.* Cement and Concrete Composites, 1999. **21**(1): p. 11-21.
142. Irassar, E., M. Gonzalez, and V. Rahhal, *Sulphate resistance of type V cements with limestone filler and natural pozzolana.* Cement and Concrete Composites, 2000. **22**(5): p. 361-368.
143. Hossain, K. and M. Lachemi, *Corrosion resistance and chloride diffusivity of volcanic ash blended cement mortar.* Cement and Concrete Research, 2004. **34**(4): p. 695-702.
144. Kumar, A. and D.M. Roy, *The effect of desiccation on the porosity and pore structure of freeze dried hardened portland cement and slag-blended pastes.* Cement and Concrete Research, 1986. **16**(1): p. 74-78.
145. Bouteiller, V., et al., *Corrosion initiation of reinforced concretes based on Portland or GGBS cements: Chloride contents and electrochemical characterizations versus time.* Cement and Concrete Research, 2012. **42**(11): p. 1456-1467.
146. Glass, G., B. Reddy, and N. Buenfeld, *The participation of bound chloride in passive film breakdown on steel in concrete.* Corrosion Science, 2000. **42**(11): p. 2013-2021.
147. Reddy, B., et al., *On the corrosion risk presented by chloride bound in concrete.* Cement and Concrete Composites, 2002. **24**(1): p. 1-5.

148. Luping, T. and L.-O. Nilsson, *Chloride binding capacity and binding isotherms of OPC pastes and mortars.* Cement and concrete research, 1993. **23**(2): p. 247-253.
149. Kayali, O., M. Khan, and M.S. Ahmed, *The role of hydrotalcite in chloride binding and corrosion protection in concretes with ground granulated blast furnace slag.* Cement and Concrete Composites, 2012. **34**(8): p. 936-945.
150. Dhir, R., M. El-Mohr, and T. Dyer, *Chloride binding in GGBS concrete.* Cement and Concrete Research, 1996. **26**(12): p. 1767-1773.
151. Khan, M., O. Kayali, and U. Troitzsch, *Chloride binding capacity of hydrotalcite and the competition with carbonates in ground granulated blast furnace slag concrete.* Materials and Structures, 2016. **49**(11): p. 4609-4619.
152. Khan, M. and O. Kayali, *Chloride binding ability and the onset corrosion threat on alkali-activated GGBFS and binary blend pastes.* European Journal of Environmental and Civil Engineering, 2018. **22**(8): p. 1023-1039.
153. Gjorv, O. *Steel corrosion in marine concrete structures—an overview*. in *Proceedings of the International Symposium on Durability of Concrete in Marine Environment, University of California, Berkeley*. 1989.
154. Arya, C. and Y. Xu, *Effect of cement type on chloride binding and corrosion of steel in concrete.* Cement and Concrete Research, 1995. **25**(4): p. 893-902.
155. Huang, R., J.-J. Chang, and J.-K. Wu, *Correlation between corrosion potential and polarization resistance of rebar in concrete.* Materials Letters, 1996. **28**(4-6): p. 445-450.
156. Loser, R., et al., *Chloride resistance of concrete and its binding capacity–Comparison between experimental results and thermodynamic modeling.* Cement and Concrete Composites, 2010. **32**(1): p. 34-42.
157. Qu, Z., Q. Yu, and H. Brouwers, *Relationship between the particle size and dosage of LDHs and concrete resistance against chloride ingress.* Cement and Concrete Research, 2018. **105**: p. 81-90.
158. Delagrave, A., et al., *Chloride binding capacity of various hydrated cement paste systems.* Advanced Cement based materials, 1997. **6**(1): p. 28-35.
159. Pan, T., K. Xia, and L. Wang, *Chloride binding to calcium silicate hydrates (CSH) in cement paste: A molecular dynamics analysis.* International Journal of Pavement Engineering, 2010. **11**(5): p. 367-379.
160. Federico, L. and S. Chidiac, *Waste glass as a supplementary cementitious material in concrete–critical review of treatment methods.* Cement and concrete composites, 2009. **31**(8): p. 606-610.
161. Vickers, N.J., *Animal communication: when i'm calling you, will you answer too?* Current biology, 2017. **27**(14): p. R713-R715.
162. Mantel, D., *Investigation into the hydraulic activity of five granulated blast furnace slags with eight different Portland cements.* Materials Journal, 1994. **91**(5): p. 471-477.
163. JIS, R., *5201 (1997) Physical testing methods for cement.* Japan Industrial Standards (confirmed in 2011).
164. Kabe, K., et al., *Evaluation of Chloride Penetration in Concrete by Resistivity.* Journal of the Society of Materials Science, Japan, 2008. **57**(10): p. 1005-1010.
165. Goto, S. and D.M. Roy, *Diffusion of ions through hardened cement pastes.* Cement and Concrete Research, 1981. **11**(5-6): p. 751-757.
166. Page, C., N. Short, and A. El Tarras, *Diffusion of chloride ions in hardened cement pastes.* Cement and concrete research, 1981. **11**(3): p. 395-406.

167. Andrade, C. *Concepts on the chloride diffusion coefficient*. in *Third International RILEM Workshop on Testing and Modeling the Chloride Ingress into Concrete*. 2002.
168. Nilsson, L.-O. *A NUMERICAL MODEL FOR COMBINED DIFFUSION AND CONVECTION OF CHLORIDE IN NON-SATURATED*. in *PRO 19: 2nd International RILEM Workshop on Testing and Modelling the Chloride Ingress into Concrete*. 2000. RILEM Publications.
169. Crank, J., *The mathematics of diffusion*. 1979: Oxford university press.
170. Atkinson, A. and A. Nickerson, *The diffusion of ions through water-saturated cement.* Journal of materials science, 1984. **19**(9): p. 3068-3078.
171. Baroghel-Bouny, V., et al., *Prediction of chloride binding isotherms of cementitious materials by analytical model or numerical inverse analysis.* Cement and concrete research, 2012. **42**(9): p. 1207-1224.
172. Castellote, M., C. Andrade, and C. Alonso, *Chloride-binding isotherms in concrete submitted to non-steady-state migration experiments.* Cement and Concrete Research, 1999. **29**(11): p. 1799-1806.
173. Whiting, D., *Rapid determination of the chloride permeability of concrete.* Final Report Portland Cement Association, 1981.
174. Luping, T. and L.-O. Nilsson, *Rapid determination of the chloride diffusivity in concrete by applying an electric field.* Materials Journal, 1993. **89**(1): p. 49-53.
175. Tang, L., *Chloride transport in concrete-measurement and prediction.* Chalmers University of Technology, Sweden, Doctor Thesis, 1996.
176. Andrade, C., *Calculation of chloride diffusion coefficients in concrete from ionic migration measurements.* Cement and concrete research, 1993. **23**(3): p. 724-742.